

**UNIVERSIDAD DE VALLADOLID**



**Control Predictivo multivariable y optimización de procesos con HITO y EcosimPro**

**Benjamin Bradu**



**DEPARTAMENTO DE INGENIERÍA  
DE SISTEMAS Y AUTOMÁTICA**

**ESCUELA TÉCNICA SUPERIOR DE INGENIEROS INDUSTRIALES**

UNIVERSIDAD DE VALLADOLID

**PROYECTO FIN DE CARRERA**

Presentado en el

DEPARTAMENTO DE INGENIERÍA DE SISTEMAS  
Y AUTOMÁTICA

de la

ESCUELA TÉCNICA SUPERIOR DE INGENIEROS  
INDUSTRIALES

para la obtención del título de

**INGENIERO INDUSTRIAL**

por

**Benjamín Bradu**

**Control Predictivo multivariable y optimización de procesos  
con HITO y EcosimPro**

*Proyecto dirigido por: Cesar de Prada Moraga*

*Director: Rogelio Mazaeda*

# Contents

<b>Introduction</b>	<b>8</b>
<b>I Identification and predictive control</b>	<b>9</b>
<b>1 Identification</b>	<b>10</b>
1.1 Identification goal and principle . . . . .	10
1.2 Identification procedure . . . . .	11
1.2.1 Signal post-processing . . . . .	11
1.2.2 Model types . . . . .	14
1.2.3 Identification . . . . .	15
1.2.4 Validation of the model . . . . .	16
<b>2 Predictive control</b>	<b>17</b>
2.1 General feature . . . . .	17
2.2 Model and Predictions . . . . .	19
2.2.1 Generalized Predictive Control (GPC) . . . . .	19
2.2.2 Dynamic Matrix Control (DMC) . . . . .	20
2.3 Calculation of the optimal control . . . . .	21
2.4 Constraints on variables . . . . .	22
2.5 Feasibility of control . . . . .	22
<b>II Communicating tanks</b>	<b>23</b>
<b>3 Identification of 2 communicating tanks</b>	<b>24</b>
3.1 Process Description . . . . .	24
3.2 Identification . . . . .	25
3.2.1 Test protocol . . . . .	25
3.2.2 Signal post-processing with HIDDEN . . . . .	25
3.2.3 Identification with HIDDEN . . . . .	26
3.3 Validation of the model . . . . .	27
<b>4 Identification of 4 communicating tanks</b>	<b>30</b>
4.1 Process description . . . . .	30
4.2 Identification . . . . .	31
4.3 Validation of the model . . . . .	32
<b>5 Predictive Control of 2 communicating tanks</b>	<b>34</b>
5.1 HITO . . . . .	34
5.2 Hardware configuration . . . . .	34
5.3 Constraints and control properties . . . . .	34
5.4 Feasibility problem . . . . .	35
5.5 Simulations . . . . .	35
5.6 Results . . . . .	37
5.7 Influence of perturbations . . . . .	38
5.8 Constraints and feasibility . . . . .	39

<b>6</b>	<b>Predictive Control of 4 communicating tanks</b>	<b>41</b>
6.1	Control parameters and simulation . . . . .	41
6.2	Results on the real plant . . . . .	42
6.3	Influence of perturbation . . . . .	43
6.4	Conclusion . . . . .	43
<b>III</b>	<b>Distillation column</b>	<b>44</b>
<b>7</b>	<b>Process and control presentation</b>	<b>45</b>
7.1	Distillation principle . . . . .	45
7.2	Process description . . . . .	46
7.3	Process operation . . . . .	47
7.4	EcoSim library of the depropanizer . . . . .	47
7.5	Process control objectives . . . . .	48
7.6	Predictive control of the depropanizer . . . . .	48
<b>8</b>	<b>Optimization of the depropanizer</b>	<b>52</b>
8.1	HITO . . . . .	52
8.2	Economic cost function . . . . .	54
8.3	Numerical Data . . . . .	56
8.4	steady-state optimization . . . . .	57
8.5	Experiments on EcoSimPro . . . . .	59
8.5.1	Basic simulations . . . . .	59
8.5.2	Moving of operating point with disturbances . . . . .	61
8.5.3	Market price influence . . . . .	61
	<b>Conclusion</b>	<b>65</b>
	<b>Bibliography</b>	<b>66</b>
	<b>Appendix A: Mathematic model of distillation columns</b>	<b>68</b>
	<b>Appendix B: A predictive control with dynamic optimization on a distillation column</b>	<b>95</b>
	<b>Appendix C: Optimization program and results in GAMS</b>	<b>104</b>

# List of Figures

1.1	Identification procedure	11
1.2	Discreet white noise simulated and its autocorrelation	12
1.3	A PRBS signal and its autocorrelation	13
1.4	Model Structure in close-loop	13
2.1	Typical global architecture with a MBPC	17
2.2	Temporal diagram of a typical MBPC	18
2.3	Smoothing of the reference trajectory $r(t)$ according to $\alpha$	18
2.4	MBPC internal architecture	19
3.1	Schema of the 2 communicating tanks	24
3.2	signals applied on the two valves	25
3.3	Inter correlation between the 2 PRBS and their autocorrelation	26
3.4	Process and model outputs	27
3.5	Correlation between residue and inputs	27
3.6	Process/model Inputs and outputs for each validation test	28
3.7	Correlations between residue $r_1$ and inputs for each validation test	28
3.8	Correlations between residue $r_2$ and inputs for each validation test	28
3.9	Process/Model inputs and outputs during "extreme" test	29
3.10	Correlations between residues and inputs during "extreme" test	29
3.11	tank levels (measured and calculated) during a predictive control	29
4.1	Schema of the 4 communicating tanks	30
4.2	steps realized on the 4 communicating tanks	31
4.3	Identification : model and process outputs, step response and correlations between residues and inputs	32
4.4	validation : Model and process outputs, correlation between residues and inputs	33
5.1	priorities to solve problem of not feasibility	36
5.2	Step responses on $L_{T1}$ for different tests	36
5.3	Real and simulated step responses with GPC and PID	37
5.4	Test on the real plant	37
5.5	Perturbation : closing of the right drain valve	38
5.6	Perturbation : closing of the exchange valve	38
5.7	priority to move MV limits or CV limits in HITO	39
5.8	Non feasible problem with higher priority to move MV limits	40
5.9	Non feasible problem with higher priority to move CV limits	40
6.1	Predictive Control simulated on the 4 tanks	41
6.2	Responses to steps of the set-points with predictive Control on the 4 tanks	42
6.3	Predictive Control of the 4 tanks	42
6.4	Perturbation on the right valve	43
6.5	Perturbation on the valve of exchange	43
7.1	Boiling point diagram at a constant pressure	45
7.2	Distillation column	46
7.3	Control architecture of the distillation column	50
7.4	Simulation of the depropanizer with a DMC controller : steps of $C_{4top}$	50
7.5	Control architecture of the distillation column in EcosimPro	51
8.1	HITO algorithm with optimization	53

8.2	Steady-state and HITO optimization . . . . .	53
8.3	Relation between the butane and the condensate . . . . .	54
8.4	In order to have a quadratic approximation, temperature range is divided in two . . . . .	57
8.5	Value of the cost function according to $Fpv$ and $T$ for each specification . . . . .	59
8.6	Simulation of the column : DMC with cost optimization with the 1 <sup>st</sup> specification . . . . .	62
8.7	Simulation of the column : DMC with cost optimization with the 2 <sup>nd</sup> specification . . . . .	63
8.8	Simulation without optimization but using Optimal set-points of the 2 <sup>nd</sup> specification on the DMC . . . . .	63
8.9	Simulation of the column with optimization at T=7 and disturbance on the feed at T=15 . . . . .	64

# Acknowledgments

This final year project has been performed in the Systems Engineering and Automatic Control Department of the University of Valladolid (Spain) in order to graduate with the Engineer degree from the *Ecole Supérieure d'Ingénieurs en Electrotechnique et en Electronique d'Amiens* (ESIEE-Amiens) and by the Master Science and Technology of the *Université Technologique de Compiègne* (UTC).

I'm especially grateful to Cesar de Prada, my Valladolid supervisor who guided me during all my work and who allowed me to meet different researchers of the control world. Moreover, I have discovered new areas such as the chemical engineering and optimization techniques. Thanks to Hervé Coppier, my ESIEE supervisor, who advised me and cared about all my work.

I would like to express my gratefulness to Augustin Mpanda, my Department leader in the ESIEE and to Christine Robert and Blanca Giménez who have helped me with administrative details. I also want to thank Enrique Blanco Viñuela who has advised me this department.

Thanks to Elena who helped me during my work about chemical engineering and a special thanks to Santiago for his knowledge about the petroleum refineries and his daily good mood in the laboratory.

Thanks to the whole ISA department for their welcome and to Smaranda Cristea for her assistance about HITO.

# Introduction

I have done my final year project in the System Engineering and Automatic Control department of the University of Valladolid in Spain. This department is composed of a dozen of researchers and of a ten of doctoral students. This department works with advanced control, modeling and simulation, process optimization, Computer Aided Control Systems Design and educational systems.

Most of the industrial processes are generally controlled and regulated with a classical Proportional, Integral and Derivative controller (PID). Nevertheless, complex processes composed of various inputs and outputs which have important delays or inverse responses can't be controlled with PID. The solution is to develop an advanced control like the Model Based Predictive Control (MBPC). The majority of users are big industries like petroleum refineries, chemical factories, nuclear plants, metallurgy, cryogenic systems, etc. This control is based on a mathematical model of the process in order to predict future behaviors. That is why the identification of the process is very important in this kind of problem, where an accurate model guarantees an efficient control. Moreover, advanced control techniques allow to reject external disturbances (measurable or stochastic) and to take into account constraints on the process in order to preserve actuators.

Another point which concerns and interests industries is the optimization of process operations. In complex processes, there are several degrees of freedom and the operating ranges are quite large, so different ways exist to control such a process. The goal of the optimization is to find an optimal operating point in order to minimize the cost of production, and so, to increase the benefits of the factory. Such an optimization can be directly included in a MBPC using the same model. Nowadays, models can be more accurate and more efficient thanks to the power of computers, components of factories are entirely simulated in numerical simulations.

I have worked on two different projects : The first project consisted in carrying out an identification and a predictive control of an existing experiment composed of two or four communicating tanks in a laboratory. My second project was to develop an optimization of a predictive control on a distillation column thanks to simulations in order to reduce the cost of production of this column which is used in the petroleum industry.

To achieve all these works, different tools and software are used. The identification is performed on Matlab thanks to a toolbox named HIDEN. Then, the predictive control of the communicating tanks is realized with a software called HITO which has been developed by my department using an OPC interface. Concerning the distillation column, numerical simulations are essential to check theoretical results before testing on the real plant. An existing model of the column developed in EcosimPro is used. The predictive control and the optimization of the column are achieved in EcosimPro thanks to an external library of HITO.

In the first part the identification and the predictive control theory will be treated in order to introduce basic concepts of these two fundamental techniques. In the second part, the communicating tanks will be studied. Identification of the process will be done before developing the predictive control of this process (a Generalized Predictive Control and a Dynamic Matrix control will be done). Finally, in the third part, the distillation column will be presented (its working and its control) in order to achieve in the following the optimization of the control. Finally, a conclusion will summarize all the results obtained in the different parts.



## Part I

# Identification and predictive control

# Chapter 1

## Identification

To control a process, particularly with a predictive control, it is necessary to have a mathematical model of the process. An identification is a transformation of the natural laws in equations. For this, two approaches are possible :

- Using the physical equations of the system (Mass conservation, energy conservation...) which are generally complex differential equations.
- Exciting the process by inputs, measuring the outputs and deducing an empirical model upon these observations: parametrical identification.

The first method needs to have an important knowledge of the process and moreover disturbances on electrical signals (noise) can't be expressed. The different parameters obtained with this method are physical constants generally not very well-known.

The second method, which will be explained in this report, allows a good reliability in taking care on all possible disturbances applied on the system. The result of this identification is a mathematical model where the different parameters haven't any physical significations. This model can be represented continuously or discretely by different way as transfer functions, states spaces, step responses, pulse responses...

### 1.1 Identification goal and principle

The principle of the parametrical identification is to extract a mathematical model from observations. Thus, it's important to have a basic knowledge of the process. It's necessary to choose a model type. For this, we have to select the properties of the models :

- SISO or MIMO model. Which inputs ? Which outputs ? Which disturbances ?
- Linear or non-linear model (and what is non-linear about what ?)
- Continuous or discreet model
- Independent or regressive model : for a regressive model the model output  $y_m$  depends on the process output  $y_p$
- Determinist or stochastic model

Then, in order to obtain a model with a good reliability, it's important to excite all frequencies, so, the signal applied to the process input have to be rich in frequencies (*ie* : having a large spectrum). One of the best signal, very rich in frequency is a Pseudo Random Binary Signal (PRBS). This signal can be set at two distinctive values (eg:1 and -1) where the order of apparition of these two values is generated by a random function during a fixed period. Then, this sequence is repeated (Figure 1.3).

When there are multiple inputs in a MIMO system, all inputs have to be uncorrelated. If two inputs ( $u_1$  and  $u_2$ ) are correlated, it exists an infinity of solutions for the two models  $M1 = \frac{y1}{u1}$  and  $M2 = \frac{y1}{u2}$ . For example, if  $u_1 = \alpha \cdot u_2$  then  $y = M1 \cdot u_1 + M2 \cdot u_2 = (\alpha \cdot M1 + M2) \cdot u_2$  and there are a lot of different solutions to find  $M1$  and  $M2$ .

Moreover, exciting one input with the other constant and vice-versa is not a good solution either. First, the time of the test and of the resolution will be longer and secondly, the dynamic of the process is not well evaluated, it's not representative of a normal process operation. So, the best method is to excite the process with all inputs together and all input signals have to be uncorrelated.

That's why it's important to develop a test protocol to have a good precision in the model. In the figure 1.1, the identification procedure is resumed [CAR04]:

- Determination of the **test protocol** : Properties of the excitation signal to cover all interesting frequencies, the ratio signal/noise must be important enough and the number of measurements must be relevant for the test (>1000).
- Determination of the **model structure** : there are a lot of models to describe a dynamic behavior and the model has to be adapted to the process. The model order and the delays have to be determined too.
- **Parameters identification** : choice of an algorithm to solve the problem and minimizing errors between process and model.
- The **validation** of the model is very important. It consists of different tests to validate the model. If the model is wrong, it's necessary to come back on previous steps.

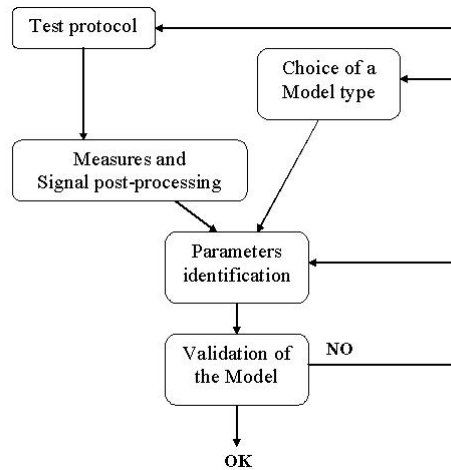


Figure 1.1: Identification procedure

## 1.2 Identification procedure

In this section, all identification steps will be described to perform a consistent identification on a real process. This procedure is the same in the HIDENT toolbox (HITO Identificación). It is a MATLAB identification toolbox developed by the *departemento de Ingeniería de Sistemas Automática* of the Valladolid university. The model obtained with this toolbox can be imported in HIDENT in order to proceed to a predictive control.

### 1.2.1 Signal post-processing

After having made a data acquisition from the process, it's necessary to filtering signals, define a sample time and analyze signals correlations in order to have correct signals to beginning the identification.

#### Signal corrections

To perform an identification, the signal must be filtered with different filters. Moreover, to keep the dynamical behavior between the filtered values, it's a paralleled filter which is applied between the manipulated and controlled variables. The different filters are :

- A high-pass filter with a turn-over pulsation  $\omega = 0rad/sec$  in order to remove the continuous component.
- A high-pass filter to remove the low-frequencies dues to the external environment (external temperature...) and not dues to the inputs.
- A low-pass filter to remove the noise. The turn-over pulsation must be superior of the input frequency in order not to loose information.

### Sampling time and Integrator

The sampling frequency can be reduced according to the dynamic of the process. Of course, the Shanon theorem has to be respected.

If the process contains integrators, it's possible to remove them by derivating the output signals to identify the process without them (a transfer function contains  $N$  integrators if there are  $N$  poles  $z = 1$  or  $p = 0$ ). It means that the process is not stable. The goal of this manipulation is to remove an eventual bias. If the process contains a pole equal to  $z = 1$ , the identification will not give a pole strictly equal to 1. Hence a bias is introduced, it's better to identify the process without the integrator (moreover the order of the model is reduced) and to add it later in multiplying the denominator of the transfer function by  $(1 - q^{-1})$ .

### Signal Analysis

After all signal post-processing, it's important to check the correlations of signals before the identification. HIDENT allows to calculate the correlations between the output and each input, correlations between the different inputs, the autocorrelations of all signals and to check all spectrums.

The correlation between 2 signals  $y$  and  $u$  represents the dependency between the value of  $y$  at the instant  $t$  and the value of  $u$  at the instant  $t - \tau$ . This relation is defined as :

$$R_{yu}(\tau) = E\{y(t) \cdot u(t - \tau)\} \simeq \frac{1}{N-1} \sum_{i=\tau}^N y(i) \cdot u(i - \tau) \quad (1.1)$$

The autocorrelation of a signal  $u$  represents the self-dependance of the signal between the instants  $t$  and  $t - \tau$ .

$$R_u(\tau) = E\{u(t) \cdot u(t - \tau)\} \simeq \frac{1}{N-1} \sum_{i=\tau}^N u(i) \cdot u(i - \tau) \quad (1.2)$$

As we said previously, all inputs have to be uncorrelated between themselves and their autocorrelations have to be more or less close to a white noise. The autocorrelation of a white noise is a Dirac impulsion, hence, it's a stationary signal (his autocorrelation function not depends of the time) and moreover, the knowledge of the signal value at the instant  $t$  does not bring any information about the value at the instant  $t + \tau$  : a white noise is completely uncorrelated. This signal doest not exist in the nature and can't be generated (his variance is infinite) but it can be approached by a disreet white noise generated numerically (Figure 1.2).

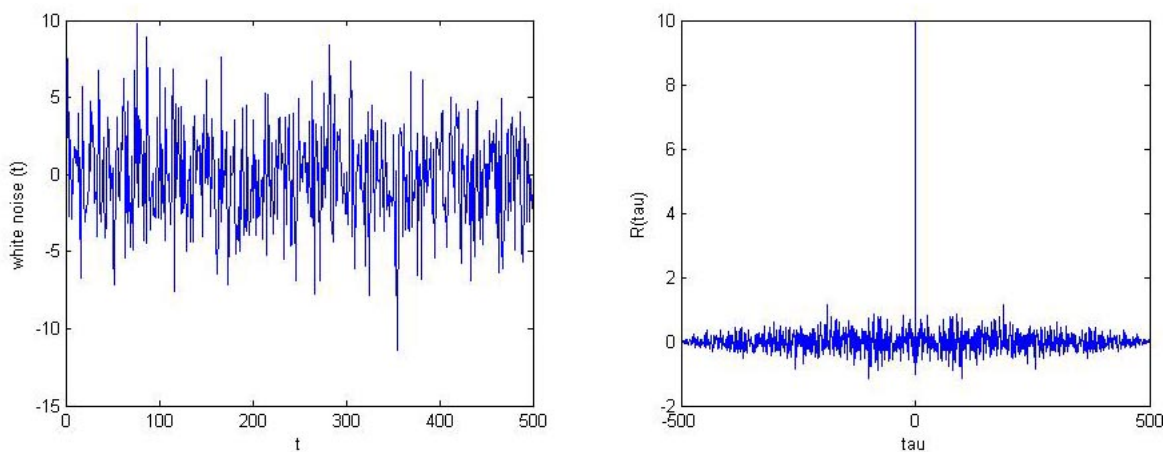


Figure 1.2: Discreet white noise simulated and its autocorrelation

Generally, a white noise can't be applied on a real process directly, because of the actuators, that's why we are using a PRBS signal (Figure 1.3). The autocorrelation of a PRBS is a weighted sum of Dirac impulsions. For a PRBS signal with a pseudo-period  $T$  and an amplitude between  $+a$  and  $-a$ , the autocorrelation of a PRBS is equal to  $R_{PRBS}(\tau) = a^2$  when  $\tau = k \cdot T$  and  $R_{PRBS}(\tau) = -\frac{a^2}{T}$  elsewhere. The advantages of a PRBS are multiple :

- The sum of the signal on one period is 1 and its average is near 0.
- Its autocorrelation is close to a discrete white noise
- The process can be permanently excited if the PRBS is well calculated.

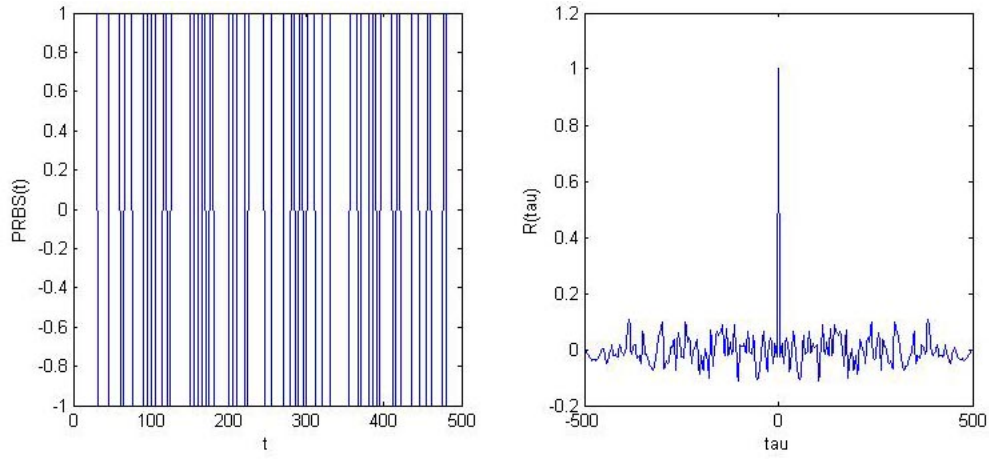


Figure 1.3: A PRBS signal and its autocorrelation

Now, it's important to know what are the different correlations between the input and output variables. In Open loop, the relation between inputs and outputs is :

$$y(t) = \sum_{i=1}^N h_i \cdot u(t-i) + v(t) \Leftrightarrow y(t) \cdot u(t-j) = \sum_{i=1}^N h_i \cdot u(t-i) \cdot u(t-j) + v(t) \cdot u(t-j) \quad (1.3)$$

Where the  $h_i$  are the coefficients of the impulse response. So, to calculate the correlation between  $y$  and  $u$  :

$$R_{yu}(j) = E \{y(t) \cdot u(t-j)\} = E \left\{ \sum_{i=1}^N h_i u(t-i) \cdot u(t-j) \right\} + E \{v(t) \cdot u(t-j)\} \quad (1.4)$$

Moreover :

$$E \left\{ \sum_{i=1}^N h_i \cdot u(t-i) \cdot u(t-j) \right\} = \sum_{i=1}^N h_i \cdot E \{u(t-i) \cdot u(t-j)\} = \sum_{i=1}^N h_i \cdot R_u(j-i) \quad (1.5)$$

In open-loop, the input  $u$  and the perturbation  $v$  are uncorrelated :  $E \{v(t) \cdot u(t-j)\} = R_{vu}(j) = 0$ . Finally we obtain :

$$R_{yu}(j) = \sum_{i=1}^N h_i \cdot R_u(j-i) \quad (1.6)$$

So, the output  $y$  is correlated to  $u$  in open-loop via the equation (1.6).

In close-loop,  $u$  can be correlated with  $v$  because of  $y$  which is dependent of  $u$  and  $v$  (Figure 1.4). So in close loop:  $E \{v(t) \cdot u(t-j)\} = R_{vu}(j) \neq 0$  and :

$$R_{yu}(j) = \sum_{i=1}^N h_i \cdot R_u(j-i) + R_{vu} \quad (1.7)$$

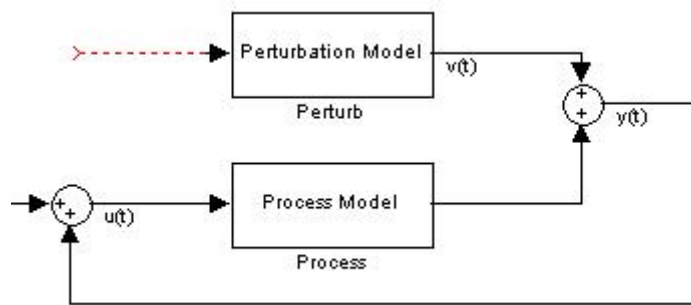


Figure 1.4: Model Structure in close-loop

## 1.2.2 Model types

There are a lot of different mathematical model types. A model can be regressive or not. A model is regressive when the output value at the instant  $t$ ,  $y(t)$ , depends on the previous values  $y(t-i)$ . Moreover, the model can include non measurable perturbation or noise  $\zeta(t)$ . In order to realize a predictive control, three main models are used :

- The pulse response
- The step response
- Transfer function in  $z$

In identification, the coefficients to find are generally put in a vector (or in a matrix with MIMO systems) called  $\theta$  and the observations of the system (previous values of inputs and outputs) in a vector (or in a matrix) called  $\phi(t)$ .

For a MIMO system,  $\Phi = [\varphi_1^T \ \cdots \ \varphi_n^T]^T$  for  $n$  outputs.

So, the system can be represented in a matrix equality :

$$y_m(t) = \phi \cdot \theta + \zeta(t) \quad (1.8)$$

### Pulse response

In this model, the model output  $y_m(t)$  depends on previous values of the different inputs and eventually of a noise  $\zeta(t)$ , for  $M$  inputs :

$$y_m(t) = \sum_{k=1}^M \sum_{i=1}^{\infty} h_{ki} \cdot u_k(t-i) + \zeta(t) \simeq \sum_{k=1}^M \sum_{i=1}^N h_{ki} \cdot u_k(t-i) + \zeta(t) \quad (1.9)$$

with a significative value of  $N$  according to the process. the coefficients  $h_i$  represent the pulse response of the process.

The different vectors in a SISO system are :

$$\begin{cases} \varphi = [ u(t-1) \ \cdots \ u(t-N) ]^T \\ \theta = [ h_1 \ \cdots \ h_N ]^T \end{cases}$$

### step response

The difference in the step response is that the output  $y_m$  depends on the variation of the input  $\Delta u = (1-q^{-1}) \cdot u$ , for  $M$  inputs :

$$y_m(t) = \sum_{k=1}^M \sum_{i=1}^N g_{ki} \cdot \Delta u_k(t-i) + \zeta(t) \quad (1.10)$$

and the coefficients  $g_i$  represent the step response of the process. The different vectors in a SISO system are :

$$\begin{cases} \varphi = [ \Delta u(t-1) \ \cdots \ \Delta u(t-N) ]^T \\ \theta = [ g_1 \ \cdots \ g_N ]^T \end{cases}$$

### Transfer function

There are different types of transfer functions according to the process. The first model which can be used is an ARX model (Auto Regressive with eXternal inputs). It's an auto regressive model containing a white noise  $\zeta(t)$  with a null average . Moreover the model includes a pure delay where  $k$  is the number (an integer) of sampling time ( $T$ ) representing the delay  $d = k \cdot T$ .

$$y(t) = q^{-k} \cdot \frac{B(q^{-1})}{A(q^{-1})} \cdot u(t) + \zeta(t) \quad (1.11)$$

Another model is the ARMAX (Auto Regressive Moving Average with eXternal inputs) model. It's a regressive model where the non measurable disturbances are assimilated to white noise  $\zeta(t)$  filtered by a transfer function with a moving average :

$$y(t) = q^{-k} \cdot \frac{B(q^{-1})}{A(q^{-1})} \cdot u(t) + \frac{T(q^{-1})}{A(q^{-1})} \cdot \zeta(t) \quad (1.12)$$

It's also possible to integrate the noise directly to obtain an ARIMAX model (or CARIMA model) :

$$y(t) = q^{-k} \cdot \frac{B(q^{-1})}{A(q^{-1})} \cdot u(t) + \frac{T(q^{-1})}{\Delta \cdot A(q^{-1})} \cdot \zeta(t) \quad (1.13)$$

$\Delta$  corresponds to the differential operator. The polynomial  $T(q^{-1})$  is often equal to 1 but can be different according to the noise model. This point will be explained later. The different vectors in a SISO system are :

$$\begin{cases} \varphi = [ y(t-1) & \cdots & y(t-N_1) & u(t-1) & \cdots & u(t-N_2) ]^T \\ \theta = [ a_1 & \cdots & a_{N_1} & b_1 & \cdots & b_{N_2} ]^T \end{cases}$$

### Model order

To proceed at the identification, the order of the model and the pure delay have to be known beforehand when the model is a transfer function and the number of samples retained for the step/impulse response too. For the pure delay, it's easy to find it during a step test in open-loop : it's the delay between the beginning of the step and the beginning of the process response. Concerning the order of  $A(q^{-1})$  and  $B(q^{-1})$ , there isn't law except the shape of the response and the experience. To choose the number of samples in the impulse/step response, a hundred of samples can be retained but it depends on the process velocity and on the sampling time.

### 1.2.3 Identification

The identification consists in finding all parameters  $\theta$  of the model from the measurements  $\phi$  to minimize the errors between the model output and the process output. The most used method to solve this problem is the Least Squares algorithm (LS). A recursive version also exists (RLS).

#### LS algorithm

The LS algorithm allows to minimize the function  $V$  which represents the sum of the quadratic errors  $\varepsilon^2$  :

$$V = \frac{1}{N} \sum_{k=1}^N \varepsilon^2 = \frac{1}{N} \sum_{k=1}^N (y(t) - y_m(t))^2 = \frac{1}{N} \sum_{k=1}^N (y(t) - \phi^T \cdot \theta)^2 \quad (1.14)$$

So, if the system to identify has a model  $y = \phi \cdot \theta$  (there isn't any noise or disturbance), the optimal  $\theta$  can be calculated with the pseudo-inverse of  $\phi$ :

$$\hat{\theta} = [\phi^T \cdot \phi]^{-1} \cdot \phi^T \cdot y \quad (1.15)$$

Of course,  $[\phi^T \cdot \phi]$  has to be invertible.

If the model is an ARX model (equation (1.11)), containing a white noise with a null average, the LS algorithm provides a consistent identification without any bias [CAR04] and the solution  $\hat{\theta}$  has the same expression. On the other hand, if the model is an ARMAX or ARIMAX model (see equations (1.12) and (1.13)), the solution will contain a bias because of the average of  $\frac{T(q^{-1})}{A(q^{-1})} \cdot \zeta(t)$  which is not null. To identify an ARIMAX model, the RELS algorithm has to be used. However, the solution can be more or less exact with the LS algorithm if the noise level is very weak (weak variance). The advantage of the LS algorithm is that it's fast to solve and so, can be used for real-time identification.

#### RLS algorithm

The RLS algorithm is the recursive algorithm of LS. So, the memory and the time of calculation are more important. It's not well adapted for a real-time identification but it's a performing algorithm for off-line identification. The algorithm is the following for each sampling time  $k$  [CAR04]:

$$\begin{cases} \hat{\theta}_k = \hat{\theta}_{k-1} + K_k \cdot \varepsilon_k \\ \varepsilon_k = (y_k - \hat{\theta}_{k-1}^T \cdot \varphi_k) \\ K_k = \frac{P_{k-1} \cdot \varphi_k}{1 + \varphi_k^T \cdot P_{k-1} \cdot \varphi_k} \\ P_k = P_{k-1} - \frac{P_{k-1} \cdot \varphi_k \varphi_k^T \cdot P_{k-1}}{1 + \varphi_k^T \cdot P_{k-1} \cdot \varphi_k} \end{cases}$$

$\hat{\theta}_k$  contains the parameters to identify,  $\varepsilon_k$  is the error between the real output and estimation calculated,  $K_k$  represents the adaptation gain Matrix which moves during the time and if the algorithm converges,  $K_k \mapsto 0$ .

There are other versions of the RLS which are modified. For example, it could be better to not take into account the first iterations of the algorithm in order to forget old values progressively. For this, a forget coefficient  $\lambda$  is inserted and the matrix  $P_k$  has become :  $P_k = \frac{1}{\lambda} \left[ P_{k-1} - \frac{P_{k-1} \cdot \varphi_k \varphi_k^T \cdot P_{k-1}}{1 + \varphi_k^T \cdot P_{k-1} \cdot \varphi_k} \right]$  with  $0 < \lambda \leq 1$ . When  $\lambda = 1$  it is the classical RLS algorithm but when  $\lambda \neq 1$ , the errors are weighted by a coefficient  $\lambda^{k-t}$ .

### RELS algorithm

The RELS algorithm (Recursive Extended Least Square) is also called PEM algorithm (Prediction Error Method). This algorithm allows to perform a consistent identification without any bias when the model is an ARMAX or ARIMAX model (see equations (1.12) and (1.13)). The principle of this method is to include the polynomial coefficients of  $T(q-1)$  of the noise in the vector  $\theta = [\hat{a}_i, \hat{b}_i, \hat{t}_i]$ . In consequence, we have to add in the observation vector  $\varphi$  the past values of the noise:

$$\varphi = [y(t-1) \cdots y(t-n), u(t-1) \cdots u(t-m), \zeta(t-1) \cdots \zeta(t-r)]^T \quad (1.16)$$

Of course, these values can't be measured, that's why this algorithm calculates the estimated noise  $\hat{\zeta}(t)$  thanks to the process model with a recursive relation (it's a predictor):

$$\hat{\zeta}(t) = y(t) + \sum_{i=1}^n \hat{a}_i \cdot y(t-i) - \sum_{i=1}^m \hat{b}_i \cdot u(t-i) - \sum_{i=1}^r \hat{t}_i \cdot \hat{\zeta}(t-i) \quad (1.17)$$

The final algorithm is the same as the RLS or the modified RLS algorithm but  $\theta$  and  $\varphi$  are augmented. Moreover the predictor  $\hat{\zeta}(t) = \varepsilon(t)$ .

### 1.2.4 Validation of the model

After having obtained a model, it's necessary to valid this model with different tests. The data used for the validation must be different from the data which have been used with the identification algorithm. If the data are the same, the validation is useless.

#### Qualitative verification

The first test is a visual verification checking if the model outputs have the same shape as the process outputs for different types of excitation at the input. Be careful, this test is necessary but not sufficient to validate the model.

#### Statistic tests

The error between the process output and the model output is called residue :  $\varepsilon(t) = y(t) - y_m(t)$ . This residue has to be close to a white noise with a null average and has to be uncorrelated with the different inputs. So it's necessary to calculate the average of the residue, its autocorrelation  $R_\varepsilon$  and its correlation with each input  $R_{\varepsilon u}$ .

#### Parameters distortion

The question is : How to change the parameters at an instant  $t$  to have a perfect model at this instant (*ie* : the residue is null) ? To be sure that the model obtained is a good model, the parameters calculated by the algorithm have to be not very distorted during the time to obtain a perfect model. It's a sign of credibility.



# Chapter 2

## Predictive control

Model Based Predictive Control (MBPC) or only predictive control is an advanced technique of control based on a process model. The principle of this technique is to predict, thanks to the model, the future outputs of the process. These predictions depend on the passed values (outputs and inputs) and on the future commands. An algorithm provides an adequate law of command which is optimal in order to follow a predefined trajectory to reach the set point until an horizon defined. This command is calculated according to constraints and minimizes a cost function (with quadratic or linear errors). Thus, feedback and feedforward disturbances can be anticipated and removed. The MBPC is an advanced control which can manage the basic control system of a system (Figure 2.1). Hence, after global steady state optimization which is defined each day and after a local optimization of the plant, the MBPC will provide (around every minute) set points and information to the classical dynamic control system (DCS) in taking account constraints and future responses of the process.

### 2.1 General feature

This technique was developed by Richalet in 1978[RIC78] and generalized in 1987 by Clarke[CLA87] in agreement with industrial groups (Shell and Adersa). The predictive control can be used with complex processes where a classical PID is insufficient. This technique is particularly interesting when processes have a long time delay and important measurable disturbances. The main users of this technology are the petroleum refineries, chemical and food industries, metallurgy, aerospace... The objectives of the predictive control are the following :

- Avoid range violations on inputs and outputs.
- Put manipulated variables to their optimal values.
- Avoid excessive variations of manipulated variables.
- Keep a robust system in case of disturbances or wrong operations (problems with actuators, signals...).

So, the predictive control allows a safety installation with an economic interest for the industry. It exists different kinds of predictive controls for linear and nonlinear systems. In this report, only the Generalized Predictive Control (GPC) based on the transfer functions and the Dynamic Matrix Control (DMC) based on the step responses will be treated for linear systems. We will describe briefly some techniques used for non-linear systems.

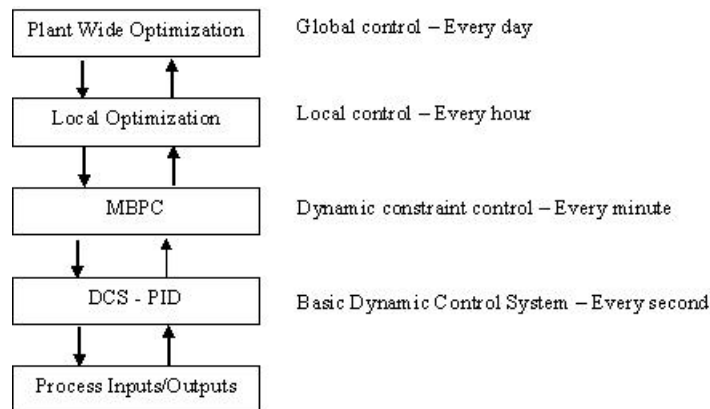


Figure 2.1: Typical global architecture with a MBPC

All MBPC techniques have to realize the same steps at each sampling time :

1. calculation of the future outputs  $\hat{y}(t + j)$  with the model for an horizon between  $N1$  and  $N2$
2. elaboration of a reference trajectory  $r(t + j)$
3. calculation of the future optimal commands  $u(t + j)$  to minimize errors according to a cost function until an horizon  $Nu$
4. Only the first element of this optimal command sequence is applied to the process, the others are rejected to be recalculated during the next sampling time : Receding Horizon Principle.

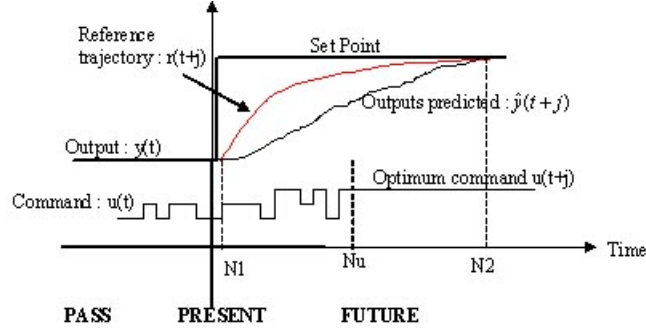


Figure 2.2: Temporal diagram of a typical MBPC

Then, the goal of the controller is to minimize a cost function. This function contains predictive quadratic errors of each controlled variable  $(\hat{y}_k - r_k)^2$  and the increments of each manipulated variable  $(\Delta u_k)^2$ . The equation (2.1) represents this cost function  $J$  for a MIMO model where  $k$  is the index of each controlled and manipulated variable (there are  $n$  controlled variables and  $m$  manipulated variables ). The tuning parameters are the following:

- $N1_k, N2_k$  : minimum and maximum horizons of the controlled variable  $y_k$ . The output has to follow the reference trajectory in this time interval. So,  $N1$  must be superior of the process delay.
- $Nu_k$  : control horizon of the manipulated variable  $u_k$
- $\gamma_k$  : weight of each controlled variable  $y_k$
- $\beta_k$  : weight of each manipulated variable  $u_k$

$$J = \sum_{k=1}^n \left( \sum_{j=N1_k}^{j=N2_k} \gamma_k (y_k(t+j) - r_k(t+j))^2 \right) + \sum_{k=1}^m \left( \sum_{j=1}^{j=Nu_k} \beta_k (\Delta u_k(t+j-1))^2 \right) \quad (2.1)$$

The reference trajectory have to be known beforehand. Generally this trajectory begins from the actual value of the output to reach the set point asymptotically. A coefficient  $\alpha$  allows to smooth the trajectory :  $r(t + j) = \alpha \cdot r(t + j - 1) + (1 - \alpha) \cdot r^\infty$  where  $r^\infty$  represents the set point to reach(Figure 2.3).

The internal architecture of a MBPC block is represented in the figure 2.4. In order to calculate predicted outputs the models need to know future inputs which are calculate thanks to an optimization program. This program take into account the cost function and the different constraints to respect. These different points will be explain later.

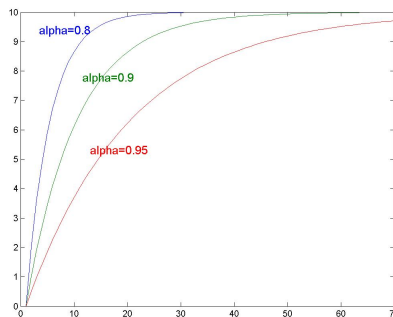


Figure 2.3: Smoothing of the reference trajectory  $r(t)$  according to  $\alpha$

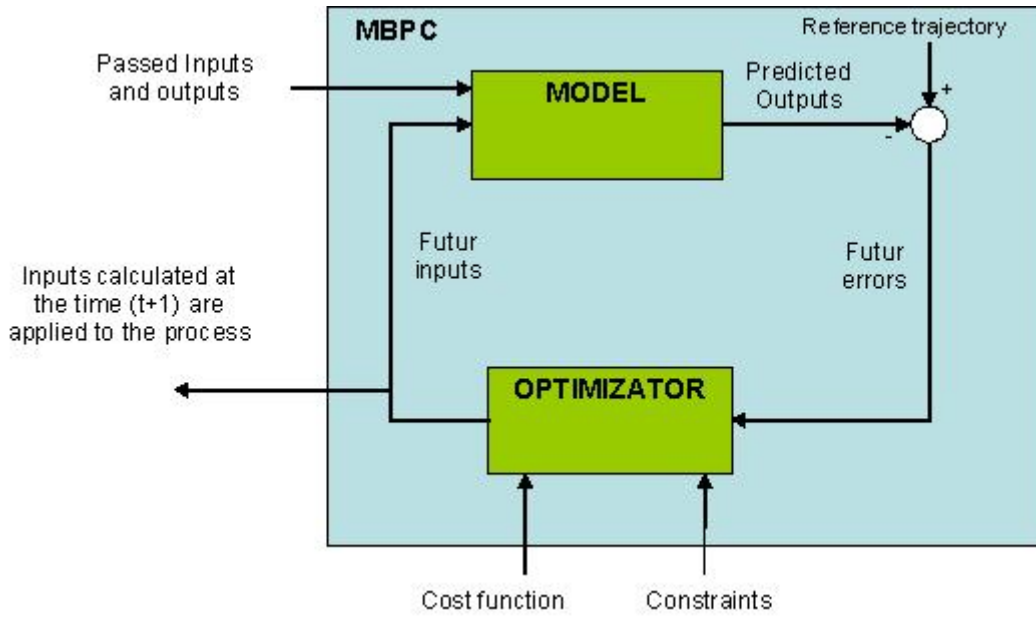


Figure 2.4: MBPC internal architecture

## 2.2 Model and Predictions

### 2.2.1 Generalized Predictive Control (GPC)

#### Model with GPC

The GPC controller uses a prediction based upon transfer functions based on a CARIMA (also called ARIMAX) model :

$$A(q^{-1}) \cdot y(t) = B(q^{-1}) \cdot u(t) + D(q^{-1}) \cdot v(t) + \frac{T(q^{-1})}{\Delta} \cdot \zeta(t) \quad (2.2)$$

This method can be used for SISO or MIMO systems. This model takes measurable disturbances  $v(t)$  and a stochastic white noise non-stationary  $\zeta(t)$  into account. For MIMO system with  $n$  controlled variables,  $m$  manipulated variables and  $\ell$  disturbances, the dimensions of matrix are :

- $y(t)$ ,  $u(t)$ ,  $v(t)$ ,  $\zeta(t)$  are vectors with a respective size of  $[n \times 1]$ ,  $[m \times 1]$ ,  $[\ell \times 1]$ ,  $[n \times 1]$
- $A$  and  $B$  are matrix  $[n \times n]$  and  $[n \times m]$
- $T$  is a diagonal matrix  $[n \times n]$  and  $T = \sigma^2 \cdot I_{n \times n}$  where  $\sigma^2$  is the variance of the white noise

#### Predictions with GPC

After having defined the process model, the cost function and the reference trajectory, the calculation of the predictions  $\hat{y}(t+j)$  are necessary. We use the principle of decomposition for linear systems to calculate the predictions :

$$\hat{y}(t+j) = y_{free}(t+j) + y_{forced}(t+j) \quad (2.3)$$

The free response  $y_{free}$  correspond to the system response when  $\Delta u(t+j) = 0 \forall j \geq 0$ . The forced response  $y_{forced}$  is the additional component according to the future command  $u(t+j)$  which will be applied in the future.

From the CARIMA model (2.2), disturbance terms  $v(t)$  can be injected in the inputs  $u(t)$  to simplify the writing. So, at the instant  $(t+j)$  the output have for expression :

$$y(t+j) = \frac{B}{A} u(t+j-1) + \frac{T}{\Delta A} \zeta(t+j) \quad (2.4)$$

Then, it's necessary to separate passed and future terms of  $\zeta$ , so we decompose  $\frac{T}{\Delta A}$  :

$$\frac{T}{\Delta A} = E_j + q^{-j} \frac{F_j}{\Delta A} \quad (2.5)$$

$E_j$  and  $F_j$  are two polynomials and  $E_j$  has a degree  $(j-1)$ . This polynomials are the solution of the Diophantine equation  $T = E_j \cdot A\Delta + q^{-j} \cdot F_j$  [BIT90].

In injecting (2.5) in (2.4) we obtain :

$$y(t+j) = \frac{B}{A}u(t+j-1) + E_j\zeta(t+j) + q^{-j}\frac{F_j}{\Delta A}\zeta(t) \quad (2.6)$$

Then, the actual value of  $\zeta(t)$  can be calculate directly from (2.2) :

$$\zeta(t) = \frac{(A \cdot y(t) - B \cdot u(t-1)) \cdot \Delta}{T} \quad (2.7)$$

After replacing  $\zeta(t)$  by (2.7) in (2.6), we obtain the following equation :

$$y(t+j) = \frac{BE_j}{T}\Delta u(t+j-1) + \frac{F_j}{T}y(t) + E_j \cdot \zeta(t+j) \quad (2.8)$$

We use the same technique as previously to separate passed and future terms of  $\frac{BE_j}{T}$  resolving the Diophantine equation  $E_jB = CG_j + q^{-j}H_j$  [BIT90]:

$$\frac{BE_j}{T} = G_j + q^{-j}\frac{H_j}{T(q^{-1})} \quad (2.9)$$

In injecting (2.9) in (2.8) we have :

$$y(t+j) = G_j \cdot \Delta u(t+j-1) + \frac{H_j}{T}\Delta u(t-1) + \frac{F_j}{T}y(t) + E_j \cdot \zeta(t+j) \quad (2.10)$$

Here, there is still a term  $E_j\zeta(t+j)$  which is independent of all measurements. Therefore, the optimal prediction  $\hat{y}(t+j)$  of  $y(t+j)$  to minimize the error variance is given deleting the term  $E_j\zeta(t+j)$ . We have finally :

$$\hat{y}(t+j) = G_j \cdot \Delta u(t+j-1) + \frac{H_j \cdot \Delta u(t-1) + F_j \cdot y(t)}{T} \quad (2.11)$$

In the equation (2.11), the free and forced responses are separated. The first part of the equation represents the forced response which depends on the futures inputs  $\Delta u(t+j-1)$ . The free response is the second part which depends on the actual values of the output  $y(t)$  and on the last change of the manipulated value  $\Delta u(t-1)$ .

## 2.2.2 Dynamic Matrix Control (DMC)

### Model with DMC

The particularity of the DMC controller is that it uses the step response model. If we take into account a controlled variable  $y$ , a manipulated variable  $u$ , a measurable disturbance  $v$  and a non-measurable disturbance  $\zeta$ , the model is :

$$y(t) = \sum_{i=1}^{\infty} g_i \cdot \Delta u(t-i) + \sum_{i=1}^{\infty} d_i \cdot \Delta v(t-i) + \zeta(t) \quad (2.12)$$

The  $g_i$  coefficients represent the step response ( $\Delta u = 1$ ) of the controlled variable and the  $d_i$  coefficients are the step response of the measurable disturbance.

### Predictions with DMC

From the equation (7.2) we can calculate the prediction of the process at the instant  $t+j$  :

$$\hat{y}(t+j) = \sum_{i=1}^{\infty} g_i \cdot \Delta u(t-i+j) + \sum_{i=1}^{\infty} d_i \cdot \Delta v(t-i+j) + \zeta(t+j) \quad (2.13)$$

If we separate the past term and the future term :

$$\hat{y}(t+j) = \sum_{i=1}^j g_i \cdot \Delta u(t-i+j) + \sum_{i=j+1}^{\infty} g_i \cdot \Delta u(t-i+j) + \sum_{i=1}^j d_i \cdot \Delta v(t-i+j) + \sum_{i=j+1}^{\infty} d_i \cdot \Delta v(t-i+j) + \zeta(t+j) \quad (2.14)$$

There isn't any model to know  $\zeta(t+j)$ , hence the DMC approach supposes that  $\zeta(t+j) = \zeta(t)$ , so we can say according to (7.2) that :

$$\zeta(t+j) = \zeta(t) = y(t) - \sum_{i=1}^{\infty} g_i \cdot \Delta u(t-i) - \sum_{i=1}^{\infty} d_i \cdot \Delta v(t-i) \quad (2.15)$$

So, if we replace  $\zeta(t+j)$  by (2.15) in (2.14) we have :

$$\hat{y}(t+j) = \sum_{i=1}^j g_i \cdot \Delta u(t-i+j) + p_j \quad (2.16)$$

and the term  $p_j$  represents the free response of the system [PRA05]:

$$p_j = y(t) + \sum_{i=j+1}^{\infty} g_i \cdot \Delta u(t-i+j) + \sum_{i=1}^j d_i \cdot \Delta v(t-i+j) + \sum_{i=j+1}^{\infty} d_i \cdot \Delta v(t-i+j) - \sum_{i=1}^{\infty} g_i \cdot \Delta u(t-i) - \sum_{i=1}^{\infty} d_i \cdot \Delta v(t-i) \quad (2.17)$$

The term  $p_j$  can be rewritten as :

$$p_j = y(t) + \sum_{i=j+1}^{\infty} (g_{j+i} - g_i) \cdot \Delta u(t-i) + \sum_{i=1}^{\infty} (d_{j+i} - d_i) \cdot \Delta v(t-i) + \sum_{i=1}^j d_i \cdot \Delta v(t+j-i) \quad (2.18)$$

The infinite sums can be reduced at a number enough high  $N$  where the coefficients  $g_{i+1} \simeq g_i$  if the system is stable :

$$p_j = y(t) + \sum_{i=j+1}^N (g_{j+i} - g_i) \cdot \Delta u(t-i) + \sum_{i=1}^N (d_{j+i} - d_i) \cdot \Delta v(t-i) + \sum_{i=1}^j d_i \cdot \Delta v(t+j-i) \quad (2.19)$$

## 2.3 Calculation of the optimal control

The future sequence of the manipulated variable  $u(t+j)$  is calculated in order to minimizing the cost function (2.1) following as much as possible the reference trajectory  $r(t+j)$ . For a SISO system ( $n = 1$  and  $m = 1$ ), the cost function (2.1) can be written in matrix equality :

$$J = (G \cdot \Delta u + y_{free} - r)^T \cdot (G \cdot \Delta u + y_{free} - r) + \Delta u^T \cdot \Delta u \quad (2.20)$$

where :

- the Matrix  $G$  contains the impulse response coefficients  $\{g_i\}$  of the transfer function  $\frac{B}{\Delta A}$  :

$$G = \begin{bmatrix} g_{N1-1} & \cdots & g_0 & 0 & \cdots & 0 \\ g_{N1} & g_{N1-1} & \cdots & \ddots & \cdots & 0 \\ \vdots & \vdots & \ddots & \ddots & \ddots & \vdots \\ g_{Nu-1} & g_{Nu-2} & g_{Nu-3} & \cdots & \cdots & g_0 \\ \vdots & \vdots & \vdots & \vdots & \vdots & \vdots \\ g_{N2-1} & g_{N2-2} & g_{N2-3} & \cdots & \cdots & g_{N2-Nu} \end{bmatrix}$$

- the vector  $y_{free} = [y_{free}(t+N1), y_{free}(t+N1+1), \dots, y_{free}(t+N2)]^T$  which represents the free response calculated previously
- the vector  $r = [r(t+N1), r(t+N1+1), \dots, r(t+N2)]^T$  which represents the reference trajectory
- the vector  $\Delta u = [\Delta u(t), \Delta u(t+1), \dots, \Delta u(t+N2-1)]^T$  the increment of the manipulated variable.

The unconstrained optimal control is then, according to [BIT90] :

$$(\Delta u(t), \Delta u(t+1), \dots, \Delta u(t+N2-1))^T = (G^T \cdot G + I)^{-1} \cdot G^T \cdot (r - y_{free}) \quad (2.21)$$

Then, for the implementation of the manipulated variable :  $u(t) = u(t-1) + \Delta u(t)$ . Only the first component is applied on the system and everything is recalculated during the next sampling time (receding horizon). The equation (2.21) is an analytical optimal solution when constraints are not taking into account. The fact to calculate the optimal control by this way and to take the nearest solution if constraints are not respected is not a good solution, and it isn't the optimal control solution.

## 2.4 Constraints on variables

To provide an optimal control with constraints, it's necessary to take into account these constraints before and calculate the optimal control solution with an algorithm of optimization.

All manipulated and controlled variables have natural *physical constraints* which are never exceeded for physical reasons and a process also has *operation constraints* to respect during a right operation. These limits can be exceed punctually in penalizing the cost function. The main constraints generally used are the following :

- Constraint on the velocity of the manipulated variable between two sampling time for  $j = 0..N_u - 1$ :

$$\Delta u_{min} \leq \Delta u(t+j) \leq \Delta u_{max} \quad (2.22)$$

- Constraint on the value of the manipulated variable for  $j = 0..N_u - 1$ :

$$u_{min} \leq u(t+j) = u(t-1) + \sum_{i=1}^j \Delta u(t+i) \leq u_{max} \quad (2.23)$$

- Constraint on the value of the controlled variable for  $j = N_3..N_4$  where the interval  $[N_3, N_4] \subset [N_1, N_2]$  represents the constraint interval:

$$y_{min} \leq \hat{y}(t+j) = \sum_{i=1}^j g_i \cdot \Delta u(t-i+j) + p_j \leq y_{max} \quad (2.24)$$

Theses three constraints are lineal with  $\Delta u$  and the goal is to find a  $\Delta u$  to minimize the cost function (2.25) which is a quadratic function in  $\Delta u$ .

$$J = \sum_{k=1}^n \left( \sum_{j=N_{1k}}^{j=N_{2k}} \gamma_k (y_k(t+j) - r_k(t+j))^2 \right) + \sum_{k=1}^m \left( \sum_{j=1}^{j=N_{u_k}} \beta_k (\Delta u_k(t+j-1))^2 + \sum_{j=1}^{N_{u_k}} \beta_{1k} (u_k(t+j-1))^2 \right) \quad (2.25)$$

This problem is a quadratic programming problem. The optimal  $\Delta u$  can be found numerically by an algorithm of optimization. This optimization problem has to be solved at every sampling time. In MBPC, sampling time are generally around the minute which is largely sufficient with actual computers.

## 2.5 Feasibility of control

Reach a specific set point in respecting all constraints is not always realizable. That's why it's important to study the feasibility in order to know if a solution  $\Delta u$  exists in respecting all constraints. If any solutions exists, operation constraints have to be changed punctually to reach the set point. As there are several constraints on different variables, it's necessary to define priorities between each variables and between each constraints inserting penalty terms [RAW99]. It's also possible to move the constraint interval  $[N_3, N_4]$  to solve the problem.

Moreover, the introduction of constraints with a feasible politic can introduce instabilities in close-loop. Generally, when there is a non feasible situation, the system is unstable, that's why it's necessary to study the stability in order to find a feasible situation [MOR95].

Part II

Communicating tanks

# Chapter 3

## Identification of 2 communicating tanks

This chapter consists in identifying a system composed of two communicating tanks with a Matlab toolbox named HIDDEN. The mathematical model found will be used later in a predictive control. After a description of the model, the identification will be performed and finally, the model will be validated by different tests.

### 3.1 Process Description

This process named "Two communicating tanks" is constituted of different elements (Figure 3.1):

- 2 plastic cylinders representing the 2 tanks  $T_1$  and  $T_2$
- 2 electro-valves  $V_1$  and  $V_2$ . The valve  $V_1$  allows to fill in the tank  $T_1$  and the valve  $V_2$  allows to fill in the tank  $T_2$ .
- 2 manual valves on each tank which allow to drain each tank.
- 1 manual valve between the two tanks which allows a communication between both. The 3 manual valves are at the same level.
- 2 capacitive level sensors measuring the level of each tank. The data are transmitted to the computer via level transmitters.
- 2 amplifiers 5Vdc/24Vdc to control the electro-valves via the computer

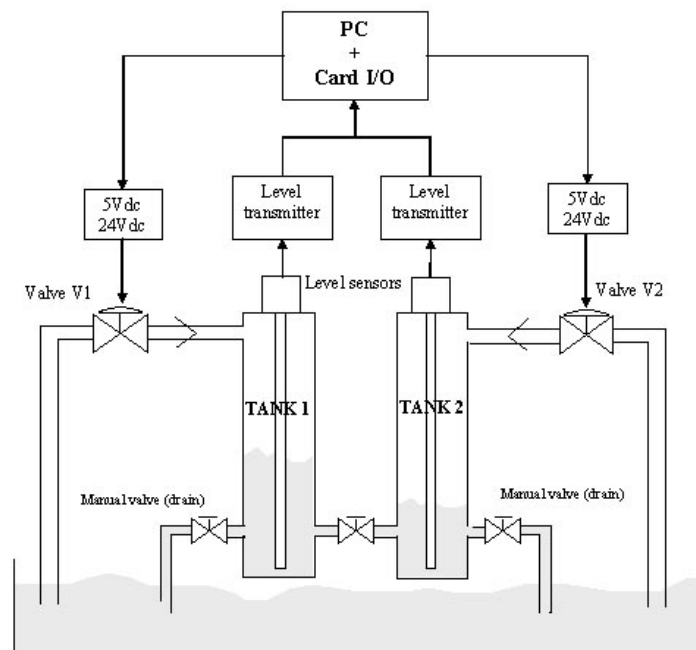


Figure 3.1: Schema of the 2 communicating tanks



Each tank can operate between 0% and 100% of its total volume and valves are working between 0% and 100%. During a normal operation, the three manual valves are opened and the goal is to control the level of the two tanks thanks to the two electro-valves. Hence, the different variables of the system and their operation limits are the following :

- Inputs : position of each valve  $V_1$  and  $V_2$ . Operation range between 0% and 90%, the operating point is 60%.
- Outputs : levels of the tanks  $L_{T1}$  and  $L_{T2}$  : operation range between 10% and 60%, operating point around 40%.
- Disturbances : positions of the three manual valves which are non-measurable (Open/Close or in semi position).

## 3.2 Identification

### 3.2.1 Test protocol

In order to proceed to the identification, we have to select two signals to apply on the the two electro-valves. According to what has been said in the previous chapter, two uncorrelated PRBS will be chosen (Figure 3.2). These signals are generated by the prbs function of MATLAB. To have a linear model, it's necessary to excite the process around its operating point. Moreover the valves have to be controlled with average values because they have non-linearities near their limits. So, the PRBS signals will have an average of 60%. The amplitudes of the two signals are fixed at 10%. In this case, the levels of the tanks are moving around the operating point of the process.

The process takes about 4 minutes to reach its stable state when the input is a step of 10%. So, in the PRBS signals, the highest time without step is 5 minutes and the shortest time is 5 seconds. These parameters allow to have a permanent excitation of the process and to explore all frequencies of the system. The time of the experience has been fixed at 30 minutes to have relevant measures and the sampling time is 0.5 second to appreciate the dynamic of the system and minimizing the data, hence we proceed to 3600 measurement points.

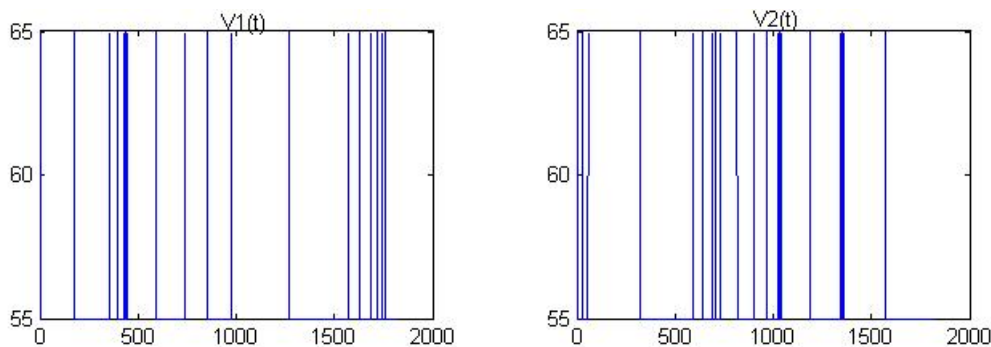


Figure 3.2: signals applied on the two valves

### 3.2.2 Signal post-processing with HIDEN

As our signals haven't a null average, the first step is to remove the continuous component of all signals. For this, we use a high-pass filter with a turn-over pulsation  $\omega = 0rad/sec$ .

Then, it's necessary to remove the noise of signals with a low-pass filter. The turn-over pulsation is chosen at  $\omega = 1.5rad/sec$  to preserve the dynamic of the system and remove high frequencies disturbances.

After these signal treatments, we check that the signals are well conditioned to proceed to the identification. For this, the correlations between inputs have to be low and the autocorrelations of each input have to be close to a white noise. HIDEN provides us the calculation of all correlations and calculates the limits not to exceed. On the Figure 3.3, the correlations between the two inputs are represented on the left by sampling time period. The two blue lines represent the limits of correlation not to exceed to have a consistent identification. Moreover, the autocorrelation of each inputs is close to a white noise (Figure 3.3 on the right), so these two signals are appropriate to perform a reliable identification.

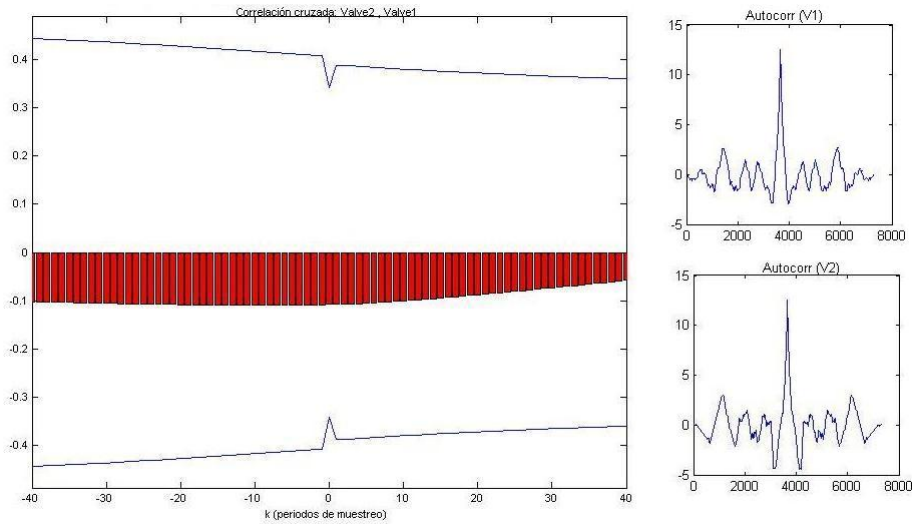


Figure 3.3: Inter correlation between the 2 PRBS and their autocorrelation

### 3.2.3 Identification with HIDENT

The first step to do is to select a model type and its characteristics. HIDENT allows to obtain different types of mathematical models (transfer functions, step/impulse responses, frequency responses). To identify the two tanks we will choose AR (Auto Regressive) transfer functions. So, there isn't any noise model and the LS and RLS algorithm can be used in this case. A priori the order of the model is unknown but we will begin with a numerator of the zero order and a denominator of the first order with a delay of one sampling time (0.5s). There are two inputs ( $V_1$  and  $V_2$ ) and two outputs ( $L_{T1}$  and  $L_{T2}$ ), so, there are four transfer functions. Each transfer function relative to the same output has the same denominator:

$$\left\{ \begin{array}{l} \frac{L_{T1}}{V_1} = q^{-1} \cdot \frac{a_{10}}{1+b_{11} \cdot q^{-1}} \\ \frac{L_{T1}}{V_2} = q^{-1} \cdot \frac{a_{20}}{1+b_{11} \cdot q^{-1}} \\ \frac{L_{T2}}{V_1} = q^{-1} \cdot \frac{a_{30}}{1+b_{21} \cdot q^{-1}} \\ \frac{L_{T2}}{V_2} = q^{-1} \cdot \frac{a_{40}}{1+b_{21} \cdot q^{-1}} \end{array} \right. \quad (3.1)$$

Then, an algorithm has to be chosen to obtain the parameters. The LS algorithm will be chosen for beginning. HIDENT provide us the following results about this identification thanks to the LS algorithm:

$$\left\{ \begin{array}{l} a_{10} = 0.0150 \\ a_{20} = 0.0121 \\ b_{11} = -0.986 \\ a_{30} = 0.0128 \\ a_{40} = 0.0133 \\ b_{22} = -0.9881 \end{array} \right. \quad (3.2)$$

These parameters not change if the RLS algorithm is used. If the order is higher, errors between models and process values are the same. So, the LS algorithm and a transfer function of the first order is sufficient and allow to minimize the calculation time and the data.

At first view, the model outputs follows the real outputs (Figure 3.4). Then an analysis of residues is necessary. Residues are errors between model and process :  $r_1(t) = y_{m1}(t) - y_{LT1}(t)$  and  $r_2(t) = y_{m2}(t) - y_{LT2}(t)$ . To estimate the value of residues, it's possible to calculate the Final Predicted Error(FPE) :  $FPE = \frac{1}{N} \cdot \frac{1+d/N}{1-d/N} \sum_{t=1}^N (y(t) - y_m(t))^2$  where  $d$  is the number of parameters estimated and  $N$  the number of samples. About  $r_1$  and  $r_2$  :  $FPE_{r1} = 1.07$  and  $FPE_{r2} = 1.21$ . These coefficients represent the average value of the quadratic error in absolute value. They allow to provide a confidence on the results.

Moreover, residues and inputs are uncorrelated (Figure 3.5). Now, we have to validate the model with other measurements. These first observations just tell us that the identification algorithm was efficient.

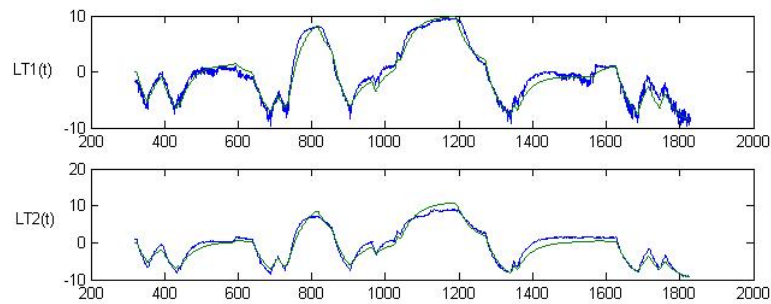


Figure 3.4: Process and model outputs

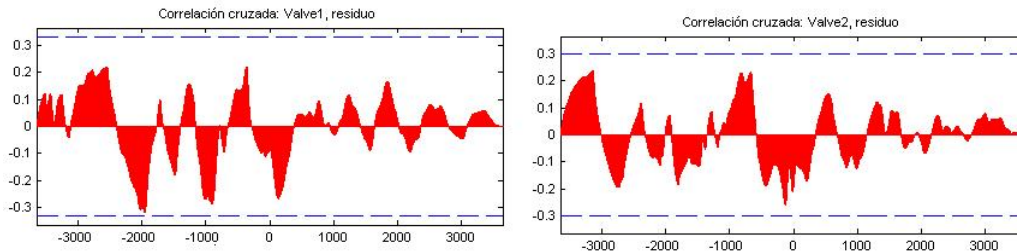


Figure 3.5: Correlation between residue and inputs

### 3.3 Validation of the model

In order to check the model, we will use three validation tests with other measurements that measurements used for the identification.

The figure 3.6 represents all responses of each validation test and the table 3.1 contains the Final Predicted Error of each test. All process responses follow more or less outputs calculated by the model found. Errors at the beginning of the simulation are due to the initial values, so they are not significant. The Final Predicted Errors are generally under 1, it means that the quadratic error on the tank level 1 or 2 is acceptable (The level calculated is exact at more or less 1%).

	$FPE_{LT1}$	$FPE_{LT2}$
Valid 1	1.6	0.97
Valid 2	0.58	0.72
Valid 3	0.62	0.66

Table 3.1: Final Predicted Errors

Moreover, we have to check that residues are not correlated to the inputs. If a correlation between both is too important, it means that the model found by identification contains a bias. The figures 3.7 and 3.8 show these correlations about the residues  $r_1$  and  $r_2$ . The main part of the correlations stay between the limits to not exceed (the two blue lines). The correlations can exceed these limits slightly very punctually.

In order to evaluate the robustness of the model and its range of validity, we can make an "extreme" test, out of the operating range with values between 0% and 100% on the two valves where the process is non-linear. The figure 3.9 show this test. The global behavior of the model is right but errors are more important. The Final Predictor Error of the residue  $r_1$  is equal to 6.1 and the FPE of  $r_2$  equal to 19.96. So, errors are more important but residues are well uncorrelated with inputs (figure 3.10).

This model have to be used for a predictive control. So, a good test is to compare during a predictive control experience, the difference between outputs measured on the process and outputs calculated thanks to the model. The figure 3.11 shows this test and the error of prediction stay between  $\pm 1\%$ . The average of the quadratic error is 0.30% on the tank level 1 and 0.19% on the tank level 2.

All these tests provide us an appreciation about the model found by the identification. There isn't a perfect proof to demonstrate the validity of a model but thanks to these positive tests, we can be confident in this model.

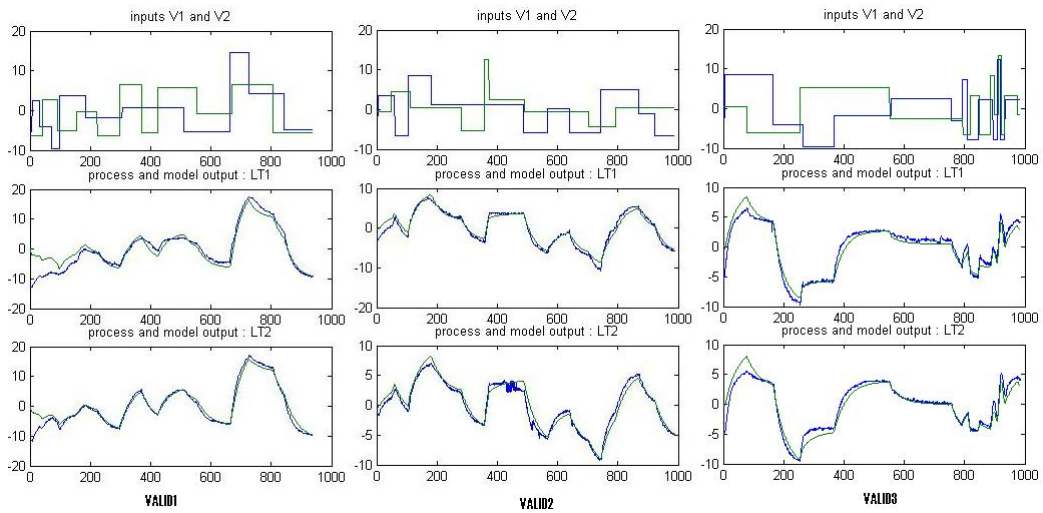


Figure 3.6: Process/model Inputs and outputs for each validation test

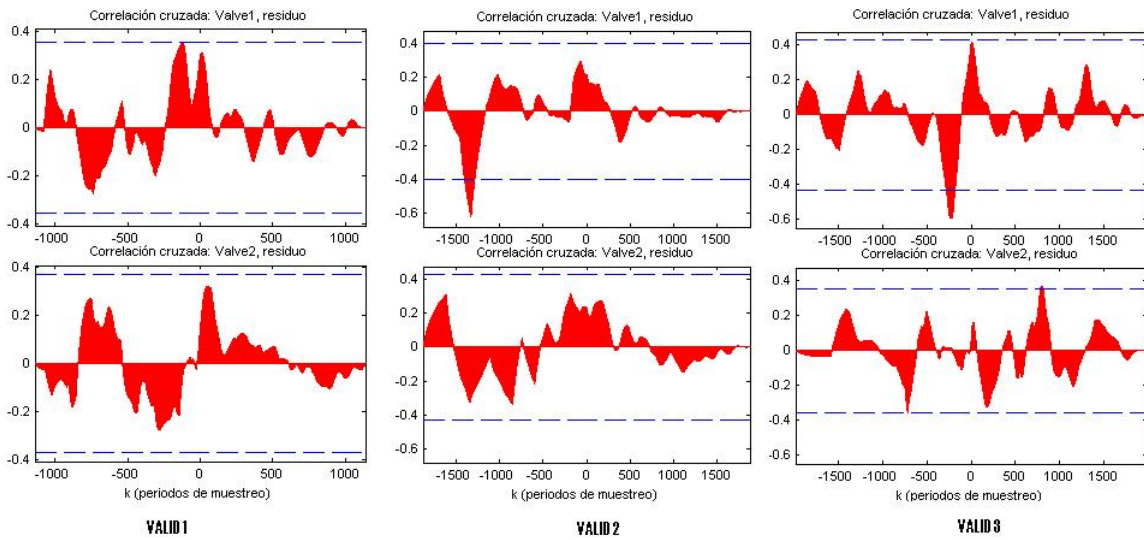


Figure 3.7: Correlations between residue  $r_1$  and inputs for each validation test

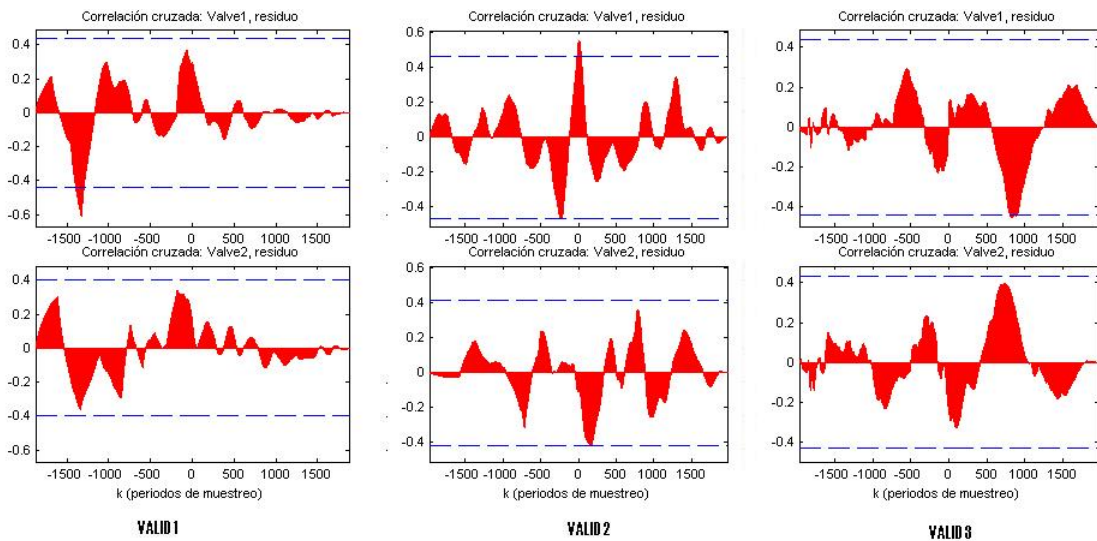


Figure 3.8: Correlations between residue  $r_2$  and inputs for each validation test

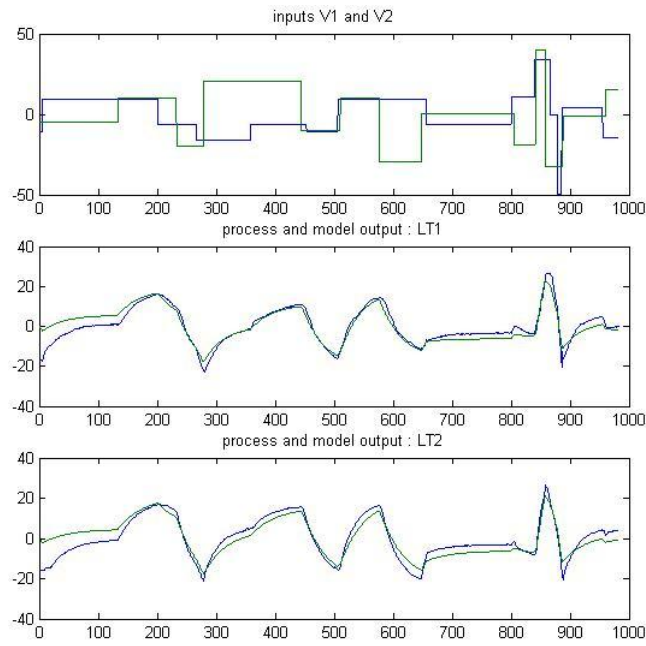


Figure 3.9: Process/Model inputs and outputs during "extreme" test

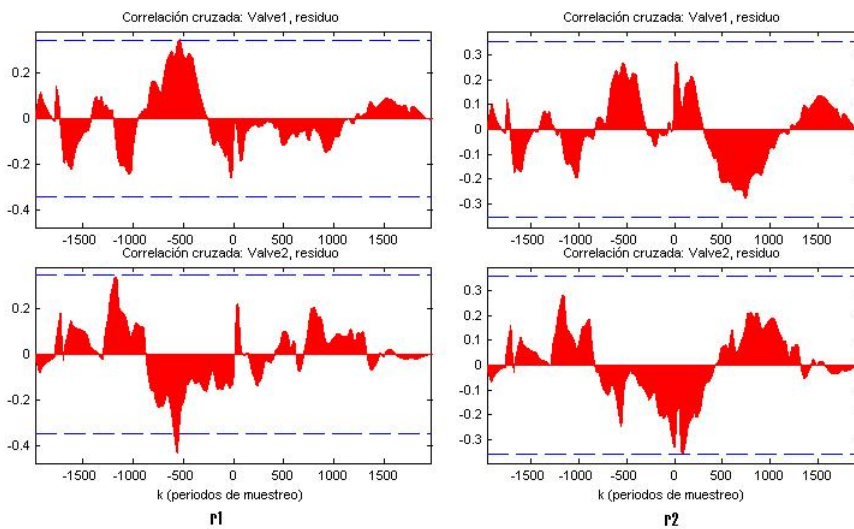


Figure 3.10: Correlations between residues and inputs during "extreme" test

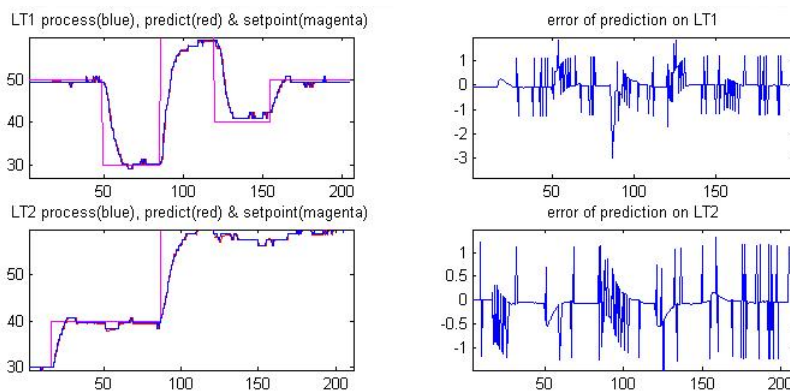


Figure 3.11: tank levels (measured and calculated) during a predictive control

# Chapter 4

## Identification of 4 communicating tanks

The goal of this chapter is to identify a system composed of four communicating tanks to a parametrical method. The interest of this identification is to perform later a predictive control using this mathematical model. After a description of the plant, the identification will be performed with the Matlab toolbox HIDENT. Then, the model will be validated by different tests.

### 4.1 Process description

This process, named "Four communicating tanks", is constituted of the same elements than the two communicating tanks but two tanks are added (Figure 4.1). There are two main tanks  $T_1$  and  $T_2$  and two intermediate tanks  $T_3$  and  $T_4$ . The valve  $V_1$  allows to fill in the the tank  $T_2$  via the intermediate tank  $T_4$ . The valve  $V_2$  allows to fill in the tank  $T_1$  via the intermediate tank  $T_3$ . The diameters of the tubes between intermediate tanks and main tanks are smaller than diameters of tubes which are between electro-valves and intermediate tanks.

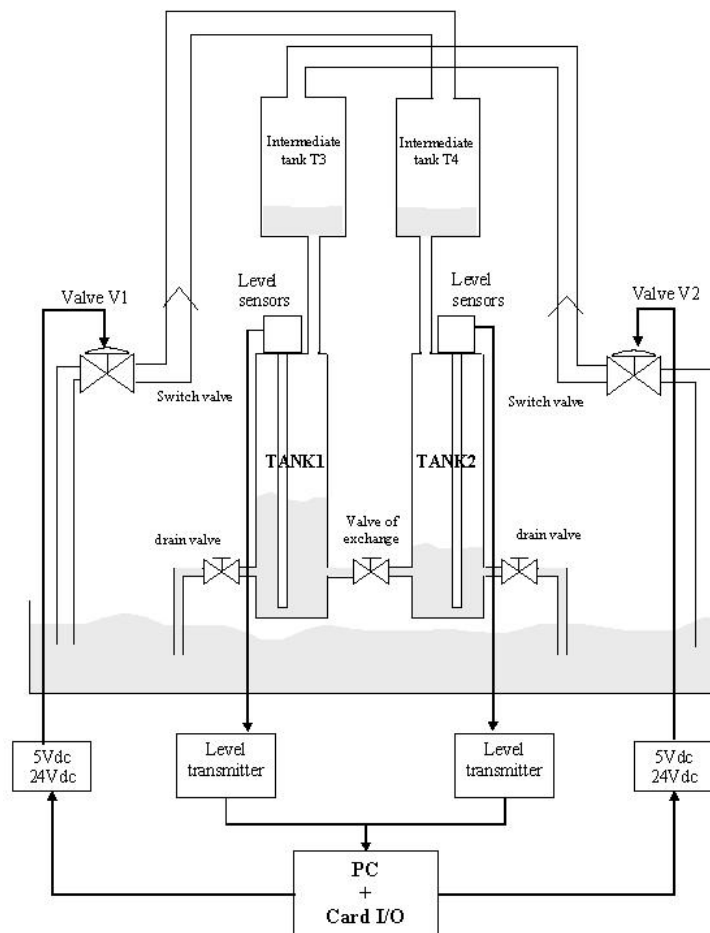


Figure 4.1: Schema of the 4 communicating tanks

Inputs, outputs and disturbances are the same than in the two communicating tanks (see chapter 3). The main difference with the previous process is that intermediate tanks introduces a new delay. The flow between intermediate and main tanks is much smaller than flow of electro-valves, this flow depends on the levels of liquid in intermediate tanks (which are not measured), not on the flow of the valves (which are measured). Moreover, intermediate tanks are much smaller than main tanks and the incoming flow is higher, so they are filled more rapidly. Hence, constraints are different because intermediate tanks must not overflow : if  $V_1$  works above 55% the intermediate tank  $T_4$  overflows and if  $V_2$  works above 60% the intermediate tank  $T_3$  overflows. The operating point is different because of this. New operating point and constraints are the following :

- Inputs : valves  $V_1$  and  $V_2$  : operation limits between 0% and 60% and the operating point is fixed respectively at 55% and 50%.
- Outputs : levels of the tanks  $L_{T1}$  and  $L_{T2}$  : operation limits between 10% and 40%, operating point around 20%.

## 4.2 Identification

The procedure of identification and input signals are the same than in the chapter 3 but the average of inputs have to be equal to the operating point (55% for  $V_1$  and 50% for  $V_2$ ), so the PRBS signal used for the identification will be composed of steps of 10% between 50% and 60%. However, the order of the model will be much higher and the delay of this system is important.

The first step is to determine the delays thanks to step responses. The figure 4.2 shows responses of the process with a step on  $V_1$  (1<sup>st</sup> column) and on  $V_2$  (2<sup>nd</sup> column). The different delays measured are the following ( $\Delta$  represents the sampling time of acquisition : 2s):

- Delay between  $V_1$  and  $L_{T1}$  :  $4s = 2\Delta$
- Delay between  $V_1$  and  $L_{T2}$  :  $4s = 2\Delta$
- Delay between  $V_2$  and  $L_{T1}$  :  $12s = 6\Delta$
- Delay between  $V_2$  and  $L_{T2}$  :  $12s = 6\Delta$

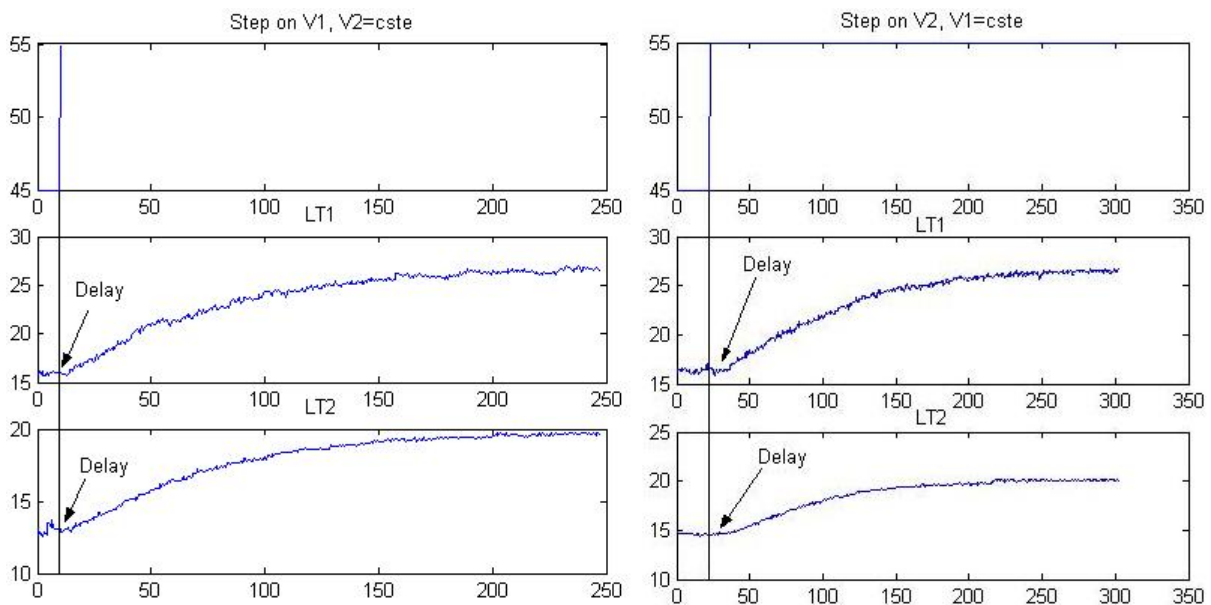


Figure 4.2: steps realized on the 4 communicating tanks

Then, to determine the order of the model, as there isn't any analytical method, we have to identify the process several times with different orders and to select the model where the residue is the smallest. After several identifications using a transfer function, results are not really good with important errors if the order remains low. So, instead of using a transfer function as model with a high order, we will use a step response model (see section 1.2.2) which can be used performing a Dynamic Matrix Control.

The model will be composed of 125 coefficients with a sampling time of 2s because the time of establishment the process is around 200s.

All coefficients are calculated thanks to HIDENT. The figure 4.3 shows at the top outputs of the model obtained and the process outputs. Coefficients of the step response are also represented. The model of the first level  $L_{T1}$  fit very well the real curve whereas there are more imprecision on the level  $L_{T2}$  but the dynamic of signal is well respected.

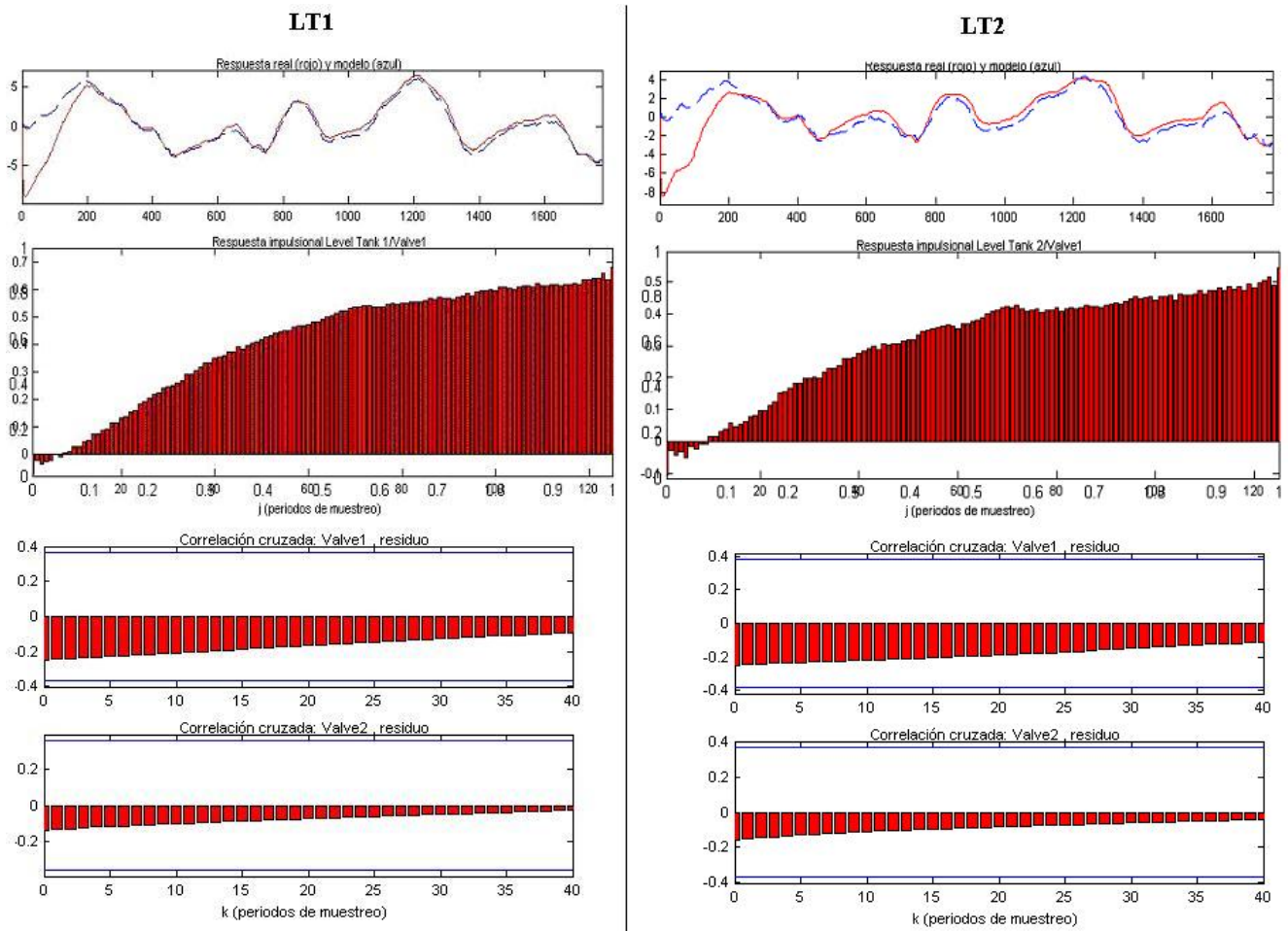


Figure 4.3: Identification : model and process outputs, step response and correlations between residues and inputs

The average of residues are respectively +0.35 and +0.4 on the levels  $L_{T1}$  and  $L_{T2}$  and the FPE of residues are 0.24 and 0.39. Moreover, autocorrelations are close to a white noise and the correlation between inputs and residues (represented at the bottom of the figure 4.3) remain between limits to not exceed (blue lines). So, residues are uncorrelated with inputs and not depend on past values (as a white noise), we can conclude that this identification is consistent. Now we have to validate the model with other measures.

### 4.3 Validation of the model

In order to validate the model, it's necessary to verify several points with measures different than measures used in the identification procedure :

- visual verification : the dynamic and the amplitude of the model response have to be close to the process response
- residues have to be uncorrelated with inputs and having an autocorrelation close to a white noise
- average of residues have to be close to 0

We will realize two validation tests staying between operating range to validate the model obtained.

The figures 4.4 shows responses of these tests and the table 4.1 summarizes information about residues. In the two tests, model and real outputs are relatively close with a FPE inferior of 1, the averages of errors are around +0.2 that's significate that the model give values slightly inferior of the reality. This error is acceptable to use this model



with a MBPC technique. Moreover, the correlation between residues and inputs on the figure 4.4 is acceptable and the autocorrelation of residues is close to a white noise autocorrelation, so we can consider an independency of residues (in the space and in the time).

These two tests allow to validate the model found previously between its operating ranges. During other tests out of these ranges, errors are more important and some dynamics are bad evaluated. This confirms that the process have non-linearities which come principally from level sensors and from intermediate tanks. Nevertheless, the process has to stay between its operation limits and the predictive control is enough robust to accept little errors of prediction.

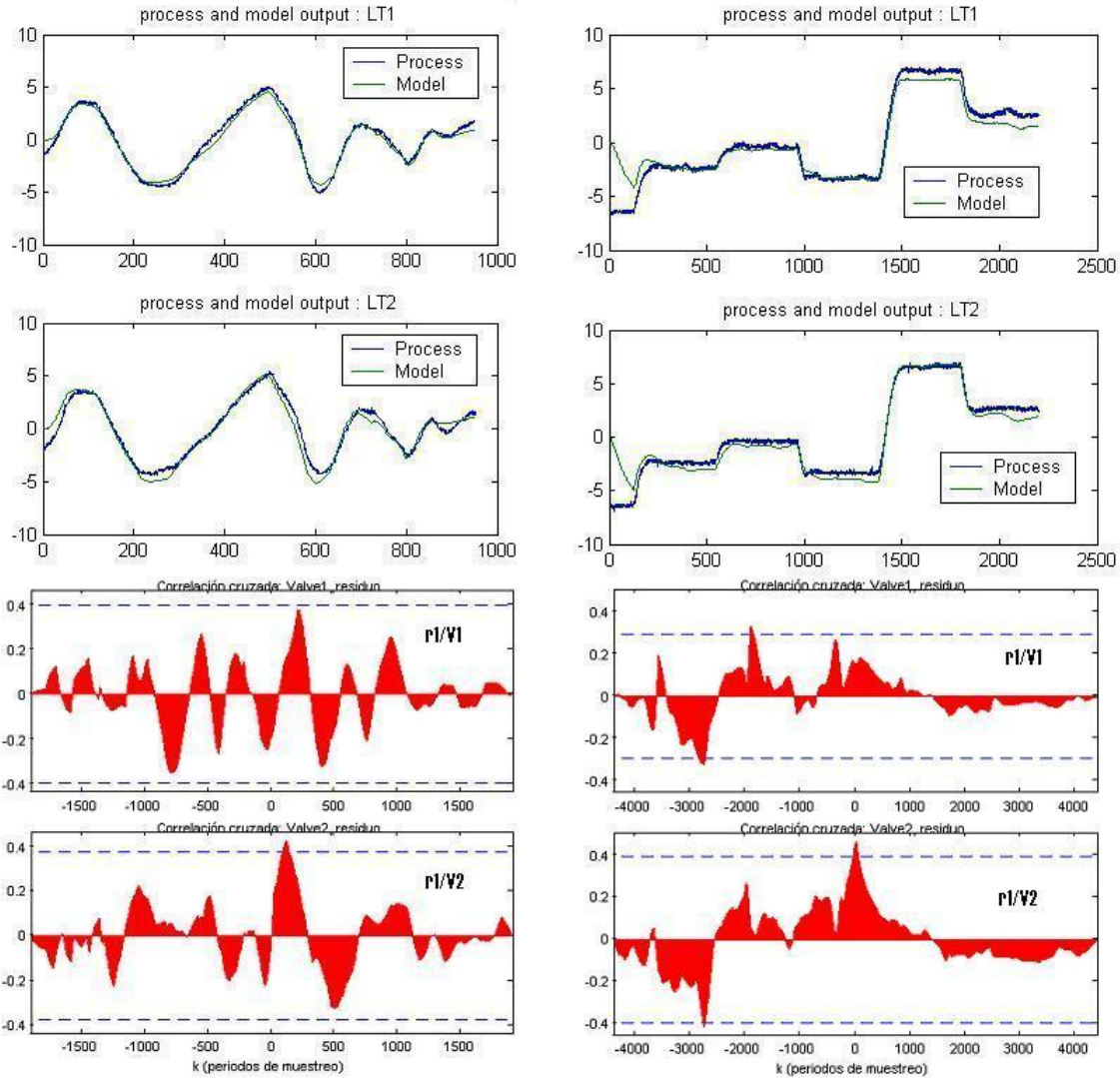


Figure 4.4: validation : Model and process outputs, correlation between residues and inputs

	$FPE_{LT1}$	$FPE_{LT2}$	average of $r1$	average of $r2$
Valid 1	0.15	0.32	+0.18	+0.23
Valid 2	0.89	0.58	+0.22	+0.22

Table 4.1: Final Predicted Errors on validation tests

## Chapter 5

# Predictive Control of 2 communicating tanks

After having realized the identification of the two communicating tanks, we can develop a model based predictive control using the model found in the chapter 3. The technique used will be a Generalized Predictive Control. This control will be performed by the software HITO.

This chapter describes the software used with its different parameters and then, a test on the real plant will be done after simulations validating the control. The robustness of the control will be studied with perturbations and the feasibility problem with a constraints management will be also mentioned.

### 5.1 HITO

HITO is a software developed by the Valladolid University in order to apply a predictive control to a MIMO system via an OPC protocol. The predictive control of the communicating tanks which have been identified before will be realized with this software. The following parameters have to be given to HITO :

- **Data source** : Select the OPC server to read input values from process and to send output values to the process
- **Controller type** : Select the predictive control method (GPC, DMC...)
- **Name of variables** : specify names of manipulated/controlled variables and perturbations with an associated state (limited, regulated, Off, auto, manual)
- **Dynamic Matrix** : All transfer functions or step responses for each couple of variables
- **Limitations** : All constraints on variables (physical, operation and optimization limits)
- **Control parameters** : predicted, control and constraint horizons, speed of the reference, weights of each variable in the cost function...
- **Feasibility** : priorities between constraints and variables

HITO calculates predictions and the future sequence of control automatically and has also an optimization algorithm to minimize the cost function with all constraints and priorities.

### 5.2 Hardware configuration

The process is described in the figure 3.1. The communication between the computer and the process uses an OPC protocol (OLE for Process Control) which is a common standard based on Microsoft technology. This protocol contains a server/client architecture to share the data with all softwares. It is an open and flexible solution to the classical proprietary driver problem, a lot of softwares for control in the industry use this standard. The computer has an IO card to send and receive the data with OPC. The inputs are the two signals from the level transmitters and the output signals go to an amplifier 5Vdc/24Vdc to manage the two electro-valves.

### 5.3 Constraints and control properties

In order to control the two tank levels, we will chose the GPC method with two manipulated variables (the two electro-valves  $V_1$  and  $V_2$ ) and two controlled variables (the two levels  $L_{T1}$  and  $L_{T2}$ ) where the four transfer functions have been found in the previous chapter. The constraints are the following :

Constraints on manipulated variables :

- The maximum evolution of a valve is fixed at  $\pm 10\%$  during one sampling time for a good operation of valves.
- The physical range of valves is  $[0\%, 100\%]$ .
- The operating range is fixed at  $[10\%, 90\%]$  in order to stay in the linear range of valves.

Constraints on controlled variables :

- The physical ranges of the tank levels are  $[0\%, 100\%]$ .
- The operating ranges are fixed at  $[20\%, 80\%]$  in order to stay around the operating point.

All horizons (predicted, constraint and control horizons) have to be chosen to have the desired response. Predicted and constraint horizons will be chosen equal because we want to respect constraints anytime. To find these parameters we will realize some simulations later.

The cost function is the same as in the chapter 2 at the equation (2.25). All weights  $\gamma_k$  and  $\beta_k$  are fixed at 1 because all variables have the same importance in this problem and the weights  $\beta_{1k}$  are null because we don't want to penalize the absolute value of the manipulated variables. So, the cost function has for expression :

$$J = \sum_{j=N_1}^{N_2} (L_{T1}(t+j) - r_{LT1}(t+j))^2 + (L_{T2}(t+j) - r_{LT2}(t+j))^2 + \sum_{j=1}^{N_u} (\Delta V_1(t+j-1))^2 + (\Delta V_2(t+j-1))^2 \quad (5.1)$$

Then, to find the solution  $\Delta u$  in respecting constraints, a quadratic solver is used in HITO.

## 5.4 Feasibility problem

The feasibility of the problem is also managed by HITO thanks to priorities on constraints which are defined by the user (Figure 5.1). The first panel (*Restablecimiento de la factibilidad en las variables manipuladas*) of the figure 5.1 defines priorities between constraints on manipulated variables. So, these parameters are used when the non-feasibility concerns a manipulated variable. Here, the highest priority is to change velocity constraint ( $\Delta u_{max}$  and  $\Delta u_{min}$ ) and if it's not sufficient, the operation limits on the position can be also changed ( $u_{max}$  and  $u_{min}$ ). The second panel (*Prioridades para restablecer la factibilidad del control predictivo*) on the right defines the priority between all controlled variables in the first column (here the level  $L_{T1}$  has higher priority than the level  $L_{T2}$ ). The other fields allow to change in priority constraints on manipulated variables ( $V_1$  and  $V_2$ ), then on controlled variable limits ( $y_{max}$  and  $y_{min}$ ) and then on the constraint horizon  $[N_3, N_4]$ . After this, if the choice is to change constraints on manipulated variables, the third panel is used (*Gestion de limites en variables manipuladas*). It defines which constraint moves in priority according to the controlled variable which presents a non-feasibility. In this case, for the two controlled variables, we will try to change firstly the velocity of the controlled variables and then operation limits of controlled variables.

## 5.5 Simulations

Before trying to control the real process, we will make simulations thanks to HITO which embed a linear simulator in order to evaluate the performance of the control and to see influences of different parameters on the control. For having a good reliability, in each test there is only one parameter which is changing. All these simulations are step responses on  $L_{T1}$ . The set point go from 40% to 45% and the set point of  $L_{T2}$  is fixed at 40%.

The sampling time of measurements is fixed at 0.5 second and in a first time the controller will be called also at this sampling time.

	controller	$N_u$	$N_1/N_2$	filt
Test 1	GPC	2	1/100	0.8
Test 2	GPC	2	1/40	0.8
Test 3	GPC	2	30/100	0.8
Test 4	GPC	2	50/150	0.8
Test 5	GPC	2	1/100	0.2
Test 6	GPC	5	1/100	0.8
Test 7	GPC	10	1/100	0.8

Table 5.1: Different parameters for the tests realized

All responses are represented on the figure 5.2. The goal of the control is to give a fast response in respecting set points without going beyond limits. Moreover, a step response on the level  $L_{T1}$  provokes a perturbation on the level  $L_{T2}$ . These tests show that the predicted horizon have to be large enough, around  $N_2 = 100$  and can begin around  $N_1 = 30$  to minimize the disturbance on the second level. The control horizon  $N_u = 2$  is sufficient. Moreover the parameter *filt* can be chosen at 0.8. The test 3 is a good compromise.

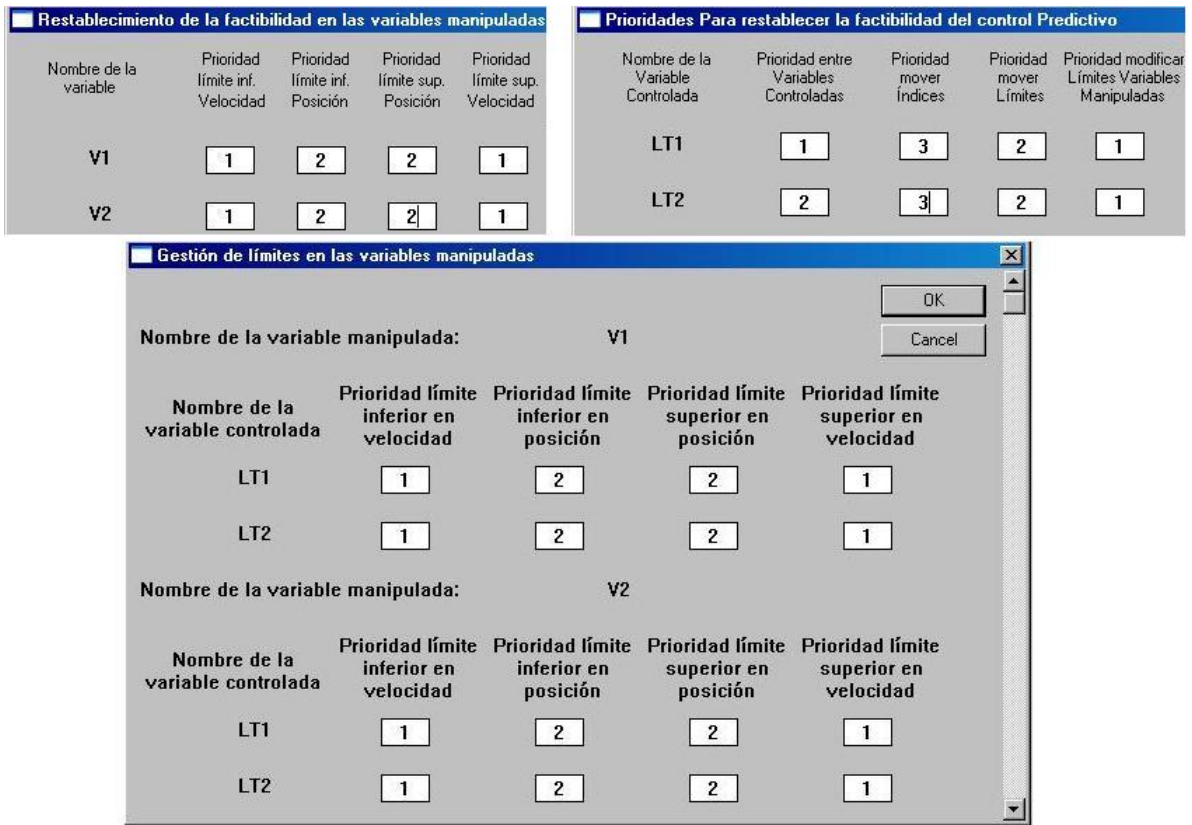


Figure 5.1: priorities to solve problem of not feasibility

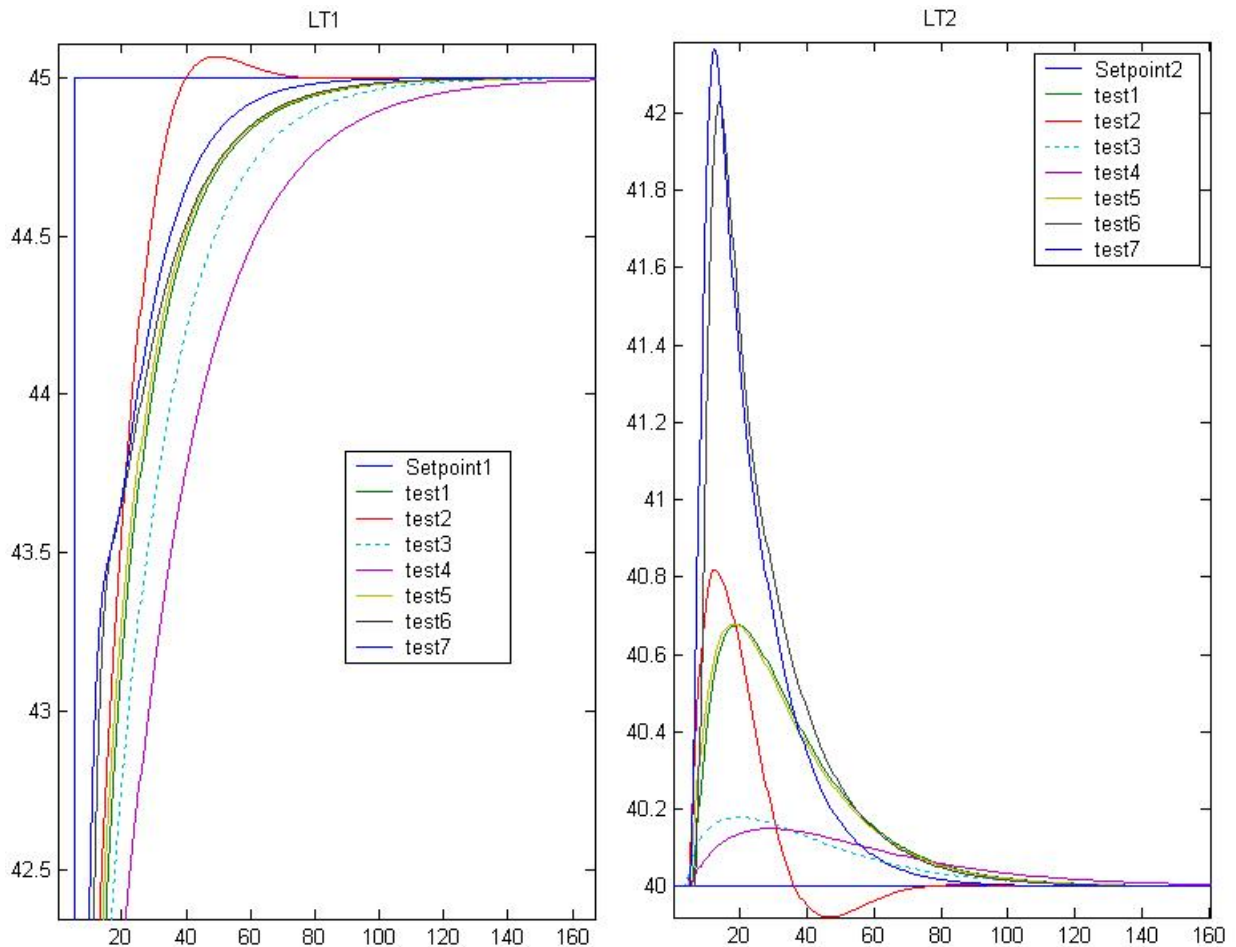


Figure 5.2: Step responses on  $LT_1$  for different tests

### 5.6 Results

After all simulations we will realize the predictive control on the real process. First, we will confirm the step response obtained in simulation. The first graph on the figure 5.3 represents the simulated and the real step response on the level  $L_{T1}$  with a generalized predictive control(GPC). The second graph shows the influence of this step (disturbance) on the level  $L_{T2}$ . The same test with a classical PID is represented on the third graph and manipulated variables ( $V_1$  and  $V_2$ ) are at the bottom.

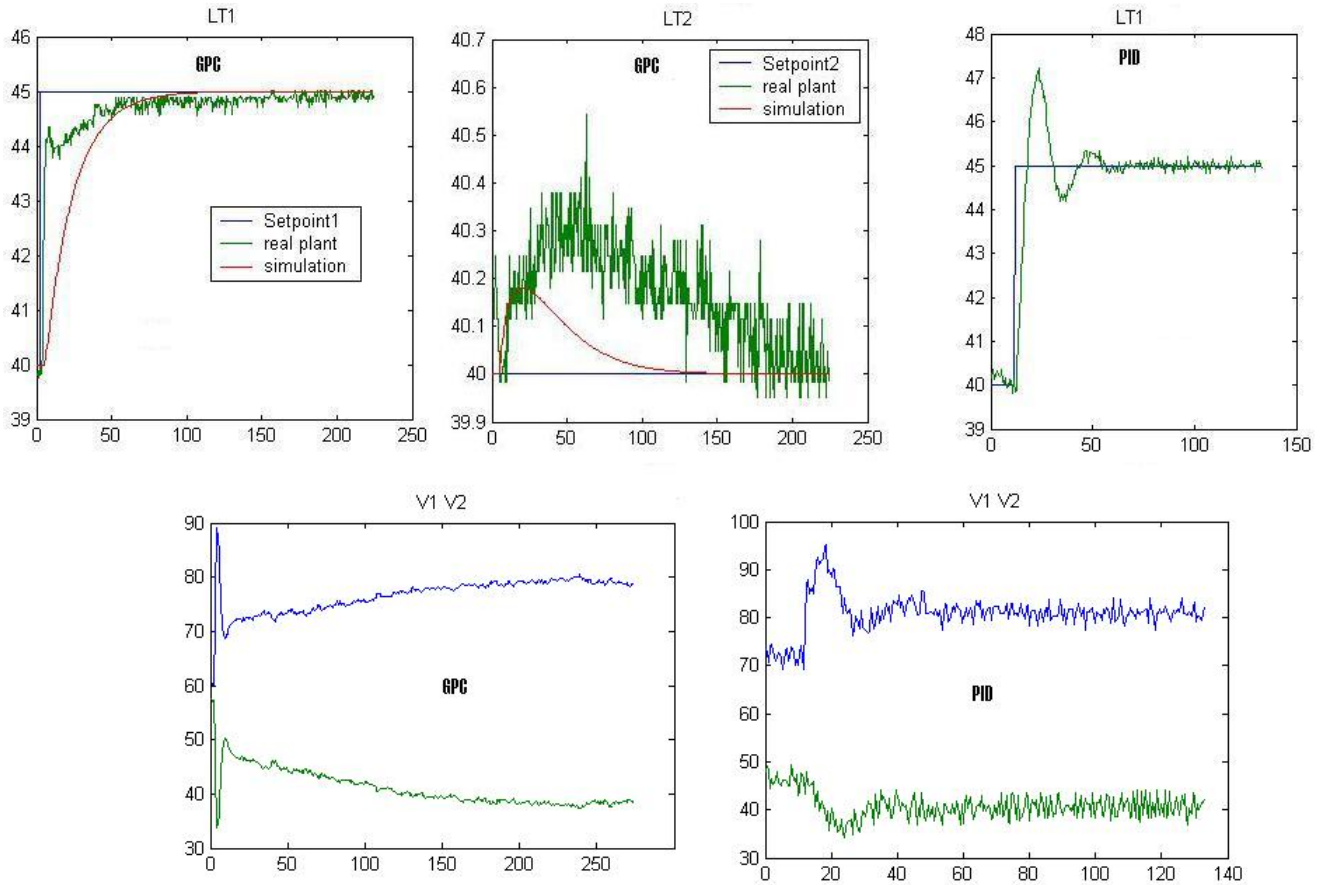


Figure 5.3: Real and simulated step responses with GPC and PID

The result obtained in simulation is confirmed, the time to reach the set-point is the same but the shape of the response is quite different because of noise and non-linearities on the sensors. The disturbance on the level  $L_{T2}$  is very low (+0.3cm) and it's erased after 2min. With the classical PID, the velocity of the response is more or less the same but there is an important overtaking with oscillations whereas this phenomena is absent with GPC. At the bottom, values of manipulated variables are represented, the GPC allows to have a more smoothed control than the PID and moreover the GPC allows to take into account constrains on variables, that's why the value of  $V_1$  not goes over 90% with GPC.

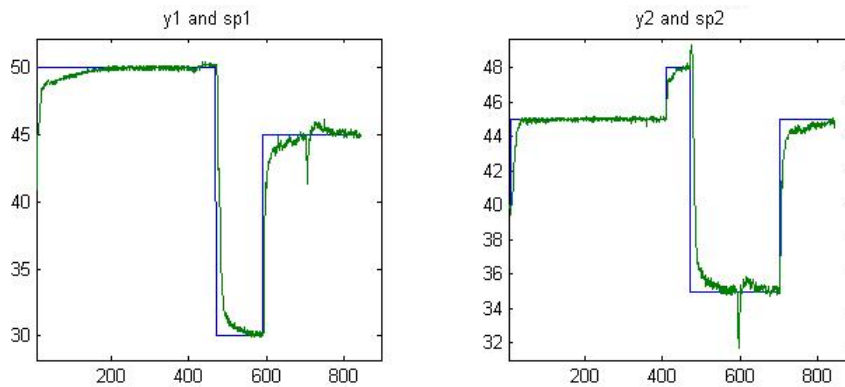


Figure 5.4: Test on the real plant

### 5.7 Influence of perturbations

We can test the reaction of the control with different perturbations in order to evaluate the robustness of the control. When there is a disturbance, the model of the real plant is modified whereas the model used to calculate future values is always the same. These disturbances can be provoked by moving the three manual valves (see figure 3.1) which allow to drain the tanks and exchanging fluids between the 2 tanks.

In a first test, each tank level is stabilized at 45% and all manual valves are open. At the time  $T_1$ , the drain valve of the second tank is half closed and reopened at the time  $T_2$ . The figure 5.5 shows the influence of this disturbance on the 2 levels.

The second test shows in the figure 5.6 consists in closing the exchange valve at the time  $T_1$  and reopening it at the time  $T_2$  while set-points of  $L_{T1}$  and  $L_{T2}$  are respectively fixed at 50% and 40%.

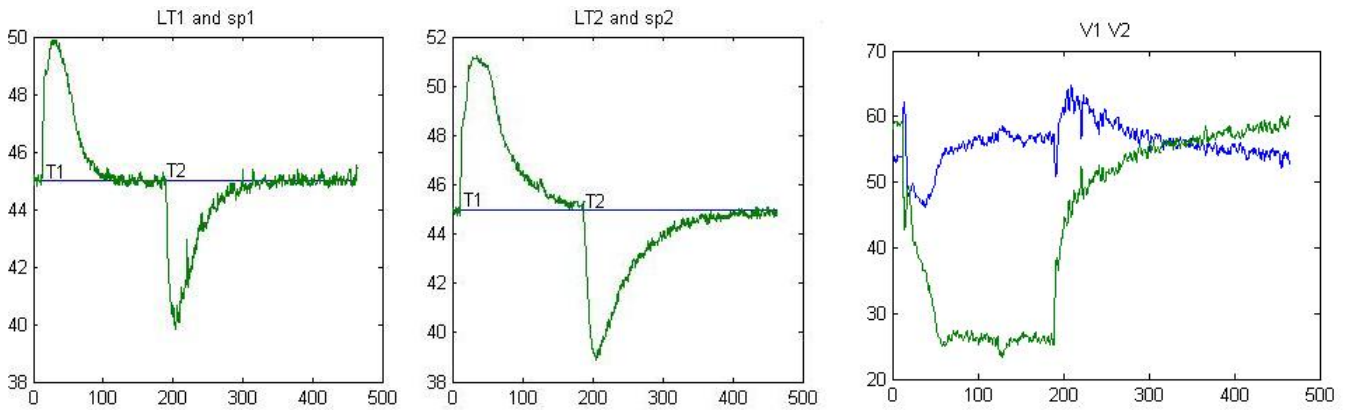


Figure 5.5: Perturbation : closing of the right drain valve

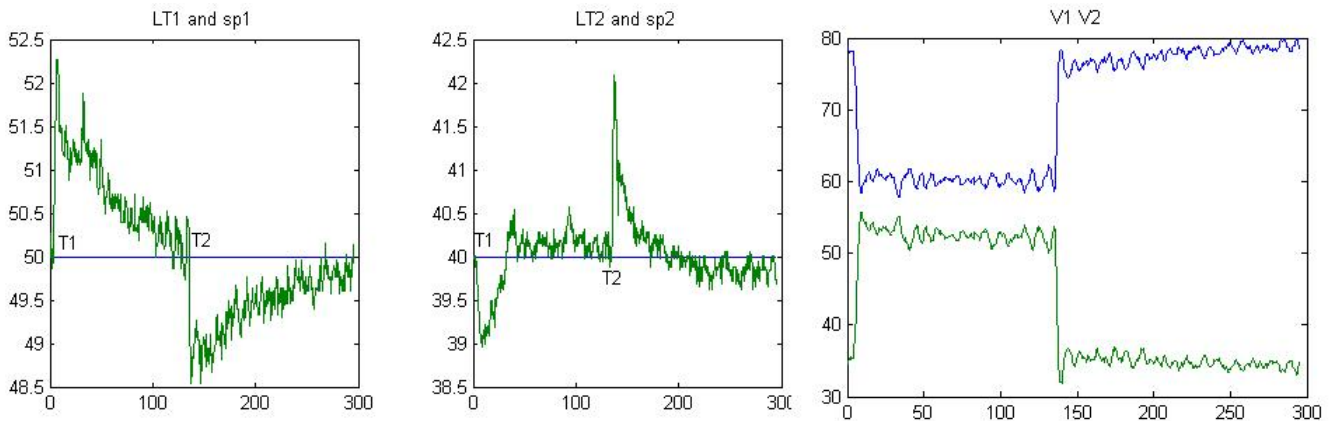


Figure 5.6: Perturbation : closing of the exchange valve

In the first perturbation test, the flow of draining in the tank 2 is reduced, so, the 2 levels goes up because there is less liquid which is going out, the model is not valid any more. Thanks to the robustness of the predictive control, a correction is automatically done on the two valves and the set-points are reached after less than 2min. When the perturbation is canceled, the inverse phenomena occur.

In the second test, as the level of the first tank is higher of 10% there is a flow from the tank 1 to the tank 2. When the exchange valve is closed, this flow is canceled and the model change. This perturbation involves an increase of the level  $L_{T1}$  and a decrease of the level  $L_{T2}$ . After 2 minutes, the set-points are reached and when the disturbance is canceled at the time  $T_2$  we observe the inverse phenomena.

In conclusion, we can appreciate the robustness of the control behavior when disturbances occurred because a model is never exact. Moreover process are changing with the time because of the ambient temperature, precision of sensors...

## 5.8 Constraints and feasibility

HITO integrates a constraint manager which takes into account the feasibility problem (see section 5.3 and 5.4). Generally, with this kind of process, the problem is always feasible and moreover there isn't any degree of freedom (2inputs/2outputs). Nevertheless, we can test the constraint manager moving operation limits of MVs and CVs such that the levels of tanks can't stay between their operation limits if the two valves also stay in their limits. For example:

- operation limits of  $L_{T1}$  and  $L_{T2}$  are fixed at [45%,90%].
- operation limits of  $V_1$  and  $V_2$  are fixed at [0%,50%].

In this configuration levels have to be superior at 45% and normally values of valves are around 60%. So, the respect of all constraints is infeasible. The operation limits are *soft constraint* (*ie* : it's possible to not respect them) contrarily to physical constraints which are *hard constraints* (*ie* : they must be respected). So, soft constraints can be not respected to solve the feasibility of the problem.

In the configuration of HITO, we have defined in the section 5.4 a higher priority to move MV operation limits in order to respect firstly constraints on the controlled variables. This configuration is generally the most employed because constraints on CVs are more important. The other solution is to give a higher priority to move CV limits, so, MV constraints are more important than CV constraints. The figure 5.7 shows these two different configuration in HITO.

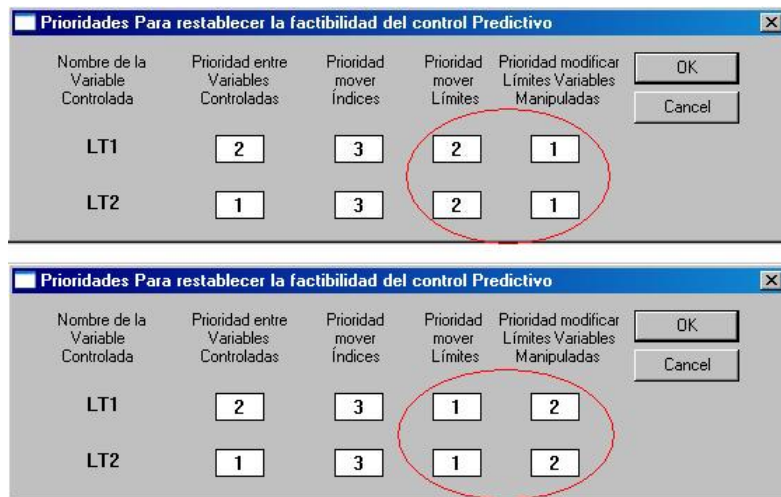


Figure 5.7: priority to move MV limits or CV limits in HITO

Tests have been done on the two communicating tanks with these two configurations to solve the infeasibility. The figures 5.8 and 5.9 show results on the real plant with these two control politics.

In the first test, HITO breaks the operation limits (staying in physical ranges) of the two valves because we have defined higher priority to move the manipulated value limits. Hence, the two levels  $L_{T1}$  and  $L_{T2}$  respect their constraints (45%).

In the second test, the valves will stay in their limits and the limits of the levels are broken. As the problem is infeasible,  $V_1$  and  $V_2$  take their maximal values (50%) and the levels  $L_{T1}$  and  $L_{T2}$  are responding according MV values without taking into account their constraints which are broken.

These example of constraint manager and of infeasible problem are "school example" and not have a real interest. In other processes more complex with more variables as distillation columns, the problem of infeasibility is much more difficult and in these cases, HITO could be a real plus.

Moreover HITO integrates an optimization mode where optimal set-points are calculated to minimize a cost function moving the operation-point of the process. Of course, to perform this, a MIMO system which contains more inputs than outputs is necessary because there are degrees of freedom. With the communicating tanks, this optimization is impossible.

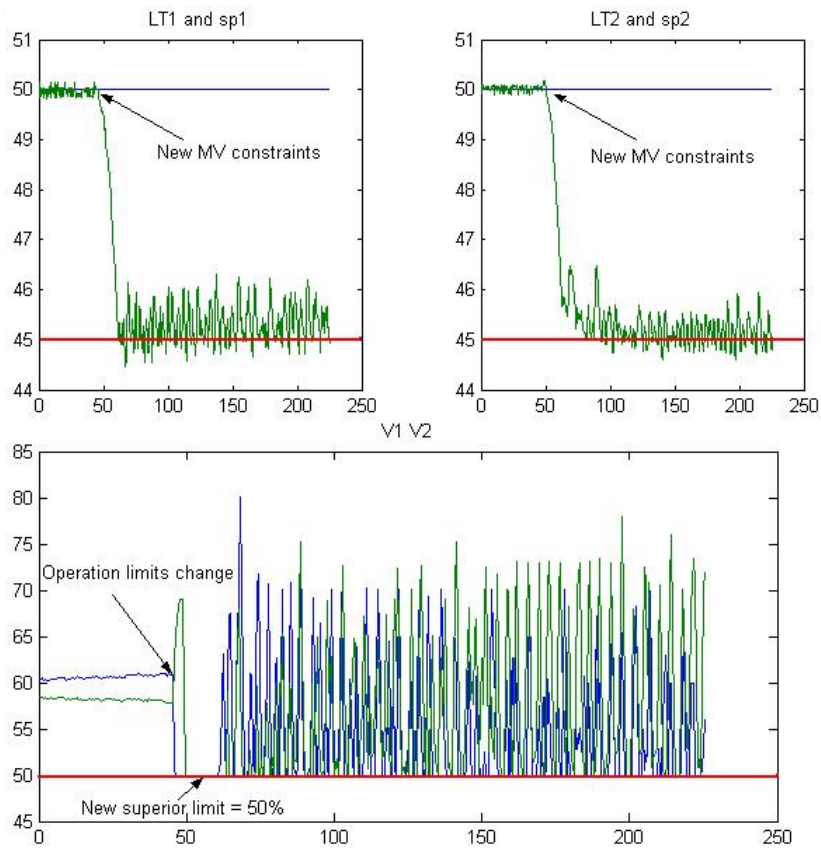


Figure 5.8: Non feasible problem with higher priority to move MV limits

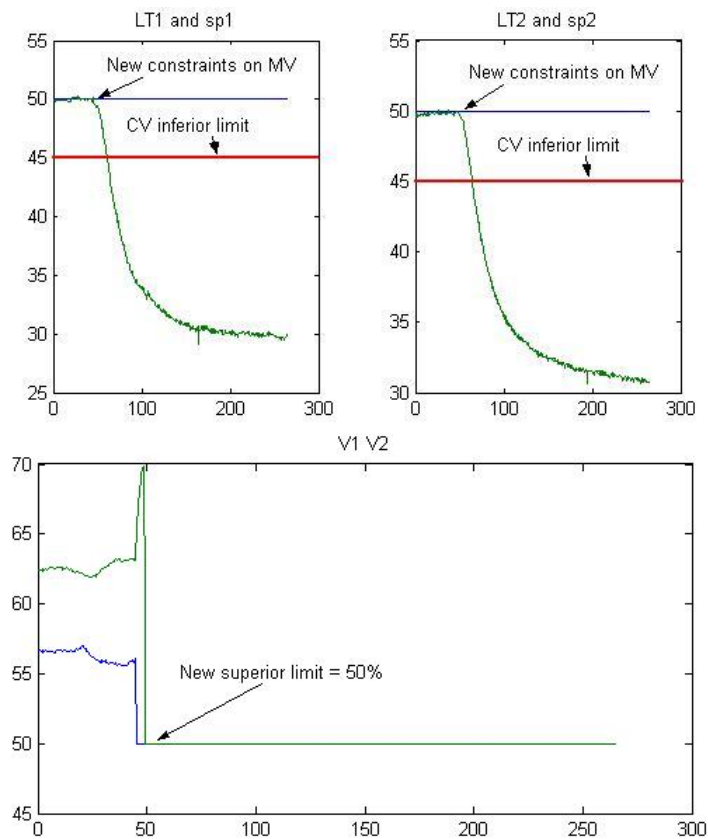


Figure 5.9: Non feasible problem with higher priority to move CV limits



## Chapter 6

# Predictive Control of 4 communicating tanks

In order to control the process identified in the chapter 4, we will use a DMC (Dynamic Matrix Control) using the model found previously. The objective of this control is to maintain the two levels of each tanks. A classical PID isn't efficient with this type of process, hence an advanced control as a DMC is an efficient way to have a good control and to respect different constraints.

First, different parameters of the predictive control will be detailed and simulations will be done, then different results on the real process will be presented with a study on the influence of different perturbations in order to appreciate the robustness of the control.

### 6.1 Control parameters and simulation

The predictive control use the model found in the chapter 4. Different parameters of the control and constraints are the following :

- Horizon of prediction :  $N_1/N_2 = 1/50 : 100s$
- Horizon of control :  $N_u = 2$
- Constraints on valves :  $0 \leq V_1/V_2 \leq 60$
- Constraints on levels :  $10 \leq L_{T1}/L_{T2} \leq 40$

Before realizing the control on the real plant, a simulation will be done thanks to the linear simulator integrated in HITO. This test consists in stabilizing  $L_{T1}$  and  $L_{T2}$  respectively at 17% and 16% and to moving set points to 21% and 20%. The result is showed in the figure 6.1

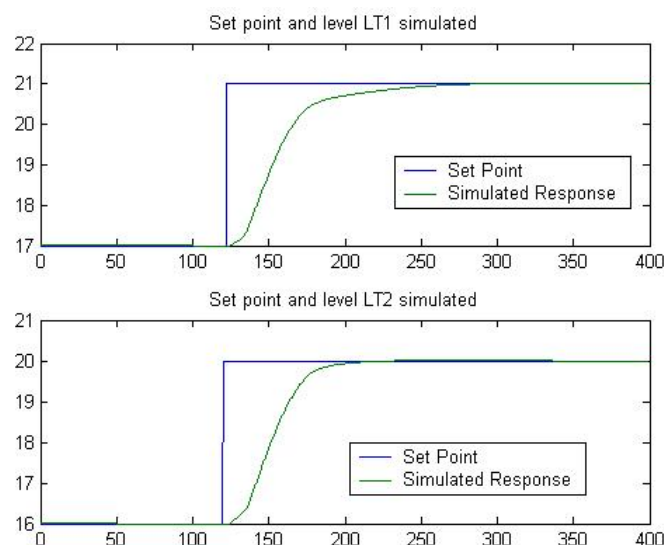


Figure 6.1: Predictive Control simulated on the 4 tanks

With this configuration, set points are reached after 2min and the controlled variables follow the reference trajectory. Now we have to confirm this result on the real plant.

## 6.2 Results on the real plant

First, the response to a step of set-point will be realized to validate the previous simulation. The figure 6.2 compare the simulation made and the real response obtained on the process. The two responses are very close, there is just a little going beyond the set-point on the level  $L_{T1}$  but this result confirms the exactitude of the model obtained and the efficiency of the predictive control following a reference trajectory.

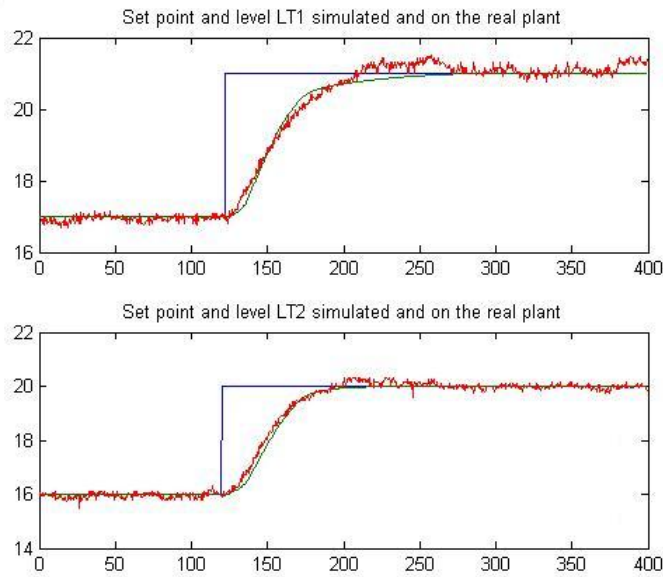


Figure 6.2: Responses to steps of the set-points with predictive Control on the 4 tanks

A longer test of 40 minutes is realized on the real plant respecting the operating range of controlled variables. The figure 6.3 shows these results. Set-points are well respected on the two levels  $L_{T1}$  and  $L_{T2}$ . When set-points remain stables, levels remain stables at  $\pm 0.2$  which is an acceptable error. When set-points are moving, the reference trajectory is correctly followed. The shape of  $V_1$  and  $V_2$  confirm the good prediction of our model because they are moving slowly and anticipate the reaction of the process, particularly the delay of the system. A such control is impossible with a classical PID where manipulated values move a lot and oscillate. So, predictive control allows to moderate actuators and to reach set points without going above the set-point.

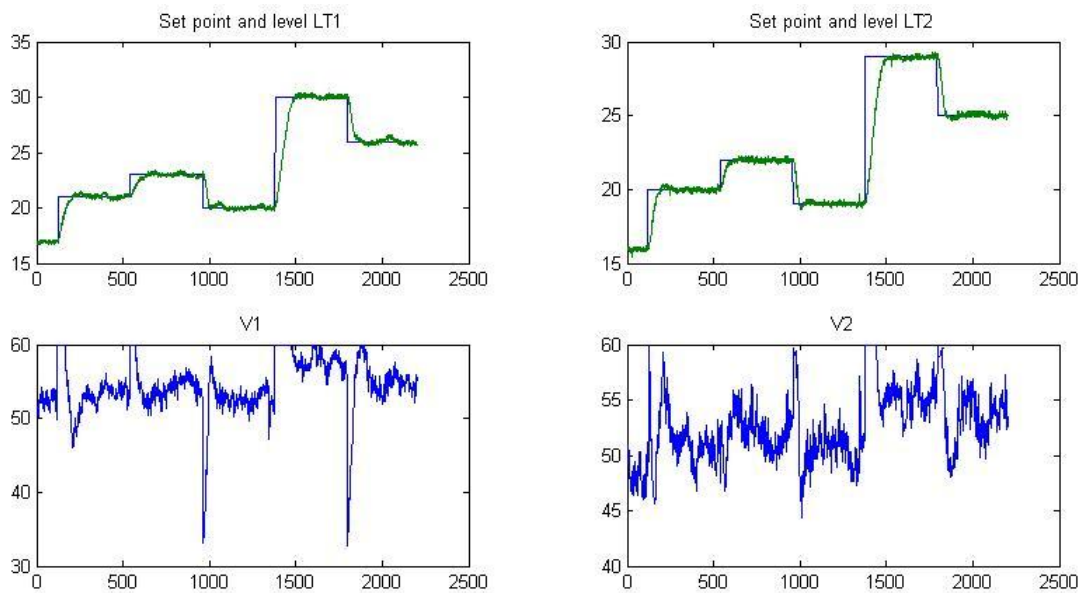


Figure 6.3: Predictive Control of the 4 tanks

### 6.3 Influence of perturbation

In order to study the robustness of the control, the same perturbation tests than in the section 5.7 will be realized :

- The right manual valve which allows to drain the tank  $T_2$  is half-closed and reopened.
- The manual valve of exchange which allows a flow between the two tanks is closed.

The figures 6.4 and 6.5 represent the process behavior with these two perturbations. The two manipulated variables ( $V_1$  and  $V_2$ ) are moving immediately after the perturbation in order to equilibrating the the two levels and respect set-points. So, the control is still efficient whereas the model of the process is different. Observations are the same than in the section 5.7.

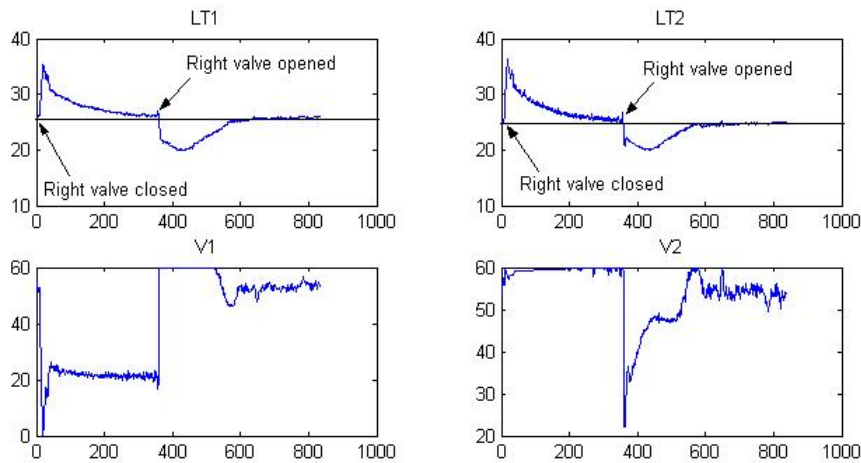


Figure 6.4: Perturbation on the right valve

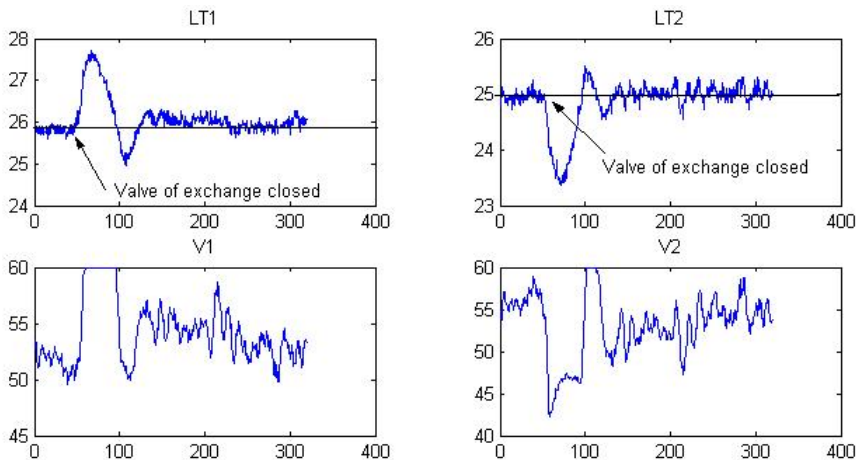


Figure 6.5: Perturbation on the valve of exchange

### 6.4 Conclusion

In this second part, a complete approach has been realized on a real process (identification and control). Two different models and two predictive control techniques have been used. A General Predictive Control (GPC) using transfer functions for the two communicating tanks and a Dynamic Matrix Control (DMC) using step responses for the four communicating tanks. The GPC was an efficient solution for the two communicating tanks which is a simple process of the first order. For the four communicating tanks, the DMC was a better choice than the GPC because of the use of a step response model instead of a transfer function with a high order.

These two methods have provided us good results and allow to regulate levels of the tanks perfectly, the disturbance rejection is also efficient.

## Part III

# Distillation column

# Chapter 7

## Process and control presentation

This chapter will explain the general operation of a distillation column used in the petroleum industry and its method of control. The column studied in this report is a depropanizer based in Tarragona (Cataluña, Spain). It allows to produce propane and butane from LPG (Liquified Petroleum Gas). The goal of the operation is to control percentage of impurities in different products.

After a succinct explanation of the distillation, the column and its operation will be described, then the existing control and the model used will be detailed.

### 7.1 Distillation principle

The goal of the distillation is to separate different components which are more or less volatile. The volatility is defined according to the boiling point of a chemical specie (more the component is volatile, more its boiling point is low). Distillation is based on the fact that the vapor of a boiling mixture is richer in the more volatile component. Therefore, when this vapor is cooled and condensed, the condensate will contain more volatile components. At the same time, the original mixture will contain more of the less volatile material. Moreover the vapor pressure and hence the boiling point of a liquid mixture depends on the relative amounts of the components in the mixture.

The figure 7.1 represents a boiling point diagram (available for a constant pressure) of a binary mixture (composed of two products A and B). The boiling point of the product A is 90 degrees and 120 degrees for the product B : A is more volatile than B. If the mixture is composed of 50% of A and 50% of B and heated from the point *a*, its concentration remains constant until it reaches the bubble-point at 100 degrees (point *b*) when it starts to boil. The vapors evolved during the boiling has the equilibrium composition given by point *c*. At this point, the concentration of A is approximately 80%, therefore the vapor contains more product A and the liquid more product B.

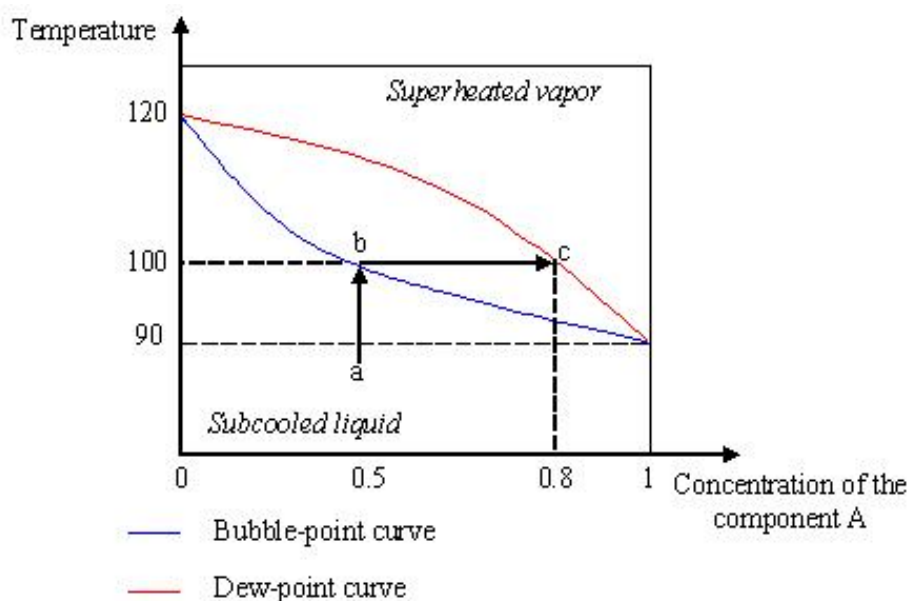


Figure 7.1: Boiling point diagram at a constant pressure

To evaluate the difficulty to separate two components, we can calculate the relative volatility  $\alpha_{ij}$  between components  $i$  and  $j$  :

$$\alpha_{ij} = \frac{y_i/x_i}{y_j/x_j} \quad (7.1)$$

In this equation  $y_i$  represents the mole fraction of component  $i$  in the vapor and  $x_i$  represents the mole fraction of component  $i$  in the liquid. So, the more important the relative volatility is, the easier the distillation of these two products is because their boiling points are very distinct.

## 7.2 Process description

A distillation column has to separate different chemical products with a desired purity. The purity is symbolized by the percentage of impurity in the final products. Distillation columns are designed to achieve this separation efficiently. In our case, the feed contains a mixture of two components which are propane ( $C_3H_8$ ) and butane ( $C_4H_{10}$ ). The distillation column has to separate propane (volatile component) and butane which is less volatile.

The figure 7.2 represents a distillation column with other necessary equipments for its operation. The equipments are the following :

- **The distillation column** is constituted of a stacking of trays. Trays are designed to allow a vapor flow from the bottom to the top of the column and to allow a liquid flow in the other way. Vapor rises through trays which contain chimneys for the vapor and the liquid falls by gravity. Moreover trays are designed to enhance the component separation forcing the contact between liquids and vapors as many as possible.
- **The reboiler** allows to generate vapor from the liquid which is at the bottom of the column. Then, the vapor produced is reintroduced in the column. To transform liquid in vapor, heat is supplied to the reboiler thanks to warm water vapor. The liquid removed from the reboiler is known as the *bottoms product* or simply, *bottoms*.
- **The condenser** allows to transform the vapor at the top in liquid. The condenser is supplied by cooling water.
- **The reflux drum** is an holding vessel which stores the condensed liquid of the condenser. Some of this liquid is recycled back to the top of the column and this is called the *reflux*. The condensed liquid that is removed from the system is known as the *distillate* or *top product*.

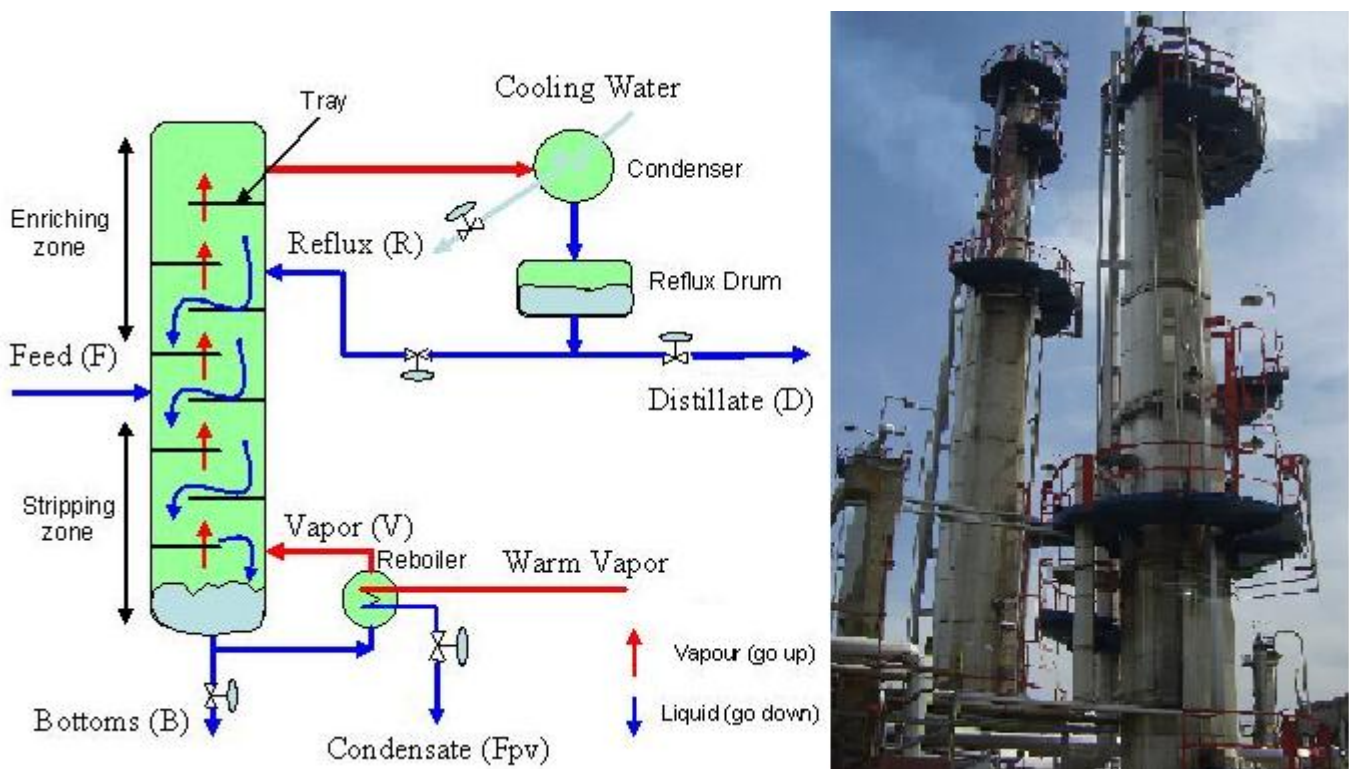


Figure 7.2: Distillation column

### 7.3 Process operation

The distillation column is fed in the middle by a mixture of components to separate (Feed). So, this feed goes down by gravity. At the bottom of the column, the liquid goes to the reboiler where it is boiled and the vapor is reintroduced in the column. This vapor contains in majority the volatile component and it will rise through the trays to reach the top of the column. Then, the vapor enters in the condenser to be transformed in liquid and stored in the reflux drum. This top product is principally composed of the volatile component. This component can be removed of the cycle (distillate) or recycled back to go down in the column (reflux). During a normal operation the levels of the reflux drum and of the bottoms products in the column have to be as constant as possible. The area located at the top of the feed is called *enriching zone* because the vapor is in contact with the reflux, therefore the purity of the vapor increases. The area located bellow is named *stripping zone* because the feed is in contact with the vapor, so, the concentration of the volatile component decreases in the liquid which is going down and the bottoms will have a better quality.

This process is a MIMO system where all manipulated and controlled variables influence all variables. That's why a regulation only with PID is inefficient. Example of correlations between variables [CAM97]:

When the Reflux increases, the quality of the distillate increases (there is less bottoms inside which are impurities) but the quality of the bottoms decreases (there is more distillate which are impurities). Moreover the working pressure (in the top of the column) decreases and the load losses increase. The reflux drum level decreases whereas the bottoms level increases.

When the vapor introduced in the column increases, the quality of the bottoms increases (there is less impurities) and the quality of the distillate decreases (there is more impurities). The reflux drum level increases whereas the level of the bottoms in the column decreases.

### 7.4 EcoSim library of the depropanizer

This column and all exterior components have been developed in EcoSimPro in order to create a library. This library is composed of the following files :

- **Properties** : contains all properties of chemical components (butane and propane)
- **Constants** : contains principal necessary constants
- **Properties water vapor** : contains properties of water and water vapor
- **Properties functions** : contains functions which are calling liquid properties
- **Mathematical functions** : contains mathematical functions in order to avoid division by zero, logarithm function...
- **Liquid properties** : contains functions which calculate enthalpy, specific heat of liquids.
- **Gas properties** : contains functions which calculate molecular mass, density, viscosity, enthalpy, conductivity, specific heat of gases
- **Ports** : Definitions of different ports for components (analog signal, liquid, gas, vapor, thermic )
- **Liquid components** : contains components as valves or tubes for incompressible fluids.
- **Liquid tanks** : contains tank components
- **exchanger** : contains heat exchanger components
- **Despropanizer** : contains the distillation column.
- **Control** : contains control components as PID, cascades.
- **Divisor** : contains a valve with 1 input and 2 outputs. This component allow to separate the reflux and the distillate after the reflux drum
- **Sources** : contains the source of the feed for the column
- **Reboiler** : The reboiler component
- **MBPC**: The DMC controller
- **Union C13 MBPC**: General architecture of the system with all connections and parameters

## 7.5 Process control objectives

The main objective of the distillation column control is to maintain the concentration of impurities in the distillate and in the bottoms between operating ranges. Other variables to control are levels. So, the different controlled variables are the following :

- Concentration of impurity at the top of the column :  $C4_{top}$
- Concentration of impurity at the bottom of the column :  $C3_{bottom}$
- Level of the distillate in the reflux drum :  $L_D$
- Level of the bottoms in the column :  $L_B$

The manipulated variables are the different flows which are controlled by a regulating valve. Hence, manipulated variables are the following :

- Flow of the distillate :  $D$
- Flow of the reflux :  $R$
- Flow of the bottoms :  $B$
- Flow of the vapor introduced in the column ( $V$ ).

The measurable disturbance is the flow of the feed.

Generally, ratios  $R/D$  (the reflux ratio) and  $V/B$  (the boilup ratio) are low, so, the level in the reflux drum ( $L_D$ ) and in the column ( $L_B$ ) are respectively controlled with  $D$  and  $B$ . For this operation, a simple  $PI$  controller should be sufficient because this two controlled variables directly depend on this two manipulated variables.

Then, to control the quality of bottoms and of distillates, an advanced control can be more efficient than a classical control for several reasons :

- All variables are linked. A multiple variables control have to be developed.
- There is a measurable disturbance (Feed) which can be taken into account only in an advanced control.
- An advanced control allows a better use of actuators and allows a control more economic for the industry.

## 7.6 Predictive control of the depropanizer

The usual technique to control this kind of process is to use a DMC predictive controller [CAM97]. Hence, the qualities of components ( $C4_{Top}$  and  $C3_{Bottom}$ ) are controlled thanks to the vapor ( $V$ ) introduced at the bottom of the column and thanks to the quantity of Reflux ( $R$ ) re-injected at the top of the column. In this specific column, a depropanizer column, the choice is a little bit different, impurities are controlled manipulating the sensible temperature ( $T$ ) at the top of the column (on the 33<sup>rd</sup> tray) and the condensate ( $F_{pv}$ ) which go out of the reboiler. This choice is more or less equivalent because the flow of the condensate is proportional to the vapor and temperature at the top is highly correlated with the Reflux. Hence, the DMC controller calculates appropriate PID set-points of the temperature and of the condensate to remove in order to respect set-points on impurities. So, variables of the DMC are the following :

- **CVs** : Impurities in the distillate (%):  $C4_{Top}$   
impurities in the bottoms (%):  $C3_{bottoms}$
- **MVs** : Sensible temperature of the column ( $^{\circ}C$ ):  $T$   
flow of the condensate in the reboiler ( $m^3/h$ ):  $F_{pv}$
- **Disturbance** : Flow of the feed ( $m^3/h$ ):  $F$

The figure 7.3 represents this control architecture. A model of this depropanizer using physic differential equations and non-linear equations has been developed by the Systems Engineering and Automatic Control department of the Valladolid University on the software EcoSimPro (see Appendix 1). A DMC controller has also been developed using a library in Ecosimpro named HITO to realize the predictive control. The DMC uses a linear model of the column (composed of step responses) which have been obtained by an identification. The figure 7.5 represents the system in EcosimPro.



The particularity of the DMC controller is that it uses a step response model [CUT79]. If we take into account a controlled variable  $y$ , a manipulated variable  $u$ , a measurable disturbance  $v$ , the model is:

$$y(t) = \sum_{i=1}^{N2} g_i \cdot \Delta u(t-i) + \sum_{i=1}^{N2} d_i \cdot \Delta v(t-i) \quad (7.2)$$

The  $g_i$  coefficients represent the step response ( $\Delta u = 1$ ) of the controlled variable and the  $d_i$  coefficients are the step response of the measurable disturbance ( $\Delta v = 1$ ).

The predictions are calculated using this model:

$$\hat{y}(t+j) = \sum_{i=1}^j g_i \cdot \Delta u(t-i+j) + p_j \quad (7.3)$$

where  $p_j$  represents the free response of the system.

Then, a cost function  $J$  is minimized to calculate the future values of the MVs. Constraints on CVs values and on MVs values and velocity are taking into account in this minimization. There are physical constraints which are physical limits of variables and operation constraints which represents operation limits of the process. The cost function used is the following for  $n$  CVs and  $m$  MVs:

$$J = \sum_{k=1}^n \left( \sum_{j=N1_k}^{j=N2_k} \gamma_k (y_k(t+j) - r_k(t+j))^2 \right) + \sum_{k=1}^m \left( \sum_{j=1}^{j=Nu_k} \beta_k (\Delta u_k(t+j-1))^2 \right) \quad (7.4)$$

There is a priority term  $\gamma_k$  on each CV and  $\beta_k$  on each MV to give a higher importance to some variables. For this distillation column, all these coefficients are equal to one (there isn't any priority). Moreover, HITO takes care of the feasibility of the control, so if the problem is unfeasible, operation constraints can be broken temporary [RAW99] [MOR95]. A priority table between constraints (on  $y$ ,  $u$  and  $\Delta u$ ) allows to solve this infeasibility breaking a such constraints rather than another one.

For the depropanizer, 150 coefficients are taking into account in the step responses with a sampling time of 2min. The horizon of prediction is  $N2 = 45$  and the control horizon is  $Nu = 2$ .

The figure 7.4 shows a simulation on the depropanizer with this predictive control where the set-point on  $C4_{Top}$  is moving by steps whereas the set-point on  $C3_{bottoms}$  remains stable. Set points are well respected and levels in the reflux drum and in the column remain stable thanks to the PI controllers. As there isn't any priority on the manipulated variables, when the set-point of  $C4_{top}$  increases, the vapor introduced in the column decreases (so the condensate  $Fpv$  decreases) and the sensible temperature  $T$  increases (so the Reflux injected at the top of the column increases).

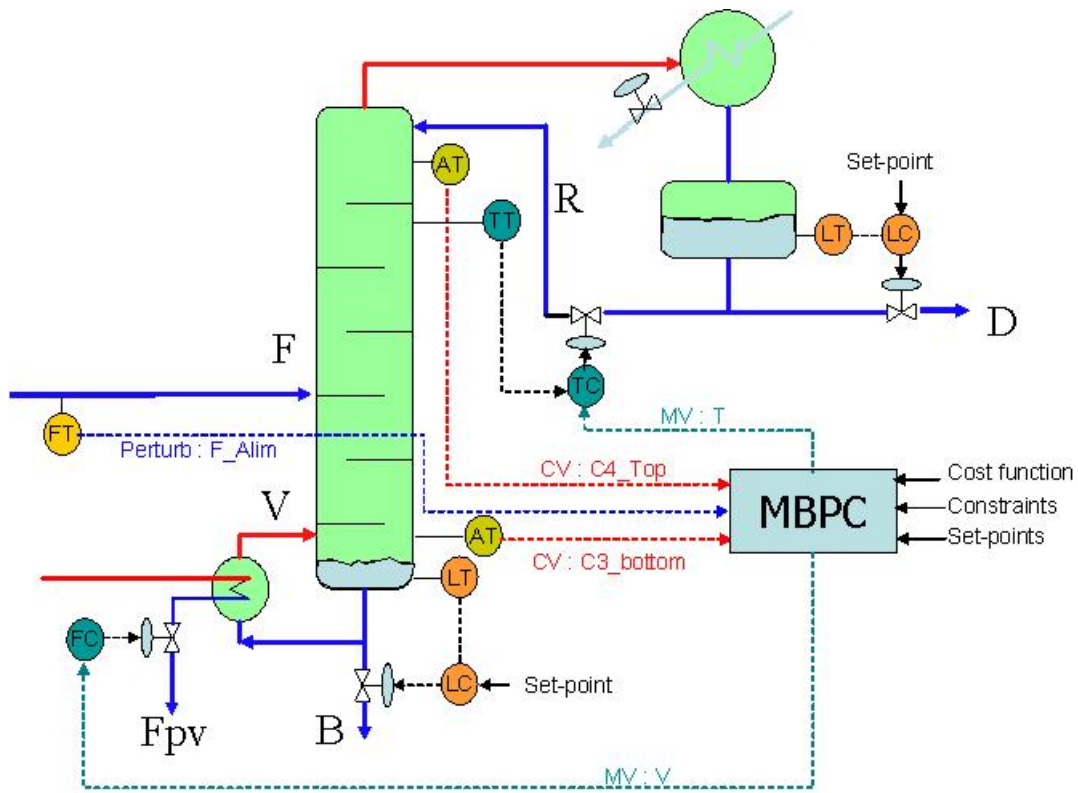


Figure 7.3: Control architecture of the distillation column

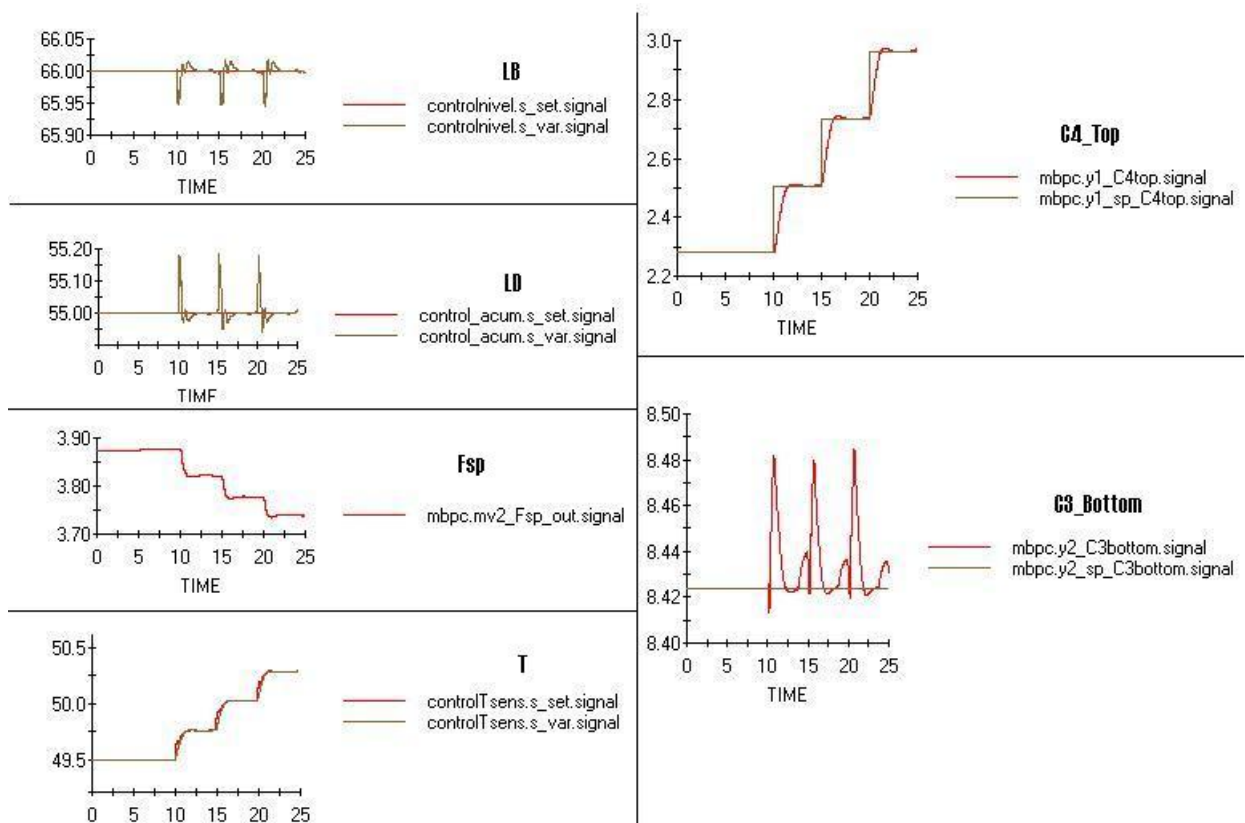


Figure 7.4: Simulation of the depropanizer with a DMC controller : steps of  $C4_{top}$

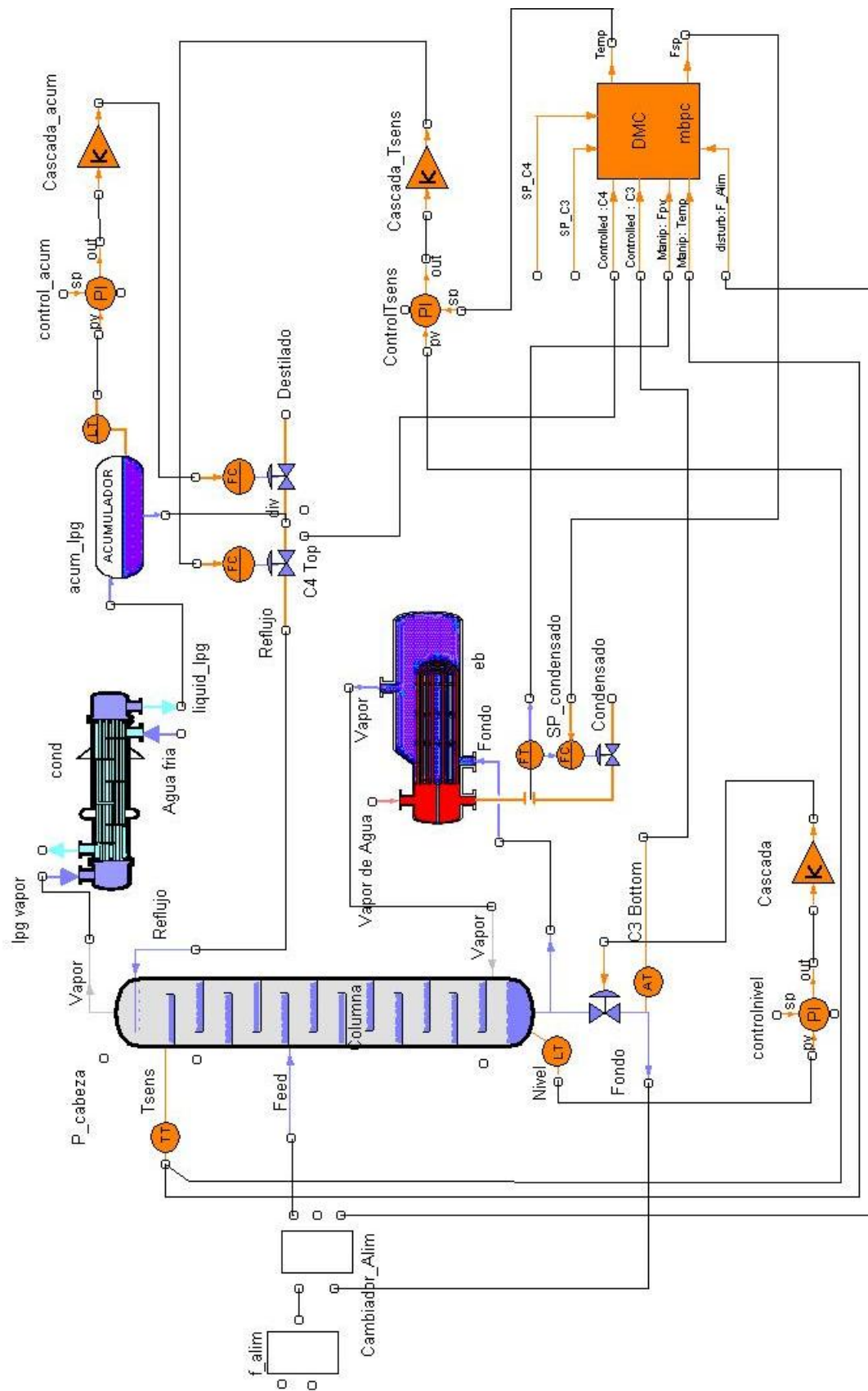


Figure 7.5: Control architecture of the distillation column in EcosimPro

# Chapter 8

## Optimization of the depropanizer

The distillation column has to furnish products (butane and propane) with a maximum amount of impurities. So, controlled variables which are these percentages of impurities has just to be maintained under this maximum limit. For example, if the maximum of propane in butane is fixed at 15% ( $C3_{botmax} = 15\%$ ), the set-point of this CV can takes values between 0% and 15%.

The aim of optimization is to calculate appropriate set-points in order to minimize the production cost during a normal operation of the process. To perform this, a cost function (quadratic or linear) subjected to constraints (linear or not) has to be minimized. The results of this minimization are values of set-points which allow to respect all constraints on the variables. So, manipulated variables are moving according to the values of set-points and if the model is consistent, all variables will stay between their optimization limits. Several studies of optimization on industrial processes have ever been done [RAM02] [LIA02] but it was steady-state optimization or with LP formulation. Here, we will study a steady-state optimization and also a dynamic optimization on the predictive horizon with a quadratic economic cost function.

First, the HITO library used for the predictive control and for the optimization will be described. Then, an economic cost function will be calculated to evaluate the operation cost of the column. After explaining different numerical data, a steady-state optimization will be achieved thanks to an optimization software (GAMS). Finally, a dynamic optimization will be purposed with HITO and simulations on EcosimPro will be done in order to confirm the different results.

### 8.1 HITO

In EcosimPro, a library called HITO (Integrated Tool for a Total Optimization) has been developed by the Engineering Systems and Automatic Control department of the Valladolid university. This library is used to achieve the predictive control. An optimization of set-points, directly included in HITO, can be also activated. The figure 8.1 resumes the general working of HITO. Steps of the algorithm are the following :

- Predictions are calculated thanks to the DMC controller using step-responses.
- Set-points of CVs are calculating minimizing an economic quadratic cost function : Optimization
- Values of MVs to apply on the process are calculated by an algorithm minimizing a cost function  $J$  respecting constraints and feasibility

To solve the problem of optimization, the algorithm of optimization minimizes a quadratic economic cost function (which can be composed of MVs, CVs and disturbances) using the predictions calculated and taking into account all constraints. One of the main advantage of HITO is that is using the same model in the DMC and in the optimization. Hence, results obtained in the DMC controller are coherent with set-points obtained in the optimization.

The parameters to give to the economic cost function are LPcosts of MVs ( $\zeta_m$ ), LPCost of CVs ( $\lambda_n$ ), LPcosts of disturbances ( $\xi_r$ ) and also a matrix which contains quadratic costs between all variables ( $\Psi_{ij}$ ). The cost function used by HITO is represented in the equation (8.1) when there are  $M$  manipulated variables,  $N$  controlled variables and  $R$  disturbances.

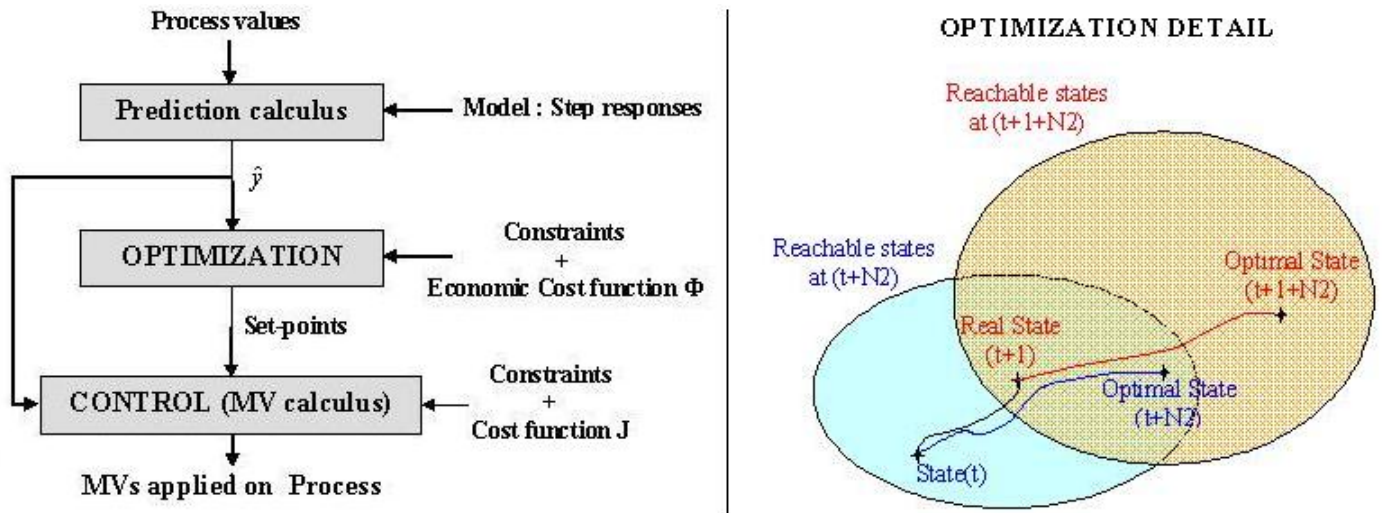


Figure 8.1: HITO algorithm with optimization

$$\begin{aligned}
 \phi = & \sum_{m=1}^M \sum_{j=1}^M \Psi_{m,j} \cdot u_m(t + Nu_m) \cdot u_j(t + Nu_j) + \sum_{n=1}^N \sum_{j=1}^N \Psi_{n+M,j+M} \cdot \hat{y}_n(t + N2_n) \cdot \hat{y}_j(t + N2_j) \\
 & + \sum_{r=1}^R \sum_{j=1}^R \Psi_{r+M+N,j+M+N} \cdot v_r(t) \cdot v_j(t) + \sum_{n=1}^N \sum_{m=1}^M \Psi_{n+M,m} \cdot \hat{y}_n(t + N2_n) \cdot u_m(t + Nu_m) \\
 & + \sum_{r=1}^R \sum_{m=1}^M \Psi_{r+M+N,m} \cdot v_r(t) \cdot u_m(t + Nu_m) + \sum_{r=1}^R \sum_{n=1}^N \Psi_{r+M+N,n+M} \cdot v_r(t) \cdot \hat{y}_n(t + N2_n) \\
 & + \sum_{m=1}^M \zeta_m \cdot u_m(t + Nu_m) + \sum_{n=1}^N \lambda_n \cdot \hat{y}_n(t + N2_n) + \sum_{r=1}^R \xi_r \cdot v_r(t)
 \end{aligned} \tag{8.1}$$

The main difference between the operating-point found by a classical steady-state optimization and by HITO which perform a dynamical optimization is that it finds a solution at the end of the prediction horizon calculating all intermediate positions at each sampling-time according to the actual operating point (see figure 8.2). Moreover HITO takes care to respect constraints on the velocity  $\Delta u$ . So, at each sampling time, the optimal operating point reachable in the predictive horizon is recalculated and normally at the end of the transitory, this operating-point should be fixed. The figure 8.1 shows the evolution of the optimization in HITO between 2 sampling time.

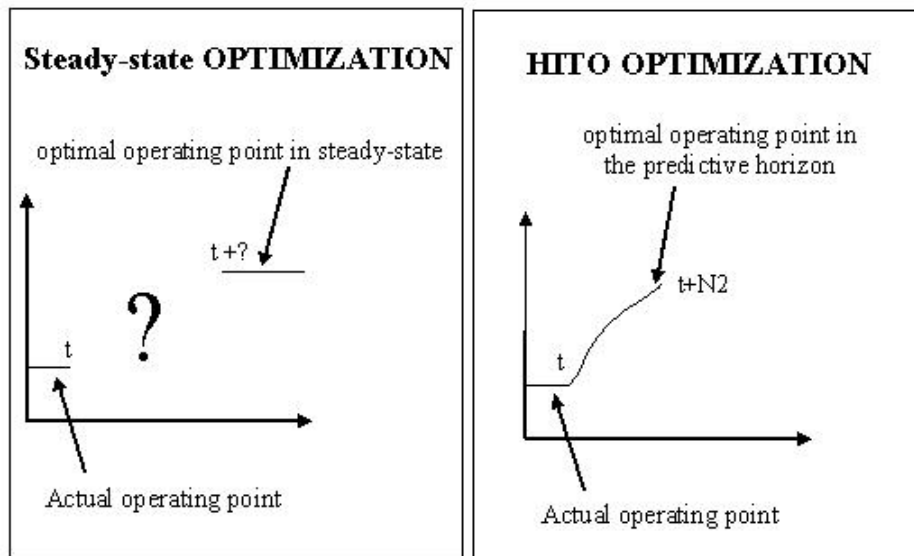


Figure 8.2: Steady-state and HITO optimization

## 8.2 Economic cost function

First, it's necessary to define all costs and gains of the process to determine an economic cost function. The costs are the quantity of steam introduced in the reboiler and of *LPG* (liquified Petroleum Gas) which fed the column in the middle. The benefits are the quantities of distillate (propane *C*<sub>3</sub>) and of bottoms (butane *C*<sub>4</sub>) which are going out and which can be sold on the market.

products	Names	unities	Costs
Feed	<i>LPG</i>	<i>Tm/h</i>	$+P_{LPG}$
Steam	<i>S</i>	<i>Tm/h</i>	$+P_S$
Distillate	<i>C</i> <sub>3</sub> : propane	<i>Tm/h</i>	$-P_{C3}$
Bottoms	<i>C</i> <sub>4</sub> : butane	<i>Tm/h</i>	$-P_{C4}$

Table 8.1: costs and benefits

According to the table 8.1 we can formulate the real cost of production  $\phi_{real}$  :

$$\phi_{real} = -C_4 \cdot P_{C4} - C_3 \cdot P_{C3} + S \cdot P_S + LPG \cdot P_{LPG} \quad (8.2)$$

The algorithm of optimization has to minimize this function finding the adequate MVs and CVs respecting all constraints. Hence, we have to transform this economic cost function  $\phi_{real}$  of the equation (8.2) in order to obtain a function  $\phi$  usable in HITO using MVs, CVs and disturbances like in the equation (8.1).

After several simulations in open-loop between operating-ranges with the non-linear model on EcosimPro, we have noticed that  $\Delta C_4$ ,  $\Delta C_3$  and  $\Delta LPG$  can be approximated by quadratic equations using  $\Delta F_{pv}$ ,  $\Delta T$  and  $\Delta F$  (see figure 8.3). Note that  $\Delta X = X - X_0$  where  $X_0$  is the initial value of  $X$ .

So, with the different results of simulations in open-loop we can explain  $C_4$ ,  $C_3$  and  $LPG$  of the equation (8.2) thanks to a quadratic equation composed of  $\Delta T$ ,  $\Delta F_{pv}$  and  $\Delta F$  using gains. Gains can be determined with an approximation of the curves obtained in simulation (figure 8.3) such that :  $\Delta Y = G_{Y/X} \cdot \Delta X + G_{Y/X^2} \cdot \Delta X^2$ .

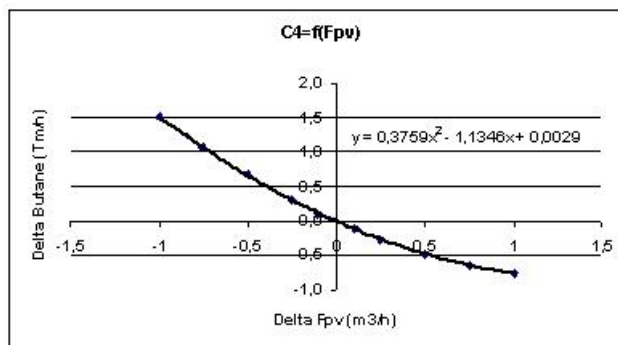


Figure 8.3: Relation between the butane and the condensate

Applying the principle of superposition we obtain the following expressions :

$$C_4 = C_{4moy} + G_{C4/T} \cdot \Delta T + G_{C4/T^2} \cdot \Delta T^2 + G_{C4/F_{pv}} \cdot \Delta F_{pv} + G_{C4/F_{pv}^2} \cdot \Delta F_{pv}^2 + G_{C4/F} \cdot \Delta F + G_{C4/F^2} \cdot \Delta F^2$$

$$C_3 = C_{3moy} + G_{C3/T} \cdot \Delta T + G_{C3/T^2} \cdot \Delta T^2 + G_{C3/F_{pv}} \cdot \Delta F_{pv} + G_{C3/F_{pv}^2} \cdot \Delta F_{pv}^2 + G_{C3/F} \cdot \Delta F + G_{C3/F^2} \cdot \Delta F^2$$

$$LPG = LPG_{moy} + G_{LPG/T} \cdot \Delta T + G_{LPG/T^2} \cdot \Delta T^2 + G_{LPG/F_{pv}} \cdot \Delta F_{pv} + G_{LPG/F_{pv}^2} \cdot \Delta F_{pv}^2 + G_{LPG/F} \cdot \Delta F$$

Moreover, the steam is proportional to the condensate:

$$S = k \cdot F_{pv} \Rightarrow P_S = \frac{P_{F_{pv}}}{k} \Rightarrow S \cdot P_S = F_{pv} \cdot P_{F_{pv}}$$

A virtual cost  $P_{F_{pv}}$  is introduced for the condensate  $F_{pv}$  because Vapor and condensate in the reboiler are strictly proportional. We can note that in all these relations, the impurities (the CVs  $C_{4top}$  and  $C_{3bot}$ ) are absent, it means that the economic cost of production not depend directly on these impurities.

So (8.2) is equivalent to :

$$\begin{aligned}
\phi_{real} = & -(C_{4moy} + G_{C4/T} \cdot \Delta T + G_{C4/Fpv} \cdot \Delta Fpv + G_{C4/F} \cdot \Delta F) \cdot PC4 \\
& -(G_{C4/T^2} \cdot \Delta T^2 + G_{C4/Fpv^2} \cdot \Delta Fpv^2 + G_{C4/F^2} \cdot \Delta F^2) \cdot PC4 \\
& -(C_{3moy} + G_{C3/T} \cdot \Delta T + G_{C3/Fpv} \cdot \Delta Fpv + G_{C3/F} \cdot \Delta F) \cdot PC3 \\
& -(G_{C3/T^2} \cdot \Delta T^2 + G_{C3/Fpv^2} \cdot \Delta Fpv^2 + G_{C3/F^2} \cdot \Delta F^2) \cdot PC3 \\
& +(LPG_{moy} + G_{LPG/T} \cdot \Delta T + G_{LPG/Fpv} \cdot \Delta Fpv + G_{LPG/F} \cdot \Delta F) \cdot PLPG \\
& +(G_{LPG/T^2} \cdot \Delta T^2 + G_{LPG/Fpv^2} \cdot \Delta Fpv^2) \cdot PLPG \\
& +Fpv \cdot P_{Fpv}
\end{aligned} \tag{8.3}$$

Now we can Factorize (8.3):

$$\begin{aligned}
\phi_{real} = & -(G_{C4/T} \cdot PC4 + G_{C3/T} \cdot PC3 - G_{LPG/T} \cdot PLPG) \cdot \Delta T \\
& -(G_{C4/Fpv} \cdot PC4 + G_{C3/Fpv} \cdot PC3 - G_{LPG/Fpv} \cdot PLPG) \cdot \Delta Fpv \\
& -(G_{C4/F} \cdot PC4 + G_{C3/F} \cdot PC3 - G_{LPG/F} \cdot PLPG) \cdot \Delta F \\
& -(G_{C4/T^2} \cdot PC4 + G_{C3/T^2} \cdot PC3 - G_{LPG/T^2} \cdot PLPG) \cdot \Delta T^2 \\
& -(G_{C4/Fpv^2} \cdot PC4 + G_{C3/Fpv^2} \cdot PC3 - G_{LPG/Fpv^2} \cdot PLPG) \cdot \Delta Fpv^2 \\
& -(G_{C4/F^2} \cdot PC4 + G_{C3/F^2} \cdot PC3) \cdot \Delta F^2 \\
& -(C_{4moy} \cdot PC4 + C_{3moy} \cdot PC3 - LPG_{moy} \cdot PLPG) \\
& +P_{Fpv} \cdot Fpv
\end{aligned} \tag{8.4}$$

Moreover  $\Delta Fpv = (Fpv - Fpv_0)$  and  $\Delta T = (T - T_0) \Rightarrow \Delta Fpv^2 = (Fpv^2 + Fpv_0^2 - 2 \cdot Fpv \cdot Fpv_0)$  and  $\Delta T^2 = (T^2 + T_0^2 - 2 \cdot T \cdot T_0)$ . So, replacing all terms and factorizing we can formulate the cost function as following :

$$\begin{aligned}
\phi_{real} = & -[G_{C4/T} \cdot PC4 + G_{C3/T} \cdot PC3 - G_{LPG/T} \cdot PLPG \\
& -2 \cdot T_0 \cdot (G_{C4/T^2} \cdot PC4 + G_{C3/T^2} \cdot PC3 - G_{LPG/T^2} \cdot PLPG)] \cdot T \\
& -[G_{C4/Fpv} \cdot PC4 + G_{C3/Fpv} \cdot PC3 - G_{LPG/Fpv} \cdot PLPG \\
& -2 \cdot Fpv_0 \cdot (G_{C4/Fpv^2} \cdot PC4 + G_{C3/Fpv^2} \cdot PC3 - G_{LPG/Fpv^2} \cdot PLPG) - P_{Fpv}] \cdot Fpv \\
& -[G_{C4/F} \cdot PC4 + G_{C3/F} \cdot PC3 - G_{LPG/F} \cdot PLPG \\
& -2 \cdot F_0 \cdot (G_{C4/F^2} \cdot PC4 + G_{C3/F^2} \cdot PC3)] \cdot F \\
& -(G_{C4/T^2} \cdot PC4 + G_{C3/T^2} \cdot PC3 - G_{LPG/T^2} \cdot PLPG) \cdot T^2 \\
& -(G_{C4/Fpv^2} \cdot PC4 + G_{C3/Fpv^2} \cdot PC3 - G_{LPG/Fpv^2} \cdot PLPG) \cdot Fpv^2 \\
& -(G_{C4/F^2} \cdot PC4 + G_{C3/F^2} \cdot PC3) \cdot F^2 \\
& +(G_{C4/T} \cdot PC4 + G_{C3/T} \cdot PC3 - G_{LPG/T} \cdot PLPG) \cdot T_0 \\
& +(G_{C4/Fpv} \cdot PC4 + G_{C3/Fpv} \cdot PC3 - G_{LPG/Fpv} \cdot PLPG) \cdot Fpv_0 \\
& +(G_{C4/F} \cdot PC4 + G_{C3/F} \cdot PC3 - G_{LPG/F} \cdot PLPG) \cdot F_0 \\
& -(G_{C4/T^2} \cdot PC4 + G_{C3/T^2} \cdot PC3 - G_{LPG/T^2} \cdot PLPG) \cdot T_0^2 \\
& -(G_{C4/Fpv^2} \cdot PC4 + G_{C3/Fpv^2} \cdot PC3 - G_{LPG/Fpv^2} \cdot PLPG) \cdot Fpv_0^2 \\
& -(G_{C4/F^2} \cdot PC4 + G_{C3/F^2} \cdot PC3) \cdot F_0^2 \\
& -C_{4moy} \cdot PC4 - C_{3moy} \cdot PC3 + LPG_{moy} \cdot PLPG
\end{aligned} \tag{8.5}$$

We can assembly constant terms in order to obtain finally :

$$\begin{aligned}
\phi_{real} = & -[G_{C4/T} \cdot PC4 + G_{C3/T} \cdot PC3 - G_{LPG/T} \cdot PLPG \\
& -2 \cdot T_0 \cdot (G_{C4/T^2} \cdot PC4 + G_{C3/T^2} \cdot PC3 - G_{LPG/T^2} \cdot PLPG)] \cdot T \\
& -[G_{C4/Fpv} \cdot PC4 + G_{C3/Fpv} \cdot PC3 - G_{LPG/Fpv} \cdot PLPG \\
& -2 \cdot Fpv_0 \cdot (G_{C4/Fpv^2} \cdot PC4 + G_{C3/Fpv^2} \cdot PC3 - G_{LPG/Fpv^2} \cdot PLPG) - P_{Fpv}] \cdot Fpv \\
& -[G_{C4/F} \cdot PC4 + G_{C3/F} \cdot PC3 - G_{LPG/F} \cdot PLPG \\
& -2 \cdot F_0 \cdot (G_{C4/F^2} \cdot PC4 + G_{C3/F^2} \cdot PC3)] \cdot F \\
& -(G_{C4/T^2} \cdot PC4 + G_{C3/T^2} \cdot PC3 - G_{LPG/T^2} \cdot PLPG) \cdot T^2 \\
& -(G_{C4/Fpv^2} \cdot PC4 + G_{C3/Fpv^2} \cdot PC3 - G_{LPG/Fpv^2} \cdot PLPG) \cdot Fpv^2 \\
& -(G_{C4/F^2} \cdot PC4 + G_{C3/F^2} \cdot PC3) \cdot F^2 \\
& +cste
\end{aligned} \tag{8.6}$$

After injecting these equalities in (8.2) we obtain a function of the HITO format (as the equation (8.1)) such that  $\phi_{real} = \phi + cste$  :

$$\phi = \zeta_T \cdot T + \psi_{T^2} \cdot T^2 + \zeta_{Fpv} \cdot Fpv + \psi_{Fpv^2} \cdot Fpv^2 + \zeta_{F} \cdot F + \psi_{F^2} \cdot F^2 \tag{8.7}$$

$\zeta_T$ ,  $\zeta_{Fpv}$  and  $\zeta_F$  represent linear costs (LPcosts),  $\psi_{T^2}$ ,  $\psi_{Fpv^2}$  and  $\psi_{F^2}$  represent quadratic costs (QPcosts).

Then, all linear and quadratic costs can be deduced by an identification (removing the constant) of (8.2) with (8.7):

$$\begin{aligned}
\zeta_T &= -G_{C4/T} \cdot P_{C4} - G_{C3/T} \cdot P_{C3} + G_{LPG/T} \cdot P_{LPG} \\
&\quad + 2 \cdot T_0 \cdot (G_{C4/T^2} \cdot P_{C4} + G_{C3/T^2} \cdot P_{C3} - G_{LPG/T^2} \cdot P_{LPG}) \\
\zeta_{Fpv} &= -G_{C4/Fpv} \cdot P_{C4} - G_{C3/Fpv} \cdot P_{C3} + G_{LPG/Fpv} \cdot P_{LPG} \\
&\quad + 2 \cdot Fpv_0 \cdot (G_{C4/Fpv^2} \cdot P_{C4} + G_{C3/Fpv^2} \cdot P_{C3} - G_{LPG/Fpv^2} \cdot P_{LPG}) + P_{Fpv} \\
\zeta_F &= -G_{C4/F} \cdot P_{C4} - G_{C3/F} \cdot P_{C3} + G_{LPG/F} \cdot P_{LPG} \\
&\quad + 2 \cdot F_0 \cdot (G_{C4/F^2} \cdot P_{C4} + G_{C3/F^2} \cdot P_{C3}) \\
\psi_{T^2} &= -G_{C4/T^2} \cdot P_{C4} - G_{C3/T^2} \cdot P_{C3} + G_{LPG/T^2} \cdot P_{LPG} \\
\psi_{Fpv^2} &= -G_{C4/Fpv^2} \cdot P_{C4} - G_{C3/Fpv^2} \cdot P_{C3} + G_{LPG/Fpv^2} \cdot P_{LPG} \\
\psi_{F^2} &= -G_{C4/F^2} \cdot P_{C4} - G_{C3/F^2} \cdot P_{C3}
\end{aligned} \tag{8.8}$$

Minimize the linear function (8.2) is equivalent to minimize the quadratic function (8.7) because  $\phi_{real} = \phi + cste$ .

### 8.3 Numerical Data

Generally, it exists two different specifications on the impurities:

- 1<sup>st</sup> spec : Propane and butane are pure at 85% minimum :  $C4_{Top} = C3_{bot} = 15\%$  maximum
- 2<sup>nd</sup> spec : Propane pure at 98% minimum and butane pure at 85% minimum :  $C4_{Top} = 2\%$ ,  $C3_{bot} = 15\%$  maximum

Other constraints are :

- Temperature on the sensible tray :  $48 \leq T \leq 57$
- Flow of the condensate :  $2.7 \leq F_{pv} \leq 4.8$

Normally, all the operating ranges of values have to be studied but relations between the temperature and  $C4$ ,  $C3$ ,  $C3_{bot}$ ,  $LPG$  can't be approximated by a quadratic function because the range of temperature is very large and so, important non-linearities happens (see graph at the top on the figure 8.4). In order to keep a quadratic approximation, the idea consists in separating the operating range of the temperature in two parts according to the specification of impurities selected. We know that if the second specification is chosen ( $C4_{top} = 2\%$  maximum) the temperature will be inferior to  $51^\circ C$  whereas if the first specification is chosen ( $C4_{top} = 15\%$  maximum) the temperature will be superior at  $51^\circ C$ . Hence, we can make 2 different quadratic approximations according to the specification (see the 2 graphs at the bottom on the figure 8.4). The table 8.2 summarizes all gains found with this method. Note that the quantity of  $LPG$  does not depend on  $F^2$  and  $C4_{Top}$  does not depend on  $T^2$  because these relations are linear, all the others are quadratic.

Now, we can calculate all LPcosts and QPcosts using equations of (8.8), gains of the tables 8.2 and original operating points of the table 8.3. The LPcost of  $T$  and the QPcost of  $T^2$  are different according to the specification selected because gains are different. All the results are in the table 8.4

	$C4_{top}(\%)$	$C3_{bottom}(\%)$	$C4$ (Tm/h)	$C3$ (Tm/h)	$LPG$ (Tm/h)
$T(^{\circ}C)$ 1 <sup>st</sup> spec	0.8848	-0.5544	-0.1615	0.2153	0.016
$T(^{\circ}C)$ 2 <sup>nd</sup> spec	0.8782	-1.9294	-0.3480	0.4829	0.0457
$Fpv(m^3/h)$	-0.0056	-6.8954	-1.1346	1.3625	0.1754
$F(m^3/h)$	-0.0024	0.5496	0.4213	0.049	0.476
$T^2$ 1 <sup>st</sup> spec	0.0	0.0302	0.0041	-0.0079	-0.0011
$T^2$ 2 <sup>nd</sup> spec	0.0	1.1018	0.17988	-0.2431	-0.0261
$V^2$	0.0068	1.5413	0.3759	-0.3672	-0.0253
$F^2$	0.0001	0.0005	0.0027	-0.0025	0.0

Table 8.2: Gains

$C4_{top0}(\%)$	$C3_{bottom0}(\%)$	$C4_0$ (Tm/h)	$C3_0$ (Tm/h)	$LPG_0$ (Tm/h)	$T_0(^{\circ}C)$	$Fpv_0(m^3/h)$	$F_0(m^3/h)$
2.279	8.423	16.196	7.624	23.928	49.5	3.875	46.9877

Table 8.3: original operating point in stable state

So, the final cost functions obtained for the two specifications are:

$$\begin{aligned}
\phi_1 &= -216.461 \cdot T + 1.908 \cdot T^2 + 126.282 \cdot Fpv - 19.786 \cdot Fpv^2 + 8.148 \cdot F - 0.116 \cdot F^2 \\
\phi_2 &= -2855.121 \cdot T + 28.184 \cdot T^2 + 126.282 \cdot Fpv - 19.786 \cdot Fpv^2 + 8.148 \cdot F - 0.116 \cdot F^2
\end{aligned} \tag{8.9}$$



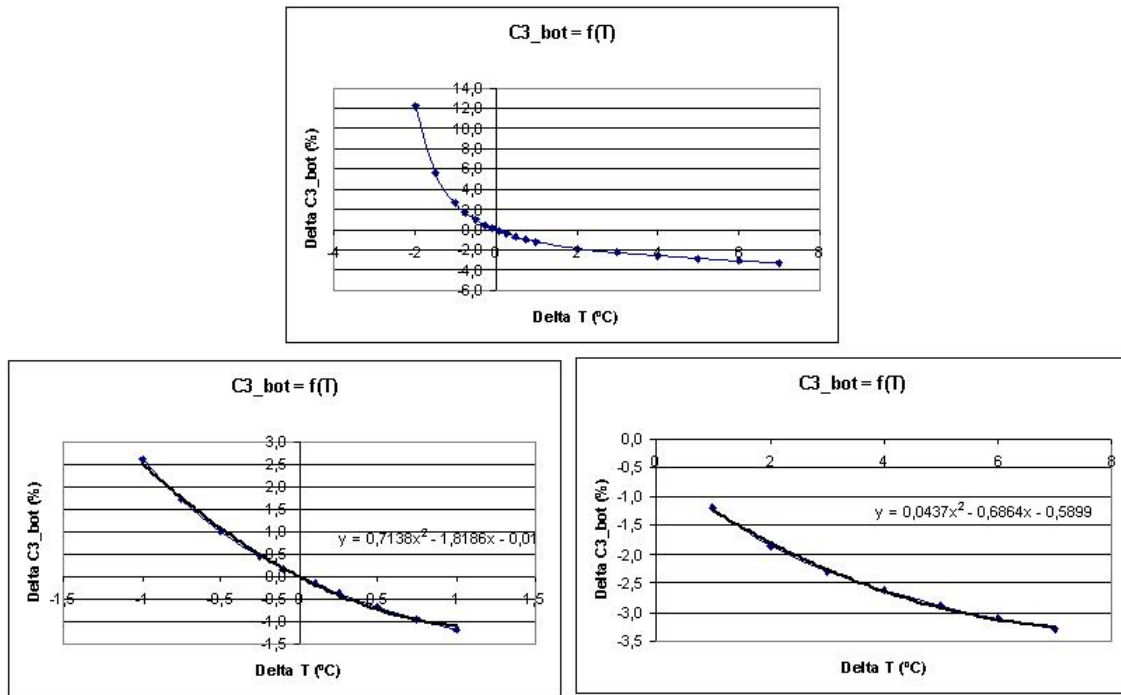


Figure 8.4: In order to have a quadratic approximation, temperature range is divided in two

LP/QP cost	1 <sup>st</sup> spec	2 <sup>nd</sup> spec
$\zeta_T$	-216.461	-2855.121
$\zeta_{Fpv}$	126.282	126.282
$\zeta_F$	8.148	8.148
$\psi_{T^2}$	1.908	28.184
$\psi_{Fpv^2}$	-19.786	-19.786
$\psi_{F^2}$	-0.116	-0.116

Table 8.4: LP and QP costs

## 8.4 steady-state optimization

To minimize the economic cost function (8.7) we have to formulate constraints on this function. So, these constraints have to be on the variables of the cost function ( $T$ ,  $Fpv$  and  $F$ ). Different constraints on the column are the following:

- Constraints on the manipulated variables  
 $[T_{inf}, Fpv_{inf}] \leq [T, Fpv] \leq [T_{sup}, Fpv_{sup}]$
- Constraints on the controlled variables  
 $[0, 0] \leq [C4_{top}, C3_{bot}] \leq [C4_{topmax}, C3_{botmax}]$
- The perturbation  $F$  fixed at its operating point  $F_0$

The problem is that CVs are absent of the economic cost function whereas there are constraints on these variables. The solution, as in the previous section, is to approximate CVs with MVs and disturbance thanks to simulations in open-loop in EcosimPro. After several simulations, the relations found are quadratic for  $C4_{top}$  and bilinear for  $C3_{bottom}$  :

$$C4_{top} = C4_{top0} + G_{C4_{top}/T} \cdot \Delta T + G_{C4_{top}/T^2} \cdot \Delta T^2 + G_{C4_{top}/Fpv} \cdot \Delta Fpv + G_{C4_{top}/Fpv^2} \cdot \Delta Fpv^2 + G_{C4_{top}/F} \cdot \Delta F + G_{C4_{top}/F^2} \cdot \Delta F^2$$

$$C3_{bot} = C3_{bot0} + G_{C3_{bot}/T} \cdot \Delta T + G_{C3_{bot}/Fpv} \cdot \Delta Fpv + G_{C3_{bot}/F} \cdot \Delta F + G_{C3_{bot}/TFpv} \cdot \Delta T \cdot \Delta Fpv$$

Now, we can formulate four inequalities equivalent to (8.16). Two inequalities from the constraint on the controlled variable  $C4_{top}$  :

$$-C4_{topsup} + C4_{top0} + G_{C4_{top}/T} \cdot \Delta T + G_{C4_{top}/T^2} \cdot \Delta T^2 + G_{C4_{top}/Fpv} \cdot \Delta Fpv + G_{C4_{top}/Fpv^2} \cdot \Delta Fpv^2 + G_{C4_{top}/F} \cdot \Delta F + G_{C4_{top}/F^2} \cdot \Delta F^2 \leq 0 \quad (8.10)$$

$$\begin{aligned} & -C_{4top0} - G_{C4top/T} \cdot \Delta T - G_{C4top/T^2} \cdot \Delta T^2 - G_{C4top/Fpv} \cdot \Delta Fpv \\ & - G_{C4top/Fpv^2} \cdot \Delta Fpv^2 - G_{C4top/F} \cdot \Delta F - G_{C4top/F^2} \cdot \Delta F^2 \leq 0 \end{aligned} \quad (8.11)$$

Two inequalities from the constraint on the controlled variable  $C3_{bot}$  :

$$\begin{aligned} & -C_{3botsup} + C_{3bot0} + G_{C3bot/T} \cdot \Delta T + G_{C3bot/Fpv} \cdot \Delta Fpv \\ & + G_{C3bot/F} \cdot \Delta F + G_{C3bot/TFpv} \cdot \Delta T \cdot \Delta Fpv \leq 0 \end{aligned} \quad (8.12)$$

$$\begin{aligned} & -C_{3bot0} - G_{C3bot/T} \cdot \Delta T - G_{C3bot/Fpv} \cdot \Delta Fpv \\ & - G_{C3bot/F} \cdot \Delta F - G_{C3bot/TFpv} \cdot \Delta T \cdot \Delta Fpv \leq 0 \end{aligned} \quad (8.13)$$

Replacing  $\Delta T$ ,  $\Delta Fpv$  and  $\Delta F$ , factorizing, we obtain finally :

$$\begin{aligned} & a_1 \cdot T^2 + b_1 \cdot Fpv^2 + c_1 \cdot F^2 + d_1 \cdot T + e_1 \cdot Fpv + f_1 \cdot F + g_1 \leq 0 \\ & -a_1 \cdot T^2 - b_1 \cdot Fpv^2 - c_1 \cdot F^2 - d_1 \cdot T - e_1 \cdot Fpv - f_1 \cdot F - h_1 \leq 0 \\ & a_2 \cdot T + b_2 \cdot Fpv + c_2 \cdot F + d_2 \cdot T \cdot Fpv + e_2 \leq 0 \\ & -a_2 \cdot T - b_2 \cdot Fpv - c_2 \cdot F - d_2 \cdot T \cdot Fpv - f_2 \leq 0 \end{aligned} \quad (8.14)$$

where :

$$\begin{aligned} a_1 &= G_{C4top/T^2} \\ b_1 &= G_{C4top/Fpv^2} \\ c_1 &= G_{C4top/F^2} \\ d_1 &= G_{C4top/T} - 2 \cdot T_0 \cdot G_{C4top/T^2} \\ e_1 &= G_{C4top/Fpv} - 2 \cdot T_0 \cdot G_{C4top/Fpv^2} \\ f_1 &= G_{C4top/F} - 2 \cdot T_0 \cdot G_{C4top/F^2} \\ g_1 &= -G_{C4top/T} \cdot T_0 - G_{top/Fpv} \cdot Fpv_0 - G_{top/F} \cdot F_0 + G_{C4top/T^2} \cdot T_0^2 + G_{C4top/Fpv^2} \cdot Fpv_0^2 + G_{C4top/F^2} \cdot F_0^2 \\ & - C_{4topsup} + C_{4top0} \\ h_1 &= -G_{C4top/T} \cdot T_0 - G_{top/Fpv} \cdot Fpv_0 - G_{top/F} \cdot F_0 + G_{C4top/T^2} \cdot T_0^2 + G_{C4top/Fpv^2} \cdot Fpv_0^2 + G_{C4top/F^2} \cdot F_0^2 \\ & - C_{4topinf} + C_{4top0} \\ a_2 &= G_{C3bot/T} - Fpv_0 \cdot G_{C3bot/TFpv} \\ b_2 &= G_{C3bot/Fpv} - T_0 \cdot G_{C3bot/TFpv} \\ c_2 &= G_{C3bot/F} \\ d_2 &= G_{C3bot/TFpv} \\ e_2 &= -G_{C3bot/T} \cdot T_0 - G_{C3bot/Fpv} \cdot Fpv_0 - G_{C3bot/F} \cdot F_0 - G_{C3bot/TFpv} \cdot T_0 \cdot Fpv_0 - C_{3botsup} + C_{3bot0} \\ f_2 &= -G_{C3bot/T} \cdot T_0 - G_{C3bot/Fpv} \cdot Fpv_0 - G_{C3bot/F} \cdot F_0 - G_{C3bot/TFpv} \cdot T_0 \cdot Fpv_0 - C_{3botinf} + C_{3bot0} \end{aligned}$$

This problem of minimization with quadratic and linear constraints can be formulated with matrix inequalities using the vector  $X = [T, Fpv]^T$  such that :

$$\min_X \phi(X, X^2) \quad (8.15)$$

Subject to :

$$g(X) \leq 0 \quad (8.16)$$

$$A \cdot X + B \leq 0 \quad (8.17)$$

The function  $\phi$  in the equation (8.15) is the economic cost function (8.7). The four quadratic inequalities of (8.14) can be formulated like in the equation (8.16).

The two constraints on the MVs ( $T$  and  $Fpv$ ) are expressed with 4 LMIs like in the equation (8.17) if:

$$A = \begin{bmatrix} 1 & 0 \\ -1 & 0 \\ 0 & 1 \\ 0 & -1 \end{bmatrix} \text{ and } B = \begin{bmatrix} -T_{sup} \\ -T_{inf} \\ -Fpv_{sup} \\ -Fpv_{inf} \end{bmatrix}$$

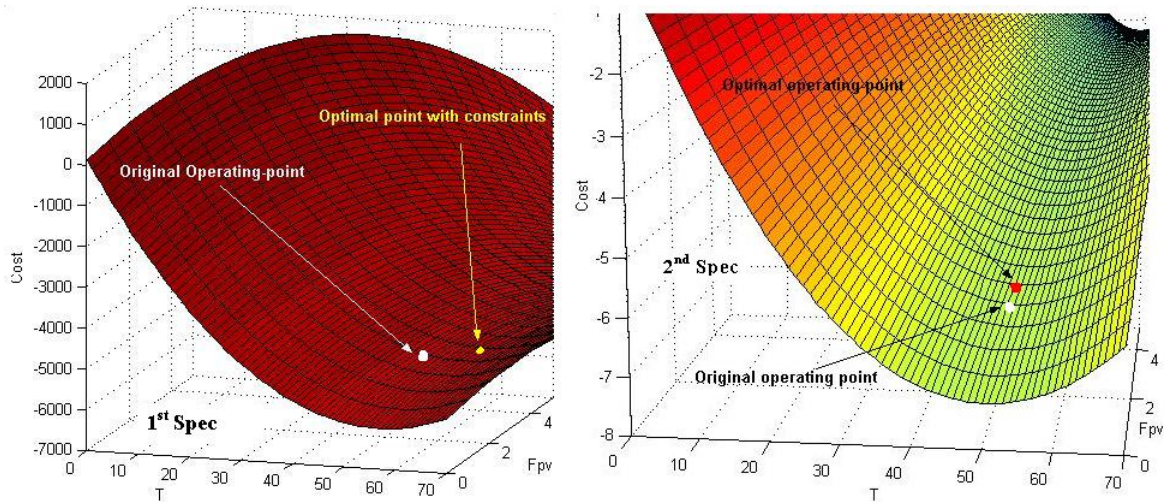
To solve this optimization problem, the software GAMS will be used. This professional software allows to solve a lot of different optimization problems (Linear, NonLinear, Mixed-Integer Linear, Mixed-Integer NonLinear Programming). We will use a NLP solver named SNOPT [MUR97]. SNOPT, (Sparse Nonlinear Optimizer) implements a sequential quadratic programming (SQP) method for solving constrained optimization problems with smooth nonlinear functions in the objective and constraints. In this method, a Quadratic Programming (QP) subproblem is solved using an estimation of the Hessian and of the Lagrangian at each iteration. So, optimal values of  $T$  and  $Fpv$  will be found minimizing the equation (8.7) subject to (8.16) and (8.17) (See the *Appendix C* for details of the GAMS program and its results).

Note that the optimal solution found by GAMS will be the solution to reach in steady-state because all relations used between variables are gains in steady-state. The transitory of variables is not assumed, there isn't any reference trajectory to follow. Optimal operating feasible points are found by GAMS for each specifications after 7 iterations of the algorithm. Results are the following :

Variable	initial value	optimal value spec 1	optimal value spec 2
$Fpv(m^3/h)$	3.875	4.8	4.8
$T(C)$	49.5	56.725	49.18
$C4_{top}(\%)$	2.279	8.672	2.00
$C3_{bottom}(\%)$	8.423	1.708	4.08
$C4(Tm/h)$	16.196	14.51	15.597
$C3(Tm/h)$	7.624	9.71	8.391
$LPG(Tm/h)$	23.92	24.12	24.05
cost function value(€)	-5719/ - 71951	-5862.3	-71970
real benefit(€)	214.77	427.19	227.32

Table 8.5: Optimal values of variables in theory

The solution of the each specification can be visualized on the figure 8.5 where the two different cost functions are represented according to  $Fpv$  and  $T$  when the perturbation  $F = F_0$ , the solution is at the bottom of the surface respecting all constraints.

Figure 8.5: Value of the cost function according to  $Fpv$  and  $T$  for each specification

With all gains and initial operating points we can calculate values of all the others variables for the optimal operating point. The table 8.5 resumes all these results. The *real benefit* corresponds to the calculation of the real cost function (8.2) but with opposite values (the benefit is the opposite of the cost).

$$real\ benefit = -\phi_{real} = C_4 \cdot PC_4 + C_3 \cdot PC_3 - Fpv \cdot P_{Fpv} - LPG \cdot P_{LPG}$$

## 8.5 Experiments on EcoSimPro

### 8.5.1 Basic simulations

In order to evaluate the performance of the optimization in EcoSimPro we will activate the optimization in the simulation after 7 min when the stationary state of the column is well established. Results of simulation are shown in the figures at the end.

In these simulations, the optimization of the HITO function gives more or less the same results as the results found with the GAMS in steady-state. All the variables take values close to the estimated values a priori. In both cases, we see that the optimization tries to maximize the quantity of propane produced reducing the quantity of butane because propane is more expensive and the column produced much more butane than propane because the concentration of butane is superior in the feed. We can also note that the two levels (of bottoms in the column and of distillate in the reflux drum) stay in acceptable limits during the transitory and remains stable in steady-state.

**1<sup>st</sup> specification**

In the first specification, the highest error is 62% on  $C3_{bottom}$  because the relation between  $\Delta T$  and  $\Delta C3_{bottom}$  is highly non-linear and the linear approximation of the DMC is not perfect. We can see on the figure 8.6 that the set-point of  $C3_{bottom}$  (the green line) found by the optimizer is not reached because of errors on predictions. But this error goes in the "right sense", so the real benefits obtained in simulation are higher than the benefits calculated previously in GAMS. With this optimization, the benefits are multiplied by two (429€ of benefits with optimization, 215€ at the original operating-point).

Variable	opt. values with dyn. optim	relative error with steady-state optim (table 8.5)
$Fpv(m^3/h)$	4.8	0%
$T(C)$	56.74	-0.03%
$C4_{top}(\%)$	8.811	+1.58%
$C3_{bottom}(\%)$	0.65	-62%
$C4(Tm/h)$	14.515	+1.83%
$C3(Tm/h)$	9.592	-1.26%
$LPG(Tm/h)$	24.103	-0.09%
cost function value(€)	-5862	+0.02%
real benefit(€)	429.70	+33.4%

Table 8.6: Optimal values of variables in simulation for the 1<sup>st</sup> specification

The steady-state is reached in more or less 10h. The main advantage is that with this dynamic optimization, the transitory is managed in order to not exceed constraints on MVs and CVs. Nevertheless we can see that the constraint on the temperature (which is a MV) is broken during a little instant at the beginning but this is not important because this constraint is just an operation constraint, not a physical constraint.

**2<sup>nd</sup> specification**

In the simulation with the second specification, the benefits found are inferior to the benefits calculated in steady-state a priori because the quantity of butane produced has been over-estimated. This benefit is very inferior to the benefit of the first specification, it is normal because the constraints are harder. We can't really compare with the initial operating-point these benefits because the initial state does not respect the constraint on the  $C4_{top}$  (which must be inferior to 2%).

The main problem easily discernable on the figure 8.7 is that the optimal operating point found by the optimization is moving at each iteration and so, the steady-state can't be reached. This phenomena comes from the cost function which is "very flat" around the operating point (see figure 8.5), so set-points are permanently moving. This phenomena not occurs with the first specification because the economic cost functions is different (LPcosts and QPcosts are not the same) and constraints are less stricted, the optimal operating-point is more insulated whereas for the second specification, the values available of the cost function are very similar.

To solve this problem, a stability policy could be achieved in order to fixe set-points when the the cost function oscillates. Here the non-stability not comes from the DMC controller or from the process but from the optimizer. During a simulation without optimizer (just with the DMC) fixing set-points on CVs which corresponds to optimal values in steady-state, the process is stable, benefits are maximized and constraints respected (figure 8.8).

Variable	opt. values with dyn. optim	relative error with steady-state optim(table 8.5)
$Fpv(m^3/h)$	4.8	0%
$T(C)$	49.16	-0.04%
$C4_{top}(\%)$	1.965	-1.78%
$C3_{bottom}(\%)$	4.09	-2.5%
$C4(Tm/h)$	15.597	-0.65%
$C3(Tm/h)$	8.392	+1.04%
$LPG(Tm/h)$	24.05	-0.04%
cost function value(€)	-71969	0.0%
gain of cost function(€)	17.501	-5%
real benefit(€)	226.74	-2.9%
real gain(€)	11.97	-53%

Table 8.7: Optimal values of variables in simulation for the 2<sup>nd</sup> specification

### 8.5.2 Moving of operating point with disturbances

A lot of exterior factors can disturb the column. In simulations, all temperatures, pressures and flows of external components are boundary variables which are fixed. Moreover, the composition of the feed can change along time according to the crude which fed the column. The only measurable disturbance takes into account in the DMC (and so, in the optimization) is the flow of the Feed ( $F$ ) which depends on the crude used. As the optimization is effectuated in real-time at each sampling-time, the optimal operating point has to move when a measurable disturbance occurs to keep an optimal operation of the column.

The flow of the feed is taking into account in the DMC, so predictions depend on this flow and we can easily understand that the optimal point will change. When the flow of the feed is moving in acceptable ranges (between 40 and 60  $m^3/s$ ), set-points of impurities are moving but we note that values of MVs are more or less the same at the optimal point with this disturbance.

If the composition (which is not measured) moves, a prediction error appears and MVs will move in order to reach the set-point ( $\Delta u \neq 0$ ). In this case, the predictions will be rectified because  $\hat{y}(t+j) = \sum_{i=1}^j g_i \cdot \Delta u(t-i+j) + p_j$  and as the predictions change during this non-measurable disturbance, the reachable states can be different and in this case, the optimization will find a new optimal set-point in this area whereas this disturbance is not measured. That is real advantage of this technique when the optimization uses predictions of the DMC.

The table 8.8 and the figure 8.9 show results when the composition of the feed change. The concentration of the feed is at the basis 56% of  $C_4$  and 44% of  $C_3$  and after 15minutes, the new composition is 65% of  $C_4$  and 35% of  $C_3$ .

Variable	initial optimal value	New optimal value with disturbance
$Fpv(m^3/h)$	4.8	4.8
$T(C)$	56.74	56.7
$C4_{top}(\%)$	8.811	9.015
$C3_{bottom}(\%)$	0.65	0.37
$C4(Tm/h)$	14.515	17.044
$C3(Tm/h)$	9.592	7.587
$LPG(Tm/h)$	24.103	24.442
cost function value(€)	-5862	-5862
real benefit(€)	429.70	403

Table 8.8: Disturbance on the composition of the Feed

As the predictions are moving, set-points move a little bit but the MVs remains stable because their values are the same for the new optimal operating-point. Of course, as the concentration of  $C_4$  is higher than previously, more butane and less propane is produced, so the real benefits decrease (the butane is cheaper than the propane) whereas the economic cost function don't move because values of MVs are the same.

### 8.5.3 Market price influence

The prices of different components (LPG, butane, propane, vapor) fluctuate according to the market. Hence, the optimal operating point varies with the prices. Moreover butane and propane prices are very close. In the previous simulations, butane was cheaper than propane but the inverse can happened on the market. That's why we have to check how the operating goes up or down with the prices.

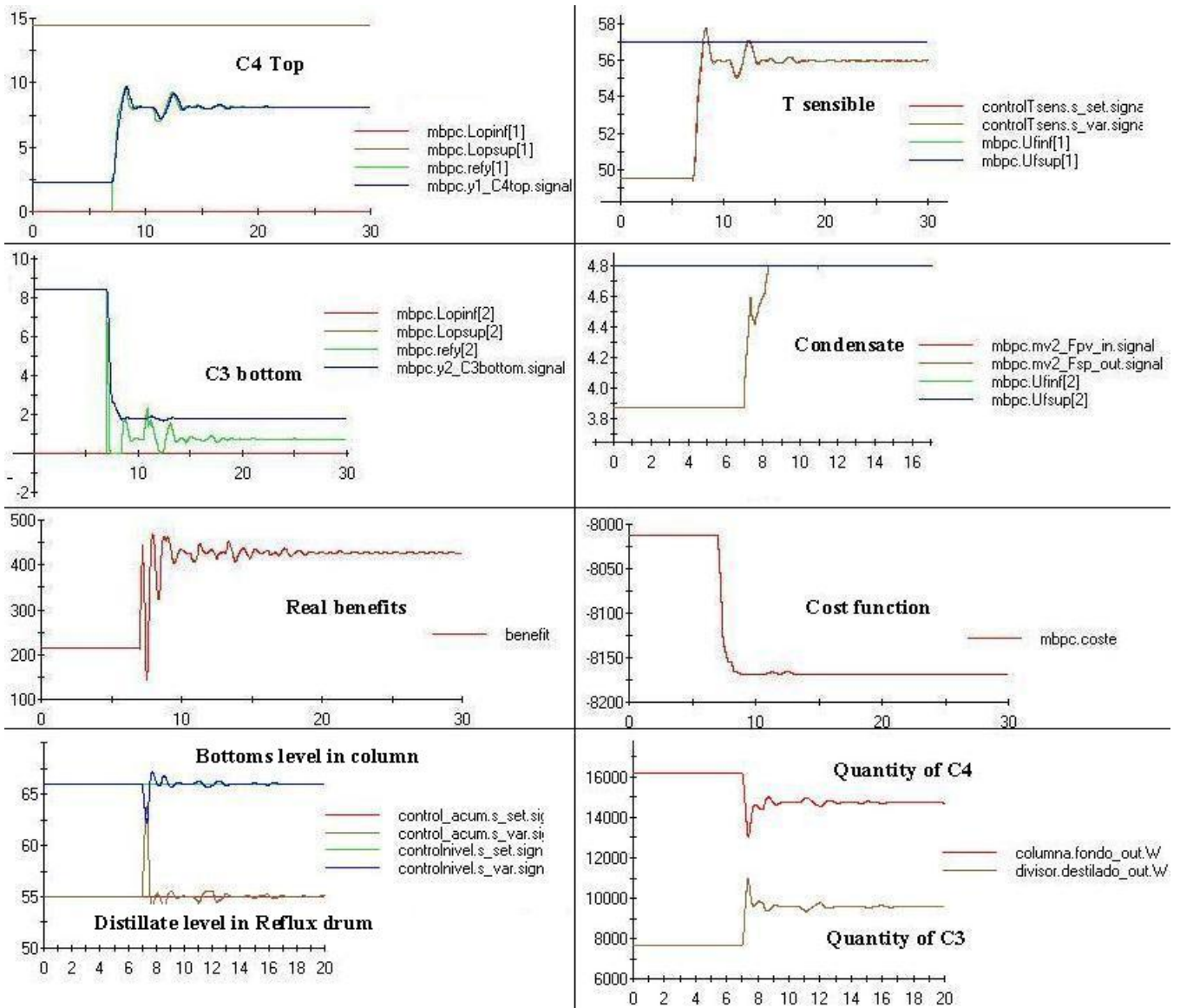


Figure 8.6: Simulation of the column : DMC with cost optimization with the 1<sup>st</sup> specification

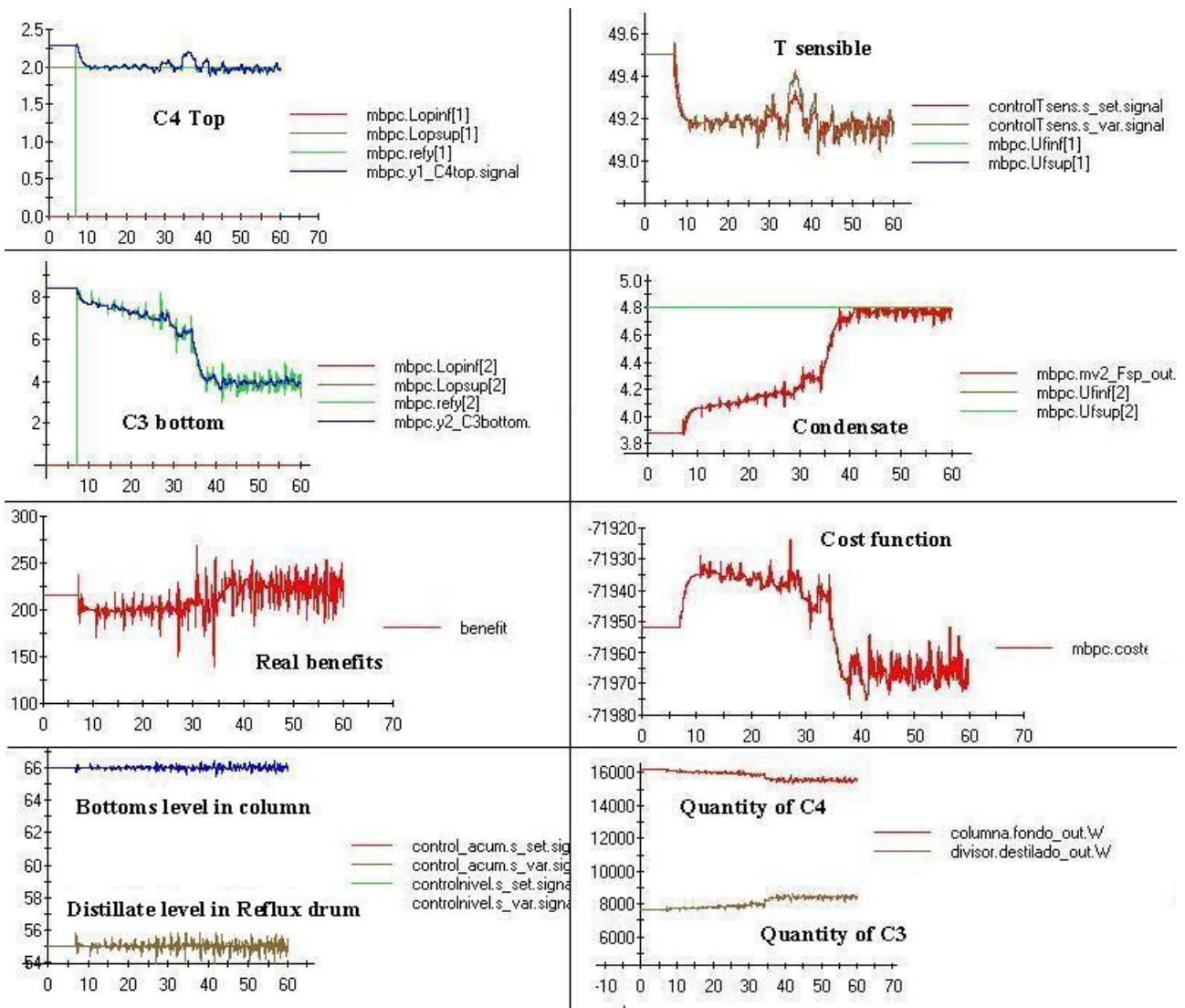


Figure 8.7: Simulation of the column : DMC with cost optimization with the 2<sup>nd</sup> specification

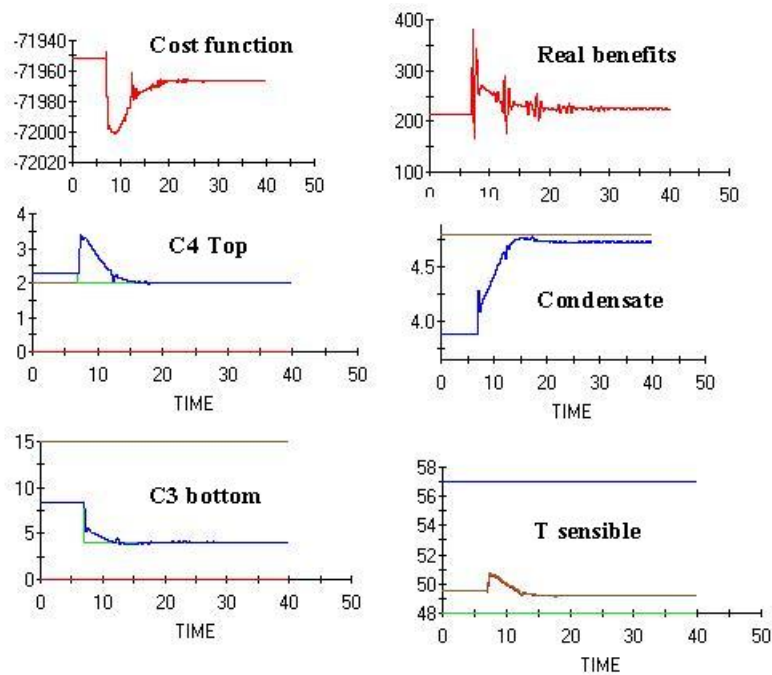


Figure 8.8: Simulation without optimization but using Optimal set-points of the 2<sup>nd</sup> specification on the DMC

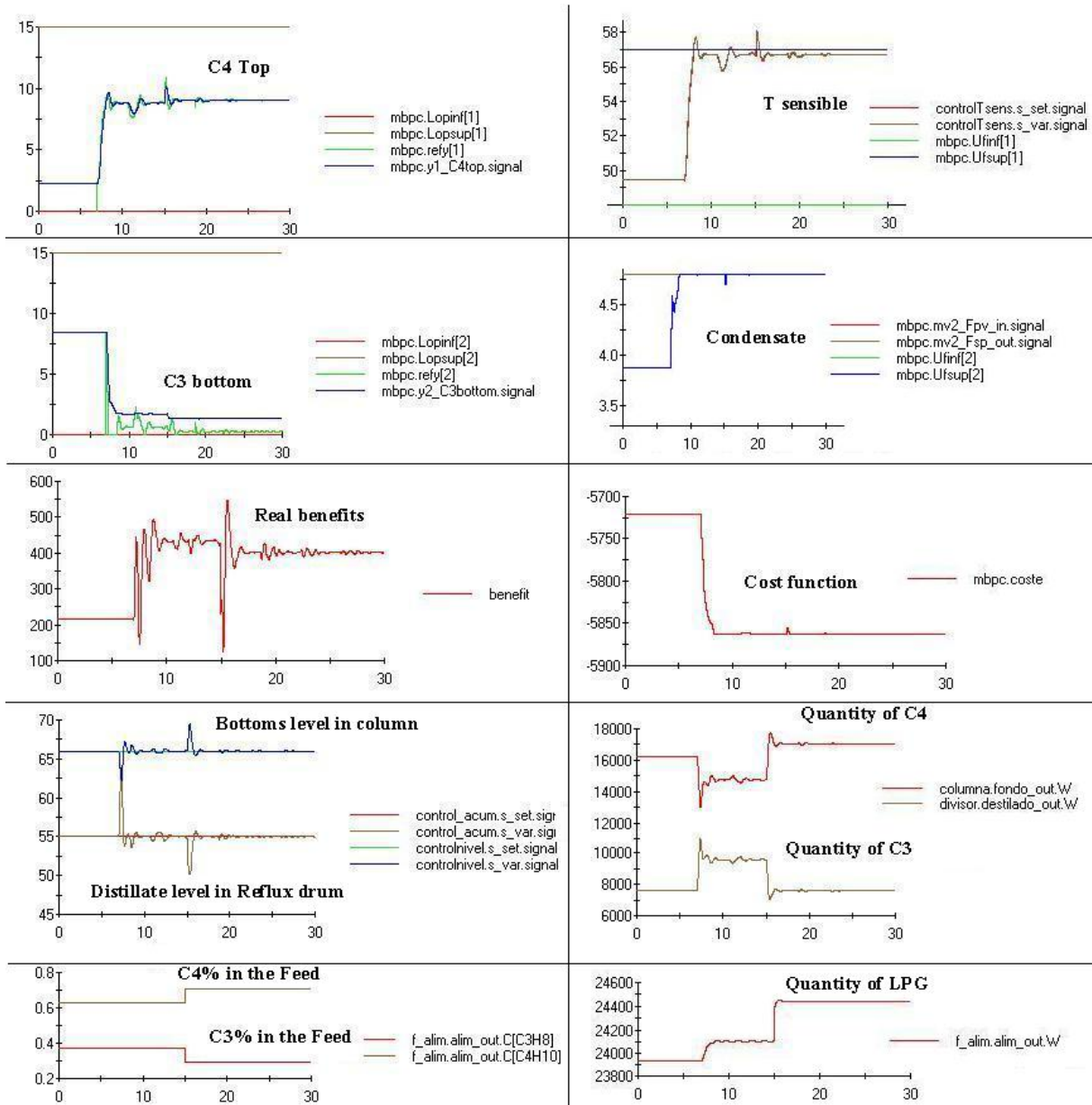


Figure 8.9: Simulation of the column with optimization at T=7 and disturbance on the feed at T=15



# Conclusion

In this report, identification, control and optimization have been studied on different processes. The common point between the different works achieved was the use of a Model Based Predictive Control (MBPC) thanks to HITO. Two different processes have been studied : a system of communicating tanks which is an experiment of the Systems Engineering and Automatic Control Department Laboratory and a distillation column based in a refinery in Tarragona, Spain.

Concerning the communicating tanks, the identification and the control have been performed on the real plant of the laboratory. Two different configurations have been studied (2 or 4 tanks). The parametrical identification used was a Least Square algorithm in both cases but different models were used according to the configuration in order to have a sufficient accuracy of the model (transfer functions for the 2 tanks and step responses for the 4 tanks). The two models found were validated with success thanks to other different experimental measurements.

Because of these different models, two different techniques were used to achieve the predictive control. A General Predictive Control (GPC) allowed to control the 2 tanks thanks to transfer functions and a Dynamic Matrix Control (DMC) controlled the 4 tanks using step responses. First, simulations have been done to check different parameters on the predictive control (horizons, sampling time..) and final tests have validated the control on the real plant. Experimental results are relatively close to the theoretical ones and the different tank levels are well regulated. This control rejects non-measurable disturbances on the manual valves and the robustness of the system is respected.

The main part of this report was the economic optimization using a predictive control of a distillation column. All the results have been performed thanks to simulation on EcosimPro with a non-linear rigorous model of the column. I have also written a paper summarizing the optimization of this distillation column (See Appendix B).

A DMC controller with an embedded dynamic optimization has been realized during this project. The main advantage is that the controller and the optimization are really correlated using the same predictions along the receding horizon. As the optimization is performed at each sampling time, the optimal operating-point is able to move rapidly when disturbances occurs or if some constraints move, it is not necessary to wait for new steady-state to perform the optimization like in the classical Real Time Optimizations (RTO). The results obtained in simulations are positive and the benefits are really maximized. Nevertheless, some problems of stability can occur during the optimization when the constraints are stronger because of the shape of the cost function. The analysis of the robustness and of the stability could be done in the future in order to find an appropriate algorithm to avoid this problem.

There are always some differences between the simulations and the real experiments even if the rigorous non-linear model used is very accurate. That is why all these results should be confirmed by tests on the real column but such systems are rarely available because they are continuously working in refineries.

This project allowed me to discover new fields of investigations with interesting applications of control theories in the chemical engineering. Many things remain to be made about control and optimization techniques for industrial plants. In the future, these kinds of techniques will be more and more used in order to reduce the consumption of energy. Moreover, nowadays processes are more and more complex and PID will not be able to control new processes. Modeling, simulations and MBPC techniques are the easiest industrial way to perform adequate control of such complex systems.

# Bibliography

- [BIT90] Bitmead, R.R., M. Gevers and V. Wertz. *Adaptive Optimal Control: the Thinking Man's GPC*. Prentice-Hall, 1990
- [CAM97] P.O. de Castro, E.F. Camacho. *Control e instrumentación de procesos quimicos*. Editorial Sintesis, 1997
- [CAR04] A.Carrière. *Identification paramétrique*. Polycopié ESIEE, 2004
- [CLA87] D. W. Clarke, C. Mohtadi, and P. S. Tuffs. *Generalized Predictive control*. Automatica, 1987
- [CUT79] C. R. Cutler, B. L. Ramaker. *Dynamic Matrix Control - a computer control algorithm*. Proceedings of the joint automatic control conference (JACC), San Francisco, CA. 1980
- [LIA02] Liankui Dai, Yang Wang *A simplified constrained multivariable controller with steady-state optimization*. 4<sup>th</sup> World Congress on Intelligent Control and Automation, 2002
- [MOR95] Zheng Z. Q. and M. Morari *Stability of model predictive control with mixed constraints*. IEEE Trans. on Automatic Control, 40(10), 1995
- [MUR97] PE Gill, W Murray, MA Saunders. *SNOPT: An SQP Algorithm for Large-Scale Constrained Optimization*. Numerical Analysis Report 97-2, Department of Mathematics, University of California, San Diego, La Jolla, CA, 1997.
- [PRA05] C. de Prada Moraga *Fundamentos de control predictivo de procesos*. Universidad de Valladolid, Dpto.de Ingeniería de Sistemas y Automática, 2005
- [RAM02] C. Ramos, J.S Senent, X.Blasco, J.Sanchis. *LP-DMC Control of a chemical plant with integral behaviour*. 15<sup>th</sup> Triennial World Congress, Barcelona, Spain, 2002
- [RAW99] James B. Rawlings. *Tutorial : Model Predictive Control Technology*. Proceedings of the American Control Conference, San Diego, California, 1999
- [RGM99] Rafael González Martín, Francisco Cifuentes Ochoa. *Curso DMCplus Basico*. Repsol Petronor, 1999
- [RGM04] Rafael González Martín. *Control multivariable predictivo : Casos y cosas practicas*. Automática e Instrumentación, n°352, 2004
- [RIC78] J. Richalet, A. Rault, J.L. Testud, J. Papon. *Model Predictive Heuristic Control : Applications to Industrial processes*. Automatica, 14, 413-428, 1978

# Appendix A: Mathematic model of distillation columns

## 2.4.2 MODELADO MATEMÁTICO DE COLUMNAS DE DESTILACIÓN

### Hipótesis de partida del modelado.

Para simular el comportamiento dinámico del proceso, se han hecho una serie de suposiciones que han sido justificadas en el apartado de alternativas:

- Alimentación en un único plato.
- La alimentación entra como líquido saturado, aunque se contempla la posibilidad de una vaporización parcial o total de ésta.
- Aunque no hay extracciones laterales, sí se tienen en cuenta en el modelo.
- No hay pérdidas de calor, la columna es adiabática.
- El condensador es total, por lo que la composición del vapor que abandona la columna por cabeza será la misma que la de la corriente de reflujo y destilado.
- El ebullidor es parcial, se vaporiza una parte de la corriente de fondo.
- El flujo de vapor se modela de dos formas distintas:
  - Como flujo de vapor no constante calculado a partir del balance de energía planteado en cada uno de los platos.
  - Como flujo molar de vapor constante en todos los platos.
- La pérdida de carga total de la columna se distribuye de forma lineal entre todos los platos.
- El flujo de líquido se calcula a partir de la fórmula de Francis para vertederos.
- El líquido acumulado en cada plato es incompresible y se encuentra como una mezcla perfecta; la composición será la misma en todos los puntos.
- La fase líquida y vapor que abandonan el plato se encuentran en equilibrio térmico, a la misma temperatura. También están a la misma presión.
- La fase líquido y vapor que abandonan el plato no están en equilibrio de fases debido a que se define una eficacia de Murphree.
- El equilibrio líquido – vapor se representa considerando:
  - Fase vapor como no ideal.
  - Fase líquida no ideal.
- Se desprecia el tiempo muerto en la corriente de vapor que va desde el último plato de la columna hasta el condensador, y también en la corriente de retorno del reflujo a la cabeza de la torre.
- Se considera la dinámica del condensador y del ebullidor en el desarrollo del modelo de la columna de destilación.
- No se considera acumulación de vapor a lo largo del sistema.

A continuación se presenta un diagrama simplificado de la columna con el fin de seguir mejor las explicaciones siguientes.

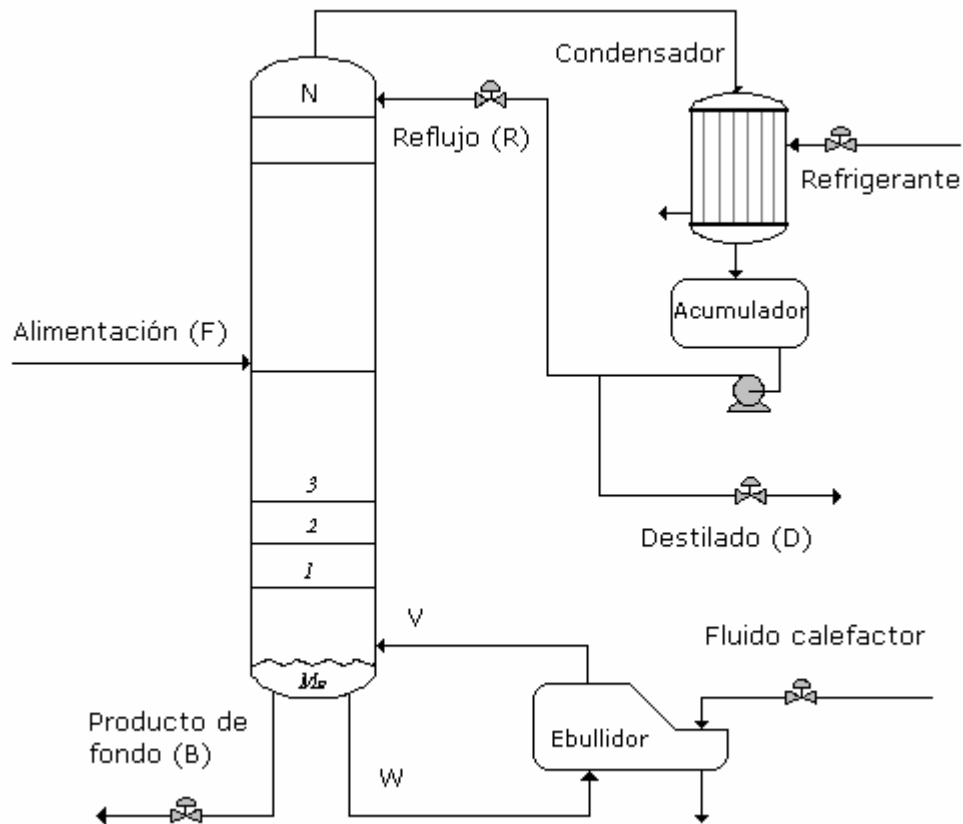


**Figura 2.1:Esquema una columna de destilación.**

A la hora de realizar el modelado se han llevado a cabo dos alternativas:

- Modelado considerando el flujo de vapor variable.
- Modelado considerando el flujo molar de vapor constante.

En este apartado se va a hacer la descripción de los balances de materia y energía, así como el resto de ecuaciones, diferenciando entre las dos alternativas de modelado cuando se requiera.

En los problemas de separación por etapas múltiples de sistemas en los que intervienen varias fases y varios componentes, es preciso proceder a la resolución simultánea, o iterativa, de cientos de ecuaciones.

Esto implica que es preciso especificar un número suficiente de variables de diseño de forma que el número de incógnitas (variables de salida) sea exactamente igual a número de ecuaciones (variables independientes).

Cuando esto ocurre, el proceso de separación está unívocamente especificado. Si se elige un número incorrecto de variables de diseño, puede que no exista una solución o bien obtener soluciones múltiples o inconsistentes.

Pero en la práctica, no se dispone de libertad para elegir las variables de diseño. Lo más frecuente es encontrarse en la situación en la que la composición de la alimentación, el número de etapas y/o las especificaciones de productos están fijadas y debe disponerse de las ecuaciones necesarias para la resolución.

### 2.4.2.1 Balances a la base de la columna.

A la base de la columna llega el líquido procedente del plato superior y la corriente de vapor procedente del ebullidor. El caudal de la corriente de fondo no es constante ya que es la variable manipulada para controlar el nivel de líquido en la base de la columna.

Un esquema sería el siguiente:

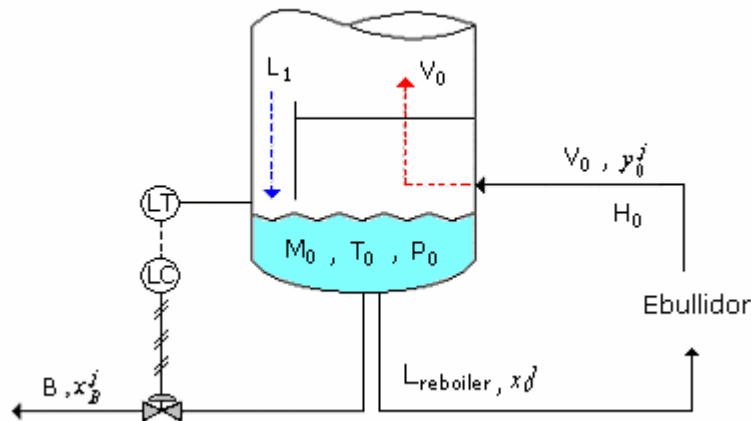


Figura 2.2: Esquema del fondo de la columna.

#### ❖ *Balances de materia, global y a los componentes.*

$$\frac{dM_0}{dt} = L_1 - B - L_{reboiler} \quad (2.1)$$

$$\frac{d(M_0 x_0^j)}{dt} = L_1 x_1^j - B x_B^j - L_{reboiler} x_B^j \quad (2.2)$$

El balance de materia se plantea para (j-1) componentes, y la fracción molar de uno de los componentes se calcula como:

$$x_B^j = 1 - \sum_{j=1}^{j=n-1} x_B^j \quad (2.3)$$

❖ **Balance global de energía.**

Tanto en la opción de modelado en la que el flujo de vapor se considera constante, como en la que es variable, es necesario plantear el balance de energía en estado no estacionario, es decir, dinámico. Como la columna se considera adiabática se obtiene:

$$\frac{d(M_0 h_0)}{dt} = L_1 h_1 - B h_0 - L_{reboiler} h_0 \quad (2.4)$$

*Cálculo de la temperatura en el fondo de la columna.*

La entalpía de la fase líquida calculada a partir de la ecuación anterior se puede expresar como una función cuadrática de la temperatura:

$$h = Atemp \cdot T^2 + Btemp \cdot T + Ctemp \quad (2.5)$$

Los parámetros *Atemp*, *Btemp* y *Ctemp* se obtienen a partir de:

$$\begin{aligned} Atemp &= \sum_{j=1}^{j=n} k_j^A x_j \\ Btemp &= \sum_{j=1}^{j=n} k_j^B x_j \\ Ctemp &= \sum_{j=1}^{j=n} k_j^C x_j \end{aligned} \quad (2.6)$$

	<i>Etanol</i>	<i>Propano</i>	<i>Butano</i>
$k_j^A$ (kJ/kmol·°C <sup>2</sup> )	$2.961 \cdot 10^{-3}$	$3.4719 \cdot 10^{-3}$	$2.8499 \cdot 10^{-3}$
$k_j^B$ (kJ/kmol·°C)	1.7158	0.9516	0.9578
$k_j^C$ (kJ/kmol)	0	0	0

**Tabla 2.1: Constantes que relacionan la entalpía del líquido con la temperatura.**

Así, a partir de la ecuación anterior se obtiene la temperatura en la base de la columna.

❖ **Presión total en la base.**

La presión en la base de la columna se calcula como la suma de las presiones parciales de los componentes, que a la vez son el producto de la presión de saturación de cada componente por la fracción molar.

$$P_B = \sum_{j=1}^j P_j = \sum_{j=1}^j (P_j^{sat} x_B^j) \quad (2.7)$$

**2.4.2.2. Balances un plato genérico.**

Las ecuaciones que representan el comportamiento de un plato genérico, son las mismas para toda la columna. En la descripción de los balances se distinguirán los dos planteamientos de modelado citados anteriormente cuando sea preciso.

Un esquema de cualquiera de estos platos sería el siguiente:

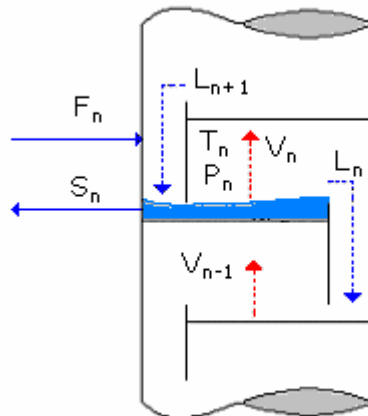


Figura 2.3: Esquema de un plato genérico.

❖ **Balances de materia, global y a los componentes.**

$$\frac{dM_n}{dt} = L_{n+1} + V_{n-1} + F_n - L_n - V_n - S_n \quad (2.8)$$

$$\frac{d(M_n x_n^j)}{dt} = L_{n+1} x_{n+1}^j + V_{n-1} y_{n-1}^j + F_n z_n^j - L_n x_n^j - V_n y_n^j - S_n x_n^j \quad (2.9)$$



El balance anterior se plantea para todos los componentes menos para uno que se calcula a partir de:

$$x_N^j = 1 - \sum_{j=1}^{j=n-1} x_N^j \quad (2.10)$$

❖ **Balance de global de energía.**

Aquí vamos a distinguir entre las dos posibilidades de modelado:

**A.** Flujo molar de vapor constante.

Esto significa que los flujos molares de vapor y líquido que abandonan cada etapa son constantes en la sección de agotamiento y de enriquecimiento de la columna. Esta afirmación únicamente será cierta cuando se cumplan las siguientes condiciones:

- Los componentes de la mezcla deben tener entalpías molares de vaporización muy similares y no debe cambiar significativamente en el rango de temperaturas en el que se opera.
- El calor específico de los componentes debe mantenerse constante en todo el rango de temperaturas de la torre.
- Los calores de mezcla no deben ser significativos.
- Las pérdidas de calor al ambiente son despreciables.

Estas condiciones se cumplen para aquellos sistemas cuyos componentes forman mezclas líquidas con un comportamiento cercano al ideal.

Pero, incluso cuando las entalpías de vaporización son significativamente diferentes, el error cometido al calcular el número de etapas suponiendo flujo molar constante es pequeño y aceptable.

En esta alternativa el flujo de vapor que recorre la columna permanece constante e igual al flujo de vapor procedente del ebullidor. Por lo tanto, se planteará el balance de energía en estado no estacionario, y a partir de él se calculará la temperatura en cada plato, como ya se ha explicado en el caso de la base de la columna.

$$\frac{d(M_n h_n)}{dt} = L_{n+1} h_{n+1} + V_{n-1} H_{n-1} + F_n h_n^F - L_n h_n - V_n H_n - S_n h_n \quad (2.11)$$

De este modo se calcularían las entalpías de la fase líquida en todos los platos, menos en el último plato.

## B. Flujo molar de vapor variable.

Si se considera esta alternativa, existen dos posibilidades a la hora de calcular el flujo de vapor que abandona cada plato de la columna de destilación.

- El flujo de vapor a través de los platos se puede calcular a partir de la pérdida de carga que hay de un plato al siguiente ( $P_{n-1} - P_n$ ) y la altura de líquido sobre el plato.

Esta altura de líquido será la suma de la altura del rebosadero ( $h_w$ ) y la altura de líquido sobre el rebosadero ( $h_{ow}$ ).

La pérdida de carga total es:

$$P_{n-1} - P_n = \frac{\rho_{L,n}(h_w + h_{ow,n})g}{10^5} + K_{DH} \rho_{V,n} (u_{V,n})^2 \quad (2.12)$$

A partir de aquí, el flujo volumétrico de vapor se calcula como:

$$\dot{V}_n = u_{V,n} A_{HOLE} \quad (2.13)$$

- El flujo de vapor también se puede calcular a partir del balance de energía en cada plato. En este caso, se tiene en cuenta la siguiente consideración:

los cambios en la entalpía específica de la fase líquida son por lo general muy pequeños comparados con la entalpía total del plato. Esto significa que, normalmente, el balance de energía se puede reducir a una ecuación algebraica a partir de la cual se calcula el flujo de vapor que abandona el plato. Por lo tanto, finalmente el balance de energía es el siguiente:

$$\begin{aligned} \frac{dh_n}{dt} &= 0 \\ V_n &= \frac{L_{n+1}(h_{n+1} - h_n) + V_{n-1}(H_{n-1} - h_n) + F_n(h_F - h_n)}{H_n - h_n} \end{aligned} \quad (2.14)$$

### ❖ Cálculo de la temperatura.

También aquí distinguimos entre las dos alternativas de modelado:

**A.** Flujo molar de vapor constante.

La temperatura se calcula, como en el caso de la base de la columna, a partir de:

$$h_n = Atemp_n \cdot T_n^2 + Btemp_n \cdot T_n + Ctemp_n$$

De este modo se calcularían las entalpías de la fase líquida y las temperaturas en todos los platos, menos en el último plato.

**B.** Flujo molar de vapor variable.

En este caso, la temperatura en cada plato no se obtiene a partir del balance de energía como ocurre en el fondo de la columna, sino que se calcula la temperatura de burbuja. La temperatura de burbuja es aquella temperatura que está en equilibrio con una composición del líquido conocida a una determinada presión también conocida.

Por lo tanto, en cada plato, el algoritmo de cálculo itera sobre la temperatura hasta que se cumple la siguiente condición:

$$1 - \sum_{j=1}^n y_j^N = 0 \quad (2.15)$$

Es decir, hasta que la suma de las composiciones de la fase vapor del plato N sea igual a la unidad.

Relación de equilibrio entre fases líquido – vapor:

$$y_{n,j}^* = \frac{\hat{\Phi}_{n,j}^{L,j} P_{n,j}^{sat}}{\hat{\Phi}_{n,j}^{v,j} P_n} x_n^j \quad (2.16)$$

❖ **Presión total en el plato n.**

**A.** Flujo molar de vapor constante.

La presión en los platos en este modelo se calcula como la suma de las presiones parciales de cada componente, que son a su vez el producto de la presión de saturación (función de la temperatura en cada plato) y de la fracción molar de cada componente en la fase líquida:

$$P_n = \sum_{j=1}^j P_n^j = \sum_{j=1}^j (P_j^{sat,j} x_n^j) \quad (2.17)$$

Se calcula así en todos los platos menos en el último, en el que la presión se mantiene fija a un valor.

**B. Flujo molar de vapor variable.**

En este caso, se fija la presión en la cabeza de la columna a un valor dado y las presiones en el resto de los platos se calculan como la presión en el plato superior más una pérdida de carga.

$$P_n = P_{n+1} + \Delta P \quad (2.18)$$

❖ **Pérdida de carga en el plato.**

La distribución de la pérdida de carga se considera lineal a lo largo de toda la columna y directamente proporcional al caudal de vapor vivo.

$$\Delta P = \left( \frac{V_0}{K} \right)^2 \quad (2.19)$$

❖ **Caudal de líquido que abandona el plato n:**

Se calcula a partir de la fórmula de Francis para vertederos segmentados:

$$h_{ow} = 664 \cdot \left( \frac{Q}{L_w} \right)^{2/3} \quad (2.20)$$

Así, el flujo de líquido que cae de un plato al inferior es:

$$Q_n = 6653.5 L_w (h_{ow,n})^{1.5} \quad (2.21)$$

$$h_{ow,n} = \frac{Vol_n - V_{plato}}{A_{plato}} \quad (2.22)$$

❖ **Caudal de vapor que abandona el plato n:**

**A. Flujo molar de vapor variable.**

En este modelo, el flujo molar de vapor que abandona cada plato es constante e igual al flujo de vapor procedente del ebullidor.

Se tiene en cuenta que el flujo de vapor en la zona de enriquecimiento de la columna puede ser distinto al de la zona de agotamiento en función de la condición térmica de la alimentación. Es decir, si la alimentación entra como líquido saturado, el flujo molar de vapor será el mismo en toda la columna. Pero si la alimentación se introduce como líquido frío, se producirá una condensación del vapor que abandona el plato de alimentación, con lo que el flujo molar de vapor en la zona de enriquecimiento será menor que el de la zona de agotamiento.

Y por el contrario, si la alimentación entra como una mezcla de líquido más vapor, el flujo molar de vapor de la zona de enriquecimiento será mayor que el de la zona de agotamiento.

### B. Flujo molar de vapor variable.

Como ya se ha dicho anteriormente, el flujo de vapor que va hacia el plato siguiente se calcula a partir del balance de energía en estado estacionario:

$$V_n = \frac{L_{n+1}(h_{n+1} - h_n) + V_{n-1}(H_{n-1} - h_n) + F_n(h_F - h_n)}{H_n - h_n} \quad (2.23)$$

#### 2.4.2.3 Balances al último plato.

Las corrientes que intervienen son:

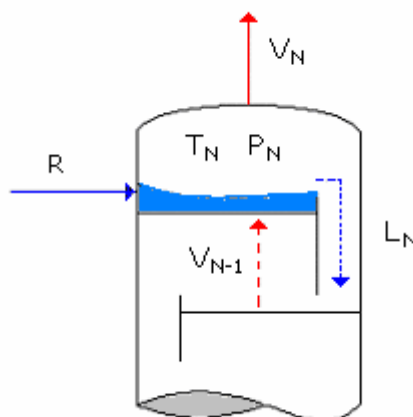


Figura 2.4: Esquema el último plato de la columna de destilación.

❖ **Balances de materia, global y a los componentes.**

$$\frac{dM_N}{dt} = V_{N-1} + R - L_N - V_N \quad (2.24)$$

$$\frac{d(M_N x_N^j)}{dt} = V_{N-1} y_{N-1}^j + R x_D^j - L_N x_N^j - V_N y_N^j \quad (2.24)$$

❖ **Balance global de energía:**

Tanto en el modelo de flujo de vapor constante como variable, el balance de energía en el último plato es en estado estacionario:

$$\frac{dh_N}{dt} = 0 \quad (2.25)$$

La temperatura se calcula de forma iterativa de manera que se cumpla la condición de que la suma de las fracciones molares de los componentes en la fase vapor sumen la unidad.

❖ **Presión en cabeza.**

La presión en cabeza se considera constante e igual a 15 bar:

$$P_{36} = 15 \text{ bar}$$

## 2.2 MODELADO DE OTROS PROCESOS UNITARIOS.

### 2.5.1 Condensador.

A la hora de realizar el modelo de un condensador debe tenerse en cuenta si se trata de un condensador parcial o total. Esto dependerá de los siguientes factores:

*La condición del destilado.*

Si el destilado puede producirse como vapor para su uso, y se cumplen el resto de los criterios expuestos a continuación, se elegirá un condensador parcial. Si, por el contrario, el destilado sólo tiene aplicación en su forma líquida, el producto debe ser enfriado o comprimido.

*Control de la relación de reflujo interna (destilado/vapor).*

Normalmente, cuando se utiliza un condensador parcial el líquido condensado se encuentra a la temperatura de burbuja y podría ser necesario un mayor caudal de reflujo líquido para aumentar la relación de reflujo interna.

Si se emplea un condensador total, el reflujo puede retornar a la columna como líquido subenfriado, y la relación de reflujo interna puede controlarse manipulando la temperatura del reflujo.

El vapor que sale del último plato entra en el condensador donde condensa totalmente. Se trata de un condensador vertical que utiliza como fluido refrigerante agua de proceso que circula por la carcasa.

Un esquema sería:

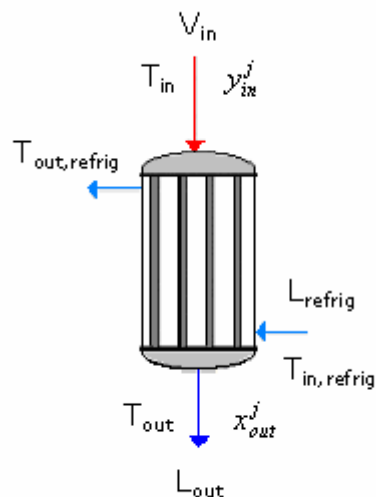


**Figura 2.5: Esquema del condensador de cabeza de la columna.**

❖ Balance de materia global y a (j-1) componentes:

$$\frac{dM_c}{dt} = V_{in} - L_{out} \quad (2.25)$$

Al producirse la condensación total del vapor que sale del último plato de la columna, la composición del condensado es la misma que la del vapor.

$$x_{out}^j = y_{in}^j \quad (2.26)$$

❖ Balance de energía a la masa de condensado.

$$\frac{d(M_c h_{out})}{dt} = V_{in} H_{in} - Q_{sub} - L_{out} h_{out} \quad (2.27)$$

El calor puesto en juego en el subenfriamiento se calcula a partir de:

$$Q_{sub} = U_{sub} A_{sub} (T_c - T_{inter,refrig}) \quad (2.28)$$

*Cálculo de la temperatura de la corriente de condensado.*

Se obtiene a partir de la entalpía calculada con el balance de energía a la masa de condensado mediante una función cuadrática que relaciona la entalpía del líquido con su temperatura.

❖ Balance de energía a la masa de refrigerante.

$$\frac{d(M_{refrig} h_{out,refrig})}{dt} = L_{refrig} (h_{out,refrig} - h_{in,refrig}) \quad (2.29)$$

## 2.5.2 Medio calefactor en columnas de destilación.

### **Kettle reboiler**

La forma habitual de producir la fase vapor en la columna es sometiendo a ebullición la mezcla líquida contenida en un ebullidor, utilizando como fluido calefactor vapor de agua.

Para ello se emplea un ebullidor tipo termosifón de circulación natural. Estos equipos pueden ser intercambiadores verticales con vaporización en los tubos o intercambiadores horizontales con vaporización en la carcasa. La circulación de líquido a través del cambiador es mantenido por la diferencia de densidad entre la mezcla bifásica de vapor y líquido en el intercambiador y por la fase líquida en la base de la columna.

Una desventaja que presentan estos ebullidor es que la base de la columna se debe elevar para proporcionar la carga hidrostática requerida para que tenga lugar el efecto termosifón. Esto incrementa los costes de las estructuras soporte de la columna.

En este caso es un ebullidor termosifón horizontal con ebullición por la parte exterior de la bancada de tubos. El flujo de vapor de calefacción es una variable independiente que se puede manipular para propósitos de control.



Un esquema sería el siguiente:

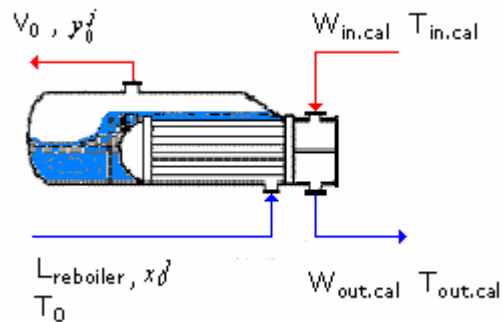


Figura 2.7: Esquema del flujo de vapor de calefacción.

En realidad, el funcionamiento de un ebullidor total es similar al de un condensador total. Por lo tanto, los balances de materia globales, a cada componente y de energía son iguales a los del condensador explicado anteriormente.

### Dinámicas de la fase vapor y líquido.

La dinámica de la fase vapor es, normalmente, mucho más rápida que la de la fase líquida. Esta es razón principal por la que la dinámica de las composiciones resulta compleja.

Variaciones en el suministro de vapor afectarán en poco tiempo a la composición del destilado. Sin embargo, la respuesta del proceso a cambios en caudales de líquido (reflujo) será mucho más lenta.

La respuesta hidráulica de un plato depende de la acumulación o disminución de líquido, que a su vez es función del diseño del plato. Un valor típico de constante de tiempo hidráulico para un plato de una aplicación industrial es de 3 a 10 s.

Se desprecia el tiempo muerto en la corriente de vapor que va desde el último plato de la columna hasta el condensador, y también en la corriente de retorno del reflujo a la cabeza de la torre. En columnas industriales esta suposición normalmente es cierta, no es así en columnas a escala de laboratorio.

### 2.5.3 Acumulador.

El flujo de condensado que abandona en condensador entra en un acumulador horizontal con una entrada y una salida, y se va a considerar mezcla perfecta.

El modelo matemático es el siguiente:

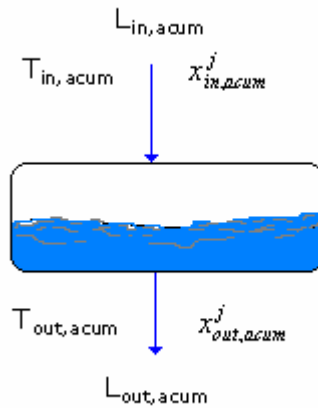


**Figura 2.6: Esquema de un deposito de acumulación horizontal.**

- ❖ Balance de materia global y a (j-1) componentes:

$$\frac{dM_{acum}}{dt} = L_{in,acum} - L_{out,acum} \quad (2.30)$$

$$\frac{d(Mx_{out}^j)}{dt} = L_{in}x_{in}^j - L_{out}x_{out}^j \quad (2.31)$$

- ❖ Balance de energía:

$$\frac{d(M_{acum}h_{out,acum})}{dt} = L_{in,acum}h_{in,acum} - L_{out,acum}h_{out,acum} \quad (2.32)$$

La temperatura se calcula, como ya se ha explicado anteriormente a partir de:

$$h_{out,acum} = Atemp_{out,acum} \cdot T_{out,acum}^2 + Btemp_{out,acum} \cdot T_{out,acum} + Ctemp_{out,acum}$$

## 2.3 DISEÑO DE LIBRERÍAS DE MODELOS CON ECOSIMPRO.

### 2.6.1 EcosimPro: lenguaje de simulación orientado a objetos.

Las librerías de modelos normalmente se conciben como un conjunto de módulos, con una determinada sintaxis, que representan unidades de proceso que pueden ser interconectadas para formar el modelo de un sistema más complejo.

Para el desarrollo de toda la simulación se ha utilizado una herramienta de modelado dinámico y simulación llamada EcosimPro.

EcosimPro utiliza un lenguaje de modelado orientado a objetos, este lenguaje utiliza modelos de conocimiento basado en ecuaciones diferenciales ordinarias y ecuaciones algebraicas.

El lenguaje de modelado de la herramienta ECOSIM se denomina EL (Ecosim Language). EL es un lenguaje de modelado continuo de sistemas orientado a objetos que permite realizar un modelado matemático de componentes complejos representados por ecuaciones algebraico-diferenciales. Los componentes se ven reflejados de una manera natural e intuitiva de entender.

EL es un lenguaje de simulación orientado a objetos que permite herencia entre componentes, agregación de componentes para la formación de otros más complejos y la modularidad de los mismos. Estas capacidades permiten al modelador reutilizar componentes ya probados para crear otros más complejos de manera incremental.

Los elementos más importantes de este lenguaje son los componentes. Un componente representa un modelo con unas variables, una topología, unas ecuaciones y un comportamiento basado en eventos. Un componente puede ser muy simple, por ejemplo una resistencia eléctrica o un condensador, con un par de ecuaciones, o muy complejo como en el caso de columnas de destilación, cientos de ecuaciones. Todo componente tiene un bloque para el manejo de ecuaciones continuas y otro para el manejo de los eventos. Además existen sentencias para describir la conexión entre componentes. Un modelo en EL de un sistema complejo consta de instancias de clases de componentes y sus sistemas de conexión. A continuación se debe generar el modelo, ECOSIM analiza el modelo del sistema de acuerdo con la sintaxis de EL y manipula simbólicamente las ecuaciones para generar automáticamente el modelo de simulación.

Una vez generado el modelo se pueden realizar experimentos sobre él. EL dispone de un lenguaje de experimentos que permite arrancar y parar la simulación, cambiar valores de parámetros, calcular estacionarios y obtener valores de las variables así como representar su evolución con el tiempo.

### **Conceptos fundamentales de EcosimPro.**

#### **❖ COMPONENT.**

Es la representación de un sistema o una parte de éste mediante ecuaciones algebraicas y diferenciales, variables, eventos discretos y topología.

Los componentes son el elemento más importante del modelado. Es donde se define el comportamiento continuo, discreto o secuencial.

En un componente se pueden distinguir 9 bloques opcionales, que son:

```
component_def ::= ABSTRACT? COMPONENT IDENTIFIER
                ( IS_A IDENTIFIER (,IDENTIFIER)* )?
                ( '(' parameters_s ')' )?
                ( PORTS port_decl_s )?
                ( DATA var_decl_s )?
                ( DECLS comp_decl_s )?
                ( TOPOLOGY topology_stm_s )?
                ( INIT seq_stm_s )?
                ( DISCRETE discrete_stm_s )?
                ( CONTINUOUS labelled_stm_s )?

                END COMPONENT
```

Los componentes pueden heredar variables y ecuaciones de un componente “padre”, o de varios (propiedad de herencia múltiple).

A continuación vamos a comentar las distintas partes de un componente:

- **Parámetros:** son variables que sirven para configurar el componente en el momento en que se instancia, luego no son variables de simulación. Se emplean para dimensionar arrays sobre un rango entero o sobre un rango enumerado (grupo de componentes químicos, por ejemplo), y para seleccionar ecuaciones alternativas.
- **Data:** en esta sección se especifican las variables cuyo valor es conocido y constante durante la simulación.
- **Decls:** en este bloque se declaran las variables y tipos locales que son visibles sólo dentro del componente y dentro de aquellos componentes que heredan de éste.
- **Topology:** representa la agregación de componentes y la conexión de éstos.
- **INIT:** aquí se declaran las variables que necesitan una inicialización en el componente.
- **Discrete:** en este bloque se definen los eventos discretos (sentencia WHEN, IF, THEN) y las comprobaciones (ASSERT).
  - ✓ IF-THEN-ELSE
  - ✓ WHILE
  - ✓ ASSERT
  - ✓ WHEN
  - ✓ DELAYED
- **Continuous:** en este bloque se definen las ecuaciones algebraicas y diferenciales que deben cumplirse a lo largo de toda la simulación. Dentro de este bloque se incluyen:

- ✓ Ecuaciones matemáticas: ODE o DAE  
 $2*y-3*\sin(\text{TIME}) = 3*x$   
 $x'' + \cos(\text{TIME}) = 4x'$
- ✓ Sentencia EXPAND: expandir una ecuación.  
EXPAND(j IN Chemical) masa\_in[j] = masa\_out[j]
- ✓ Sentencia ZONE: permite cambiar de modelo mientras la simulación se ejecuta en función de una condición.  
 $X = \text{ZONE}(m>0) \quad y + z$   
 $\text{ZONE}(m>1) \quad y + 3*\sin(\text{TIME})$   
OTHERS 5

## ❖ PORT.

Los puertos sirven de conexión entre un componente y otro. Pueden crearse diferentes tipos de puertos en función de las necesidades de modelado.

La misión de los puertos es el intercambio entre componentes de unas determinadas variables definidas en el puerto. Tiene como ventaja el que no hay que conectar variable a variable, y permite introducir “inteligencia” a las variables al permitir definir las como SUM, EQUAL, etc.

## ❖ PARTITION.

Una partición es el modelo matemático asociado a un componente.

EcosimPro presenta tres opciones a la hora de realizar la partición de un componente:

1. Definir una partición por defecto.
2. Definir una partición manual, de manera que si se detecta un modelo matemático incompleto o con problema, EcosimPro lanza unos asistentes para obtener la información necesaria del usuario.
3. Definir una partición de diseño. En este caso se puede convertir un dato en variable y continual haciendo la partición manual.

Pueden presentarse los siguientes casos:

- Si hay más variables que ecuaciones, éstas deben darse en forma de condiciones de contorno.
- En el caso de formarse lazos algebraicos, el usuario debe indicar con qué variables se rompe.

- Si se presenta el caso de Índice Superior, hay que indicar qué variables no son de estado.

### ❖ EXPERIMENT:

De cada uno de los modelos pueden realizarse distintos casos de simulación o experimentos.

Los experimentos se realizan después de haber generado la partición del componente, y pueden definirse múltiples experimentos sobre la misma partición. Dentro del experimento se puede implementar cualquier sentencia secuencial.

Los bloques de un experimento son:

```

experiment_def ::= experiment_item_s
                EXPERIMENT IDENTIFIER ON scoped_id
                ( DECLS var_decl_s )?
                ( INIT expt_assign_stm_s )?
                ( BOUNDS expt_assign_stm_s )?
                ( BODY seq_stm_s )?
                END EXPERIMENT
experiment_item_s ::= ( use_stm | extern_func_decl |
                    function_def ) *

```

Las principales funciones son:

- ✓ INTEG(), INTEG\_TO, INTEG\_CINT, INTEG\_STEP
- ✓ TIME, TSTOP
- ✓ SAVE\_STATE, RESTORE\_STATE
- ✓ REPORT\_TABLE

### ❖ LIBRARY.

En las librerías se agrupan los distintos componentes, puertos, enumerados o variables globales que están relacionados con una misma disciplina.

Dentro de una librería puede haber: COMPONENTS, PORTS, FUNCTIONS, EXTERNAL FUNCTIONS PRE-DECLARATIONS, EXPERIMENTES, ENUMERATIVE TYPES, GLOBALS CONSTANT Y VARIABLES.

Una librería puede utilizar elementos de otra empleando la sentencia USE.

## 2.6.2 Creación de librerías

La definición de los modelos de cada componente básico no difiere mucho del modo en el que se definen en otros lenguajes de modelado orientados a objetos, (puertos, datos,

declaración de variables locales, topología, parte continua del modelo, parte discreta del modelo y condiciones de inicialización).

Sin embargo una de las particularidades de ECOSIMPRO que le hacen útil para el modelo de sistemas de la industria de procesos es la capacidad de definir productos de modo que cada uno de ellos está formado por un subconjunto de compuestos químicos de entre todos los que pueden aparecer en un producto. De este modo se pueda particularizar el modelo de cada unidad elemental en función de los productos que reciban en cada uno de sus puertos. Como ejemplo de modelo de unidades elementales se muestra el código del modelo de una bomba centrífuga, así como su ubicación dentro de la librería a la que pertenece. Dicha ubicación se realiza usando las propiedades de herencia y agregación de ECOSIMPRO.

La librería de modelos desarrollada actualmente tiene tres grandes partes. En la primera se definen un conjunto de funciones que encapsulan las propiedades físicas necesarias en los modelos, fundamentalmente formadas por ecuaciones algebraicas que relacionan las diversas variables que pueden aparecer en los modelos.

La segunda en la que se definen todos los posibles conectores o tipos de puertos a utilizar.

La última contiene un conjunto de librerías de las unidades de proceso, de modo que existe una librería de unidades comunes

#### ❖ **Librería de Propiedades Físico – Químicas.**

Para realizar la simulación es necesario implementar previamente una serie de propiedades físicas de cada uno de los componentes de forma individual, así como de funciones de propiedades medias de mezclas y constantes globales.

A continuación se va a desarrollar brevemente cómo se ha llevado a cabo esta librería de propiedades físico-químicas.

#### **Implementación.**

- Definición de Enumerados.

En primer lugar es necesario definir todas las especies químicas que van a formar parte de los modelos que se desarrollarán posteriormente. Para ello, se emplea la sentencia *ENUM* propia de EcosimPro.

También es necesario implementar todos los subconjuntos de especies químicas que se van a emplear en las distintas operaciones básicas. En este caso, la sentencia utilizada es *SET\_OF*.

```

ENUM Chemical = {H2O, azucar, marco, impz, sacarosa, cristales, CaO, CaOH2, \ O2, N2, CH4, C3H8,
                CO, CO2, EtOH, PrOH, Iso, CH3, CH2, \ OH, CH3OH, CH3CO, CH,
                no_azucar}
SET_OF (Chemical)humos = {O2, N2, CH4, C3H8, CO, CO2, H2O}

```

- Definición de Propiedades Físico-Químicas de cada especie.

El siguiente paso es la implementación de las propiedades físico-químicas necesarias de cada una de las especies químicas definidas en el enumerado. Estas propiedades están definidas tanto para la fase líquido como para la fase vapor de los compuestos químicos. Se encuentran en forma de ecuaciones o de tablas y se calculan a partir de los argumentos correspondientes en cada caso (presión, temperatura, concentración, etc). Algunas de estas propiedades son las siguientes:

- Densidad.
- Presión de saturación.
- Temperatura de saturación.
- Entalpía específica.
- Viscosidad.
- Conductividad.
- Etc...

Un ejemplo de implementación de una propiedad en forma de ecuación sería el siguiente:

```

-- PRESIÓN DE SATURACIÓN (bar) en función de la temperatura (°C) del vapor de agua
FUNCTION REAL pres_sat_w (REAL T)
DECLS
  REAL P
BODY
  P = exp (11.68346 - 3816.44 / (T + 273.15 - 46.13))
  RETURN P
END FUNCTION

```

Diagrama de anotaciones:

- Una flecha azul apunta desde el texto "Variable Independiente" a la variable **T** en el parámetro de la función.
- Otra flecha azul apunta desde el texto "Variable Dependiente" a la variable **P** en el cuerpo de la función.

Y en forma de tabla sería:

```

-- CALOR ESPECÍFICO DEL VAPOR DE AGUA SATURADO
FUNCTION REAL Cpv_wsat_T (REAL T)
DECLS
  REAL H
  TABLE_1D cesp_vsatsat = {{1., 5., 10., 15., 20., 40., 60., 80., 100., 120., 140.}, \

```



```

                {2.027,2.329,2.595,2.820,3.025,3.788,4.613,5.600,6.770,8.158,10.150} }
BODY
    H = linearInterp1D(cesp_vsate, T)
    RETURN H
END FUNCTION

```

- Definición de Propiedades Físico-Químicas “generales”.

En este caso se trata de implementar funciones en las que con una única llamada se puedan calcular propiedades físico-químicas medias de los distintos enumerados que se han definido previamente.

```

FUNCTION REAL entalp_liquido (SET_OF(Chemical)Mix, REAL T, REAL C[Mix])
DECLS
    REAL h
    CONST STRING mensaje = "el liquido requerido no está incluido en la función de cálculo"
BODY
    IF(setofCmp(Mix, agua)) THEN
        h = entalp_w(T)
        RETURN h
    ELSEIF(setofCmp(Mix, lechada)) THEN
        h = entalp_lechada(T, C[CaOH2])
        RETURN h
    ELSEIF(setofCmp(Mix, destila)) THEN
        h = entalp_destila(Mix, T, C)
        RETURN h
    ELSEIF(setofCmp(Mix, especies)) THEN
        h = entalp_especies(Mix, T, C)
        RETURN h
    ELSE
        PRINT (mensaje)
    END IF
    RETURN 0.
END FUNCTION

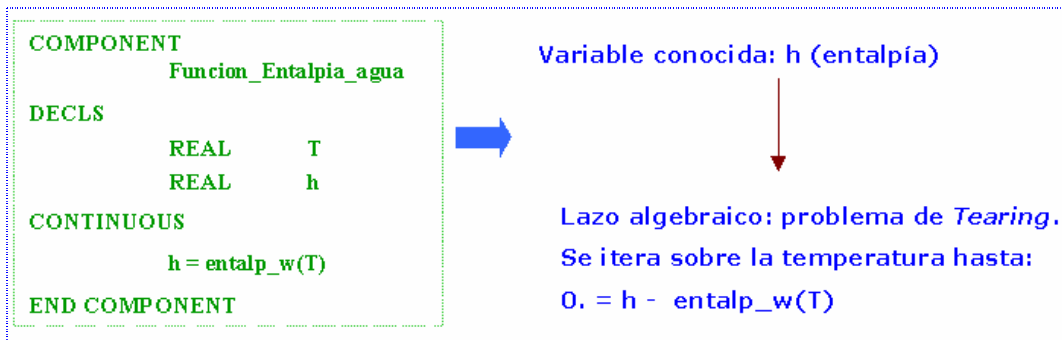
```

❖ **Problemas encontrados y soluciones propuestas.**

- Aparición de lazos algebraicos.

Cuando en una ecuación no lineal se conoce la variable dependiente en lugar de la independiente, aparece un lazo algebraico. En este caso, la forma de calcular la propiedad físico-química correspondiente es iterando sobre la variable independiente hasta que se satisfaga la ecuación no lineal.

Así por ejemplo,



Esto puede ocasionar en algún momento problemas de convergencia a la hora de realizar las simulaciones. La solución propuesta en este caso es la utilización de la función *INVERSE*, que evita la aparición del lazo algebraico:

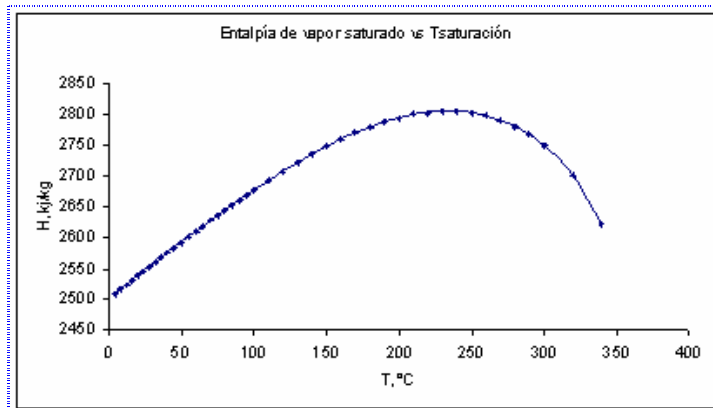
```

COMPONENT           Funcion_Entalpia_agua
DECLS
  REAL    T
  REAL    h
CONTINUOUS
  h = entalp_w(T)
  INVERSE(T) T = T_agua_H(h)
END COMPONENT

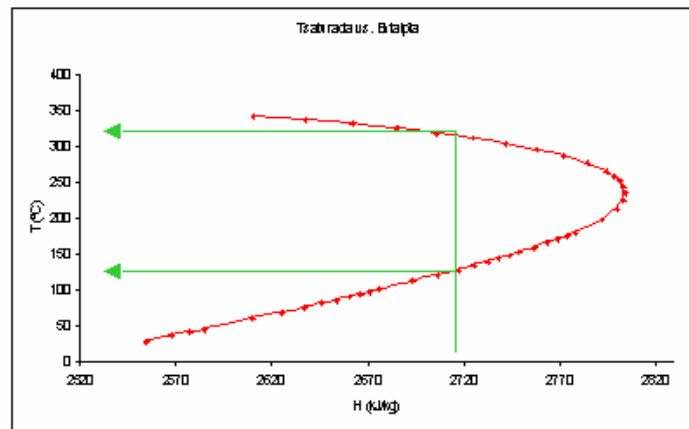
```

- Tablas cuya inversión dan lugar a más de una solución.

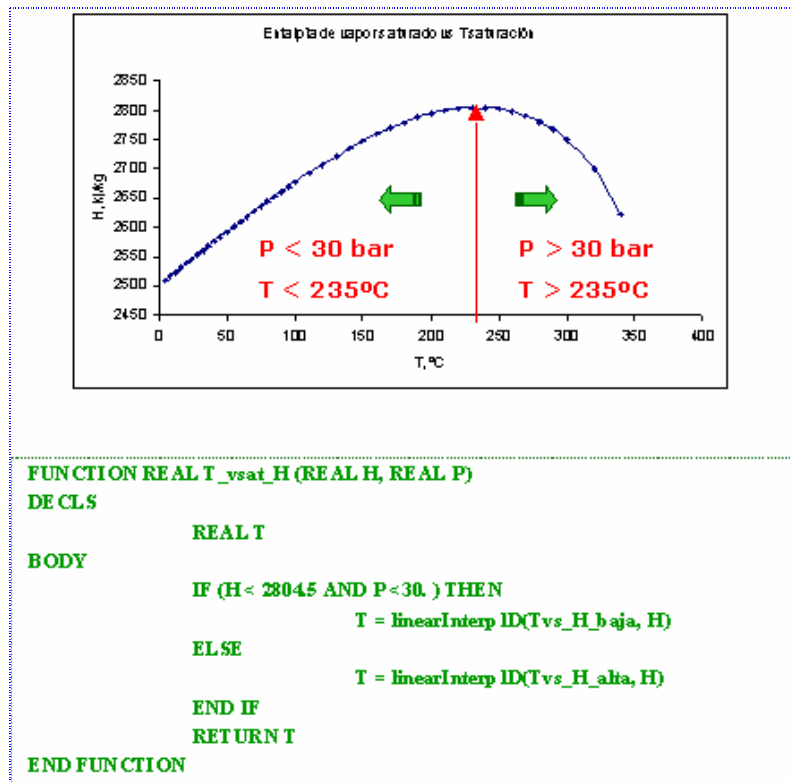
Puede ocurrir que en una propiedad fisico-química definida en forma de tabla, conocida la variable dependiente, tenga dos posibles soluciones. Son funciones de la siguiente forma:



Si se invierte la gráfica



La solución propuesta para este caso es invertir la tabla en dos tramos en función de dos argumentos de entrada:



### ❖ Librería de Puertos.

Los puertos son los elementos que permiten la conexión entre los distintos componentes. En ellos se definen aquellas variables que representan el intercambio de información entre componentes. Los puertos evitan el tener que conectar los componentes variable a variable, y crear componentes divisores y uniones.

Para permitir una utilización de los puertos de la forma más general posible se han utilizado ciertas características de EcosimPro que suponen una gran potencialidad y versatilidad a la hora de reutilizar componentes. Así los puertos de tipo líquido o gas se han parametrizado con un SET\_OF de forma que cuando se utiliza un puerto de conexión dentro de un componente no hay más que definir entre paréntesis el tipo de enumerado que le corresponde y todas las propiedades del puerto serán las correspondientes a ese enumerado.

La asignación inteligente de propiedades descrita en el apartado anterior permite además que las llamadas a las funciones sean las que el usuario quiera en función de este SET\_OF.

Otra característica de Ecosim que se ha utilizado es la sentencia EXPL, con ella se evita que ciertas variables con malas propiedades de convergencia aparezcan como variables de Tearing en los lazos algebraicos, o que Ecosim intente despejarlas a la hora de ordenar las ecuaciones. Con esto evitamos posibles problemas numérico Cada disciplina requiere un puerto propio (química, física, eléctrica, etc). Por lo tanto, los puertos desarrollados para esta librería son:

- Puerto líquido.
- Puerto gas.
- Puerto vapor de agua (saturado / no saturado).
- Puerto analógico.

❖ Librería de Elementos de Flujo.

Dentro de esta librería están las tuberías de líquido y vapor, válvulas, bombas, etc..

❖ Librería de Elementos de Control.

Se encuentran los componentes de los controladores:

- Controlador.
- Controlador proporcional.
- Controlador proporcional-integral.
- Controlador en cascada.

❖ Librería de Funciones Matemáticas.

Se implementan funciones matemáticas especiales que facilitan el funcionamiento de la simulación, como por ejemplo:

- Función para evitar divisiones por cero.
- Función para calcular la parte entera de un número.
- Función que limita una variable entre un máximo y un mínimo.

❖ Librería de Elementos de la Destilación de Gases Licuados del Petróleo (LPG).

- Columna de destilación (Despropanizadora).
- Condensador total.
- Ebullición total.

# Appendix B: A predictive control with dynamic optimization applied on a distillation column

# A predictive control with dynamic optimization applied on a distillation column

Benjamin Bradu\*, César de Prada Moraga\*\*

\* Ecole supérieure d'Ingénieurs en Electrotechnique et Electronique d'Amiens (ESIEE-Amiens)

14 Quai de la Somme, 80 000 Amiens, France

Email : [bbradu@autom.uva.es](mailto:bbradu@autom.uva.es)

\*\* Departamento de Ingeniería de Sistemas y Automática, Universidad de Valladolid

C/ Real de Burgos s/n, 47011, Valladolid, España

Email : [prada@autom.uva.es](mailto:prada@autom.uva.es)

**Abstract** — the purpose of this paper is to study a dynamic set-point optimization of a constrained multivariable predictive control in order to increase the benefits of a distillation column used in petroleum refineries. This optimization is embedded in a DMC controller and uses the same model and the predictions than the DMC in order to have a real coherence between the set-points found by the optimization and the controller. This dynamic optimization minimizes a quadratic economic cost function subject to linear constraints on controlled and manipulated variables. Results are validated thanks to simulations using a rigorous non-linear model of the column in EcoSimPro and are compared with a classical steady-state optimization. Influences of physical disturbances and of market prices on the optimal operating-point are also studied.

**Index Terms** — distillation column, predictive control, dynamic optimization

## II. PROCESS DESCRIPTION

Cesar...

## I. INTRODUCTION

Cesar...

III. CONTROL POLICY

The main objective of the distillation column control is to maintain the concentration of impurities in the distillate and in the bottoms between operating ranges. Other variables to control are the level of bottoms in the column and the level of distillate in the reflux drum.

Generally, the reflux ratio and the boilup ratio are low, so, the level in the reflux drum and the level in the column are respectively controlled with D and B. For this operation, a simple PI controller should be sufficient because these two controlled variables directly depend on these two manipulated variables. Then, to control the quality of bottoms and of distillates, an advanced control can be more efficient than a classical control for several reasons: all variables are linked. A multiple variables controller has to be developed, moreover there is a measurable disturbance (the flow of the feed:  $F$ ) which can be taken into account only in an advanced control and an advance control allows a better use of actuators and allows a more economic control for the industry. The usual technique to control this kind of process is to use a DMC predictive controller [1]. Hence, the qualities of components ( $C4_{Top}$  and  $C3_{Bottom}$ ) are controlled thanks to the vapor ( $V$ ) introduced at the bottom of the column and thanks to the quantity of Reflux ( $R$ ) re-injected at the top of the column. In this specific column, a depropanizer column, the choice is a bit different, impurities are controlled manipulating the sensible temperature ( $T$ ) at the top of the column (on the 33rd tray) and the condensate ( $Fpv$ ) which goes out of the reboiler. This choice is more or less equivalent because the flow of the condensate is proportional to the vapor and temperature at the top is highly correlated with the reflux. Hence, the DMC controller calculates appropriate PID set-points of the temperature and of the condensate to remove in order to respect set-points on impurities. So, variables of the DMC are the following:

- **CVs** : Impurities in the distillate (%):  $C4_{Top}$   
 Impurities in the bottoms (%):  $C3_{bottom}$
- **MVs** : Sensible temperature of the column ( $^{\circ}C$ ):  $T$   
 flow of the condensate (m3/h):  $Fpv$
- **Disturbance** : Flow of the feed (m3/h):  $F$

The Figure 1 represents this control architecture. A model of this depropanizer using physic differential equations and non-linear equations has been developed by the Systems Engineering and Automatic Control Department of the University of Valladolid on the software EcoSimPro. A DMC controller has also been developed using a library in Ecosimpro called HITO to realize the predictive control. The DMC uses a linear model of the column (composed of step responses) which has been obtained by identification. The Figure 2 represents the system in EcosimPro. The particularity of the DMC controller is that it uses the step response model [2]. If we take into account a controlled variable  $y$ , a manipulated variable  $u$ , a measurable disturbance  $v$ , the model is:

$$y(t) = \sum_{i=1}^{N_2} g_i \cdot \Delta u(t-i) + \sum_{i=1}^{N_2} d_i \cdot \Delta v(t-i) \tag{1}$$

The  $g_i$  coefficients represent the step response ( $\Delta u=1$ ) of the controlled variable and the  $d_i$  coefficients are the step response of the measurable disturbance ( $\Delta v=1$ ). The predictions are calculated using this model:

$$\hat{y}(t+j) = \sum_{i=1}^j g_i \cdot \Delta u(t-i+j) + p_j \tag{2}$$

$p_j$  represents the free response of the system. Then, a cost function  $J$  is minimized to calculate the future values of the MVs. Constraints on CVs values and on MVs values and velocity are taken into account in this minimization. There are physical constraints which are physical limits of variables and operation constraints which represent operation limits of the process. The cost function used is the following for  $n$  CVs and  $m$  MVs:

$$J = \sum_{k=1}^n \left( \sum_{j=N_{1k}}^{N_{2k}} \gamma_k (\hat{y}_k(t+j) - r_k(t+j))^2 \right) + \sum_{k=1}^m \left( \sum_{j=1}^{Nu_k} \beta_k (\Delta u_k(t+j-1))^2 \right) \tag{3}$$

There is a priority term  $\gamma_k$  on each CV and  $\beta_k$  on each MV to give a higher importance to some variables. For this distillation column, all these coefficients are equal to one (there is no priority). Moreover, HITO takes care of the feasibility of the control, so if the problem is unfeasible, operation constraints can be broken temporary [6] [7]. A priority table between constraints (on  $y$ ,  $u$  and  $\Delta u$ ) allows for solving this infeasibility breaking such constraints rather than another one.

For the depropanizer, 150 coefficients are taken into account in the step responses with a sampling time of 2min. The horizon of prediction is  $N2 = 45$  and the control horizon is  $Nu = 2$ .

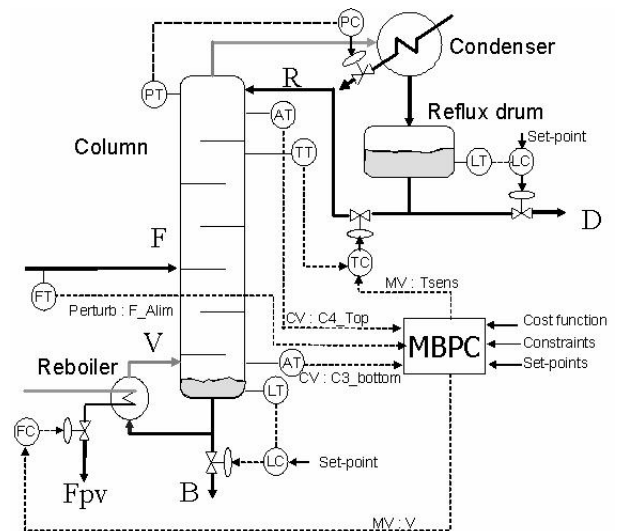


Fig. 1. Control architecture of the distillation column



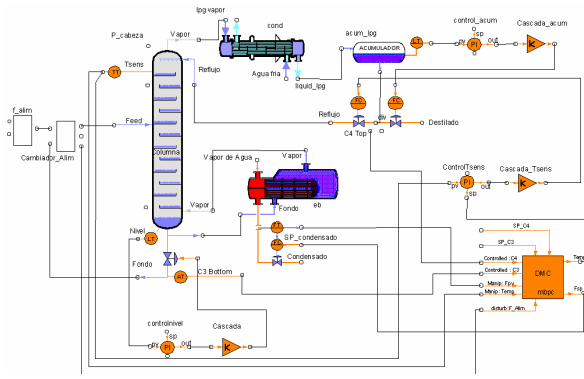


Fig. 2. Control architecture in EcosimPro

#### IV. OPTIMIZATION

The distillation column has to furnish products (butane and propane) with a maximum amount of impurities. So, controlled variables which are these percentages of impurities have just to be maintained under this maximum limit. For example, if the maximum of propane in butane is fixed at 15% ( $C3_{botmax} = 15\%$ ), the set-point of this CV can takes values between 0% and 15%. The aim of optimization is to calculate appropriate set-points in order to minimize the production cost during a normal operation of the process. To perform this, a cost function (quadratic or linear) subjected to constraints (linear or not) has to be minimized. The results of this minimization are values of set-points which allow to respect all constraints on the variables. So, manipulated variables are moving according to the values of set-points and if the model is consistent, all variables will stay between their optimization limits. Several studies of optimization on industrial processes have ever been done [3] [5] but it was steady-state optimization or with LP formulation. Here, we will study a steady-state optimization and also a dynamic optimization on the predictive horizon with a quadratic economic cost function.

##### A. HITO

In EcosimPro, a library called HITO (Integrated Tool for a Total Optimization) has been developed by the Engineering Systems and Automatic Control department of the Valladolid university. This library is used to achieve the predictive control. An optimization of set-points, directly included in HITO, can be also activated. The figure 3 resumes the general working of HITO. Steps of the algorithm are the following:

- Predictions are calculated thanks to the DMC controller using step-responses.
- Set-points of CVs are calculating minimizing an economic quadratic cost function: Optimization
- Values of MVs to apply on the process are calculated by an algorithm minimizing a cost function  $J$  respecting constraints and feasibility.

To solve the problem of optimization, the algorithm of optimization minimizes a quadratic economic cost function (which can be composed of MVs, CVs and disturbances) using the predictions calculated and taking into account all

constraints. One of the main advantages of HITO is that it is using the same model in the DMC and in the optimization. Hence, results obtained in the DMC controller are coherent with set-points obtained in the optimization. The parameters to give to the economic cost function are LPcosts of MVs ( $\zeta_m$ ), LPCost of CVs ( $\lambda_n$ ), LPcosts of disturbances ( $\xi_r$ ) and also a matrix which contains quadratic costs between all variables ( $\Psi_{i,j}$ ). The cost function used by HITO is represented by (4) when there are M manipulated variables, N controlled variables and R disturbances.

$$\begin{aligned}
 \phi = & \sum_{m=1}^M \sum_{j=1}^M \Psi_{m,j} \cdot u_m(t + Nu_m) \cdot u_j(y + Nu_j) \\
 & + \sum_{n=1}^N \sum_{j=1}^N \Psi_{n+M,j+M} \cdot \hat{y}_n(t + N2_n) \cdot \hat{y}_n(t + N2_j) \\
 & + \sum_{r=1}^R \sum_{j=1}^R \Psi_{r+N+M,r+N+M} \cdot v_r(t) \cdot v_j(t) \\
 & + \sum_{n=1}^N \sum_{m=1}^M \Psi_{n+M,m} \cdot \hat{y}_n(t + N2_n) \cdot u_m(t + Nu_m) \\
 & + \sum_{r=1}^R \sum_{m=1}^M \Psi_{r+M+N,m} \cdot v_r(t) \cdot u_m(t + Nu_m) \\
 & + \sum_{r=1}^R \sum_{n=1}^N \Psi_{r+M+N,n+M} \cdot v_r(t) \cdot \hat{y}_n(t + N2_n) \\
 & + \sum_{m=1}^M \zeta_m \cdot u_m(t + Nu_m) + \sum_{n=1}^N \lambda_n \cdot \hat{y}_n(t + N2_n) \\
 & + \sum_{r=1}^R \xi_r \cdot v_r(t)
 \end{aligned} \tag{4}$$

The main difference between the operating-point found by a classical steady-state optimization and by HITO which perform dynamic optimization is that it finds a solution at the end of the prediction horizon calculating all intermediate positions at each sampling-time according to the actual operating point (see Figure 4). Moreover HITO is careful to respect constraints on the velocity  $\Delta u$ . So, at each sampling time, the optimal operating point reachable in the predictive horizon is recalculated and normally at the end of the transitory, this operating-point should be fixed. The Figure 5 shows the evolution of the optimization in HITO between 2 sampling times.

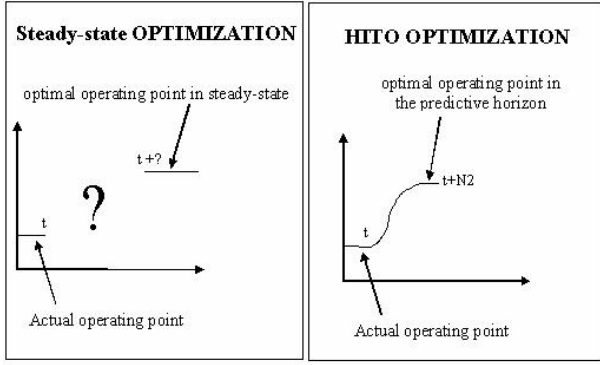


Fig. 4. Steady-state and HITO optimization

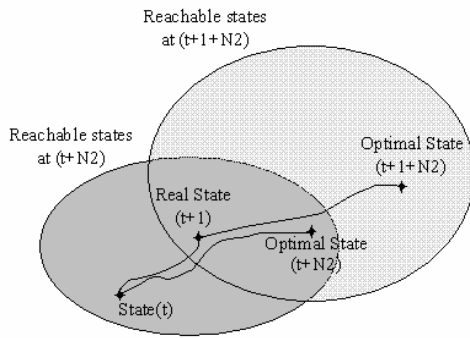


Fig. 5. HITO optimization for 2 sampling time

### B. Economic cost function

First, it is necessary to define all costs and gains of the process to determine an economic cost function. The costs are the quantity of steam introduced in the reboiler and of LPG (liquefied Petroleum Gas) which fed the column in the middle. The benefits are the quantities of distillate (propane, C4) and of bottoms (butane C3) which are going out and which can be sold on the market.

Products	Names	Units	Costs
Feed	LPG	Tm/h	+P <sub>LPG</sub>
Steam	S	Tm/h	+P <sub>S</sub>
Distillate	C3 (propane)	Tm/h	-P <sub>C3</sub>
Bottoms	C4 (butane)	Tm/h	-P <sub>C4</sub>

TABLE I. COSTS AND BENEFITS

According to the Table 1 we can formulate the real cost of production  $\Phi_{real}$ :

$$\phi_{real} = -C_4 \cdot P_{C4} - C_3 \cdot P_{C3} + S \cdot P_S + LPG \cdot P_{LPG} \quad (5)$$

The algorithm of optimization has to minimize this function finding the adequate MVs and CVs respecting all constraints. Hence, we have to transform this economic cost function (5) in order to obtain a function usable in HITO using MVs, CVs and disturbances like in (4).

After several simulations in open-loop between operating-ranges with the non-linear model on EcosimPro, we have

noticed that  $\Delta C4$ ,  $\Delta C3$  and  $\Delta LPG$  can be estimated by quadratic equations using  $\Delta Fpv$ ,  $\Delta T$  and  $\Delta F$ . Note that  $\Delta X = (X - X_0)$  where  $X_0$  is the initial value of  $X$ . So, with the different results of simulations in open-loop we can estimate  $C4$ ,  $C3$  and  $LPG$  of the equation (5) thanks to a quadratic equation composed of  $\Delta T$ ,  $\Delta Fpv$  and  $\Delta F$  using gains. Gains can be determined with an estimation of the curves obtained in simulation (figure 6) such that:  $\Delta Y = G_{Y/X} \Delta X + G_{Y/X^2} \Delta X^2$

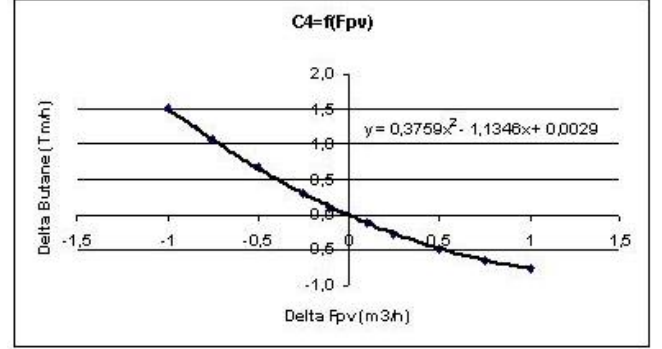


Fig. 6. Relation between the butane and the condensate in open-loop

Applying the principle of decomposition, we obtain the following expressions:

$$\rightarrow C4 = C4_{moy} + G_{C4/T} \cdot \Delta T + G_{C4/T^2} \cdot \Delta T^2 + G_{C4/Fpv} \cdot \Delta Fpv + G_{C4/Fpv^2} \cdot \Delta Fpv^2 + G_{C4/F} \cdot \Delta F + G_{C4/F^2} \cdot \Delta F^2$$

$$\rightarrow C3 = C3_{moy} + G_{C3/T} \cdot \Delta T + G_{C3/T^2} \cdot \Delta T^2 + G_{C3/Fpv} \cdot \Delta Fpv + G_{C3/Fpv^2} \cdot \Delta Fpv^2 + G_{C3/F} \cdot \Delta F + G_{C3/F^2} \cdot \Delta F^2$$

$$\rightarrow LPG = LPG_{moy} + G_{LPG/T} \cdot \Delta T + G_{LPG/T^2} \cdot \Delta T^2 + G_{LPG/Fpv} \cdot \Delta Fpv + G_{LPG/Fpv^2} \cdot \Delta Fpv^2 + G_{LPG/F} \cdot \Delta F$$

Moreover, the steam is proportional to the condensate:

$$S = k \cdot Fpv \Rightarrow P_S = P_{Fpv} / k \Rightarrow S \cdot P_S = Fpv \cdot P_{Fpv}$$

A virtual cost  $P_{Fpv}$  is introduced for the condensate  $Fpv$  because Vapor and condensate in the reboiler are strictly proportional. We can note that in all these relations, the impurities (the CVs  $C4_{top}$  and  $C3_{bot}$ ) are absent, it means that the economic cost of production do not depend directly on these impurities. After injecting these equalities in (5) we obtain a function of the HITO format (as in (4)) such that

$$\phi_{real} = \phi + cte$$

$$\phi = \zeta_T \cdot T + \psi_{T^2} \cdot T^2 + \zeta_{Fpv} \cdot Fpv + \psi_{Fpv^2} \cdot Fpv^2 + \zeta_F \cdot F + \psi_{F^2} \cdot F^2$$

$\zeta_T$ ,  $\zeta_{Fpv}$ ,  $\zeta_F$  and represent linear costs (LPcosts),  $\psi_{T^2}$ ,

$\psi_{Fpv^2}$  and  $\psi_{F^2}$  represent quadratic costs (QPcosts). Then, all linear and quadratic costs can be deduced by an identification (removing the constant) of (5) with (6):

$$\begin{aligned} \rightarrow \zeta_T &= -G_{C4/T} \cdot P_{C4} - G_{C3/T} \cdot P_{C3} + G_{LPG/T} \cdot P_{LPG} \\ &+ 2T_0 \cdot (G_{C4/T^2} \cdot P_{C4} + G_{C3/T^2} \cdot P_{C3} - G_{LPG/T^2} \cdot P_{LPG}) \\ \rightarrow \zeta_{Fpv} &= -G_{C4/Fpv} \cdot P_{C4} - G_{C3/Fpv} \cdot P_{C3} + G_{LPG/Fpv} \cdot P_{LPG} \\ &+ 2Fpv_0 \cdot (G_{C4/Fpv^2} \cdot P_{C4} + G_{C3/Fpv^2} \cdot P_{C3} \\ &- G_{LPG/Fpv^2} \cdot P_{LPG}) + P_{Fpv} \\ \rightarrow \zeta_F &= -G_{C4/F} \cdot P_{C4} - G_{C3/F} \cdot P_{C3} + G_{LPG/F} \cdot P_{LPG} \\ &+ 2F_0 \cdot (G_{C4/F^2} \cdot P_{C4} + G_{C3/F^2} \cdot P_{C3}) \\ \rightarrow \psi_{T^2} &= -G_{C4/T^2} \cdot P_{C4} - G_{C3/T^2} \cdot P_{C3} + G_{LPG/T^2} \cdot P_{LPG} \\ \rightarrow \psi_{Fpv^2} &= -G_{C4/Fpv^2} \cdot P_{C4} - G_{C3/Fpv^2} \cdot P_{C3} + G_{LPG/Fpv^2} \cdot P_{LPG} \\ \rightarrow \psi_{F^2} &= -G_{C4/F^2} \cdot P_{C4} - G_{C3/F^2} \cdot P_{C3} \end{aligned}$$

Minimize the linear function (5) is equivalent to minimize the quadratic function (6) because  $\phi_{real} = \phi + cte$

## V. RESULTS

First, the optimal operating point will be calculated in steady-state thanks to an optimization Software : GAMS. Then a dynamic optimization will be achieved with HITO during simulations on EcosimPro.

### A. Steady-State optimization with GAMS

To minimize the economic cost function (6) we have to formulate constraints on this function. So, these constraints have to be on the variables of the cost function (T, Fpv and F). Different constraints on the column are the following:

- Constraints on the manipulated variables  
 $[T_{inf}, Fpv_{inf}] \leq [T, Fpv] \leq [T_{sup}, Fpv_{sup}]$
- Constraints on the controlled variables  
 $[0, 0] \leq [C4_{top}, C3_{bot}] \leq [C4_{top\ max}, C3_{bot\ max}]$
- The perturbation F is fixed at its operating point  $F_0$

The problem is that CVs are absent of the economic cost function whereas there are constraints on these variables. The solution, as in the previous section, is to estimate CVs with MVs and disturbance thanks to simulations in open-loop in EcosimPro. After several simulations, the estimation of  $C4_{Top}$  is quadratic and the estimation of  $C3_{Bottom}$  bilinear:

$$\begin{aligned} \rightarrow C4_{top} &= C4_{top0} + G_{C4top/T} \cdot \Delta T + G_{C4top/T^2} \cdot \Delta T^2 \\ &+ G_{C4top/Fpv} \cdot \Delta Fpv + G_{C4top/Fpv^2} \cdot \Delta Fpv^2 \\ &+ G_{C4top/F} \cdot \Delta F + G_{C4top/F^2} \cdot \Delta F^2 \end{aligned}$$

$$\begin{aligned} \rightarrow C3_{bot} &= C3_{bot0} + G_{C3bot/T} \cdot \Delta T + G_{C3bot/Fpv} \cdot \Delta Fpv \\ &+ G_{C3bot/T \cdot Fpv} \cdot \Delta T \cdot \Delta Fpv + G_{C3bot/F} \cdot \Delta F \end{aligned}$$

After injecting these equalities in the CV constraints and replacing differential terms, we finally obtain four non-linear inequalities (the different coefficients  $a_1, b_1, \dots$  are constants which depend on gains  $G_{x/y}$  and on initial values):

$$\begin{aligned} a_1 \cdot T^2 + b_1 \cdot Fpv^2 + c_1 \cdot F^2 \\ + d_1 \cdot T + e_1 \cdot Fpv + f_1 \cdot F + g_1 \leq 0 \end{aligned} \quad (7)$$

$$\begin{aligned} -a_1 \cdot T^2 - b_1 \cdot Fpv^2 - c_1 \cdot F^2 \\ -d_1 \cdot T - e_1 \cdot Fpv - f_1 \cdot F - h_1 \leq 0 \end{aligned} \quad (8)$$

$$a_2 \cdot T + b_2 \cdot Fpv + c_2 \cdot F + d_2 \cdot T \cdot V + e_2 \leq 0 \quad (9)$$

$$-a_2 \cdot T - b_2 \cdot Fpv - c_2 \cdot F - d_2 \cdot T \cdot V + f_2 \leq 0 \quad (10)$$

Moreover, linear inequalities on MVs can be expressed such that:

$$A \cdot X + B \leq 0 \quad (11)$$

$$\text{With: } A = \begin{bmatrix} 1 & 0 \\ -1 & 0 \\ 0 & 1 \\ 0 & -1 \end{bmatrix} \quad \text{and } B = \begin{bmatrix} -T_{sup} \\ -T_{inf} \\ -Fpv_{sup} \\ -Fpv_{inf} \end{bmatrix}$$

This problem of minimization with non-linear constraints can be formulated using the vector  $X = [T, Fpv]^T$  such that :

$$\min_X \phi(X, X^2) \quad (12)$$

$$\begin{aligned} \text{Subject to:} \\ g(X) \leq 0 \end{aligned} \quad (13)$$

The function  $\Phi$  in (12) is the economic cost function (6). The four non linear inequalities (7) (8) (9) (10) and the linear inequalities (12) can be formulated in (13).

To solve this optimization problem, the software GAMS will be used. This professional software allows for solving a lot of different optimization problems (LP, NLP, MILP, MINLP). We will use a NLP solver named SNOPT [4] as the cost function is nonlinear and uses only continuous variables. SNOPT, (Sparse Nonlinear Optimizer) implements a sequential quadratic programming (SQP) method for solving

constrained optimization problems with smooth nonlinear functions in the objective and constraints. In this method, a Quadratic Programming (QP) sub problem is solved using estimation of the Hessian and of the Lagrangian at each iteration. So, optimal values of T and Fpv will be found minimizing the equation (12) subject to (13)

Note that the optimal solution found by GAMS will be the solution to reach in steady-state because all relations used between variables are gains in steady-state. The transitory of variables is not assumed, there is not in this case reference trajectory to follow. The optimal values found by GAMS are summarized in the Table 2. The real benefit corresponds to the calculation of the real cost function (5) but with opposite values (the benefit is the opposite of the cost).

Variables	Initial Values	Optimal Values
Fpv (m <sup>3</sup> /h)	3.875	4.8
T(°C)	49.5	56.72
C4 <sub>Top</sub> (%)	8.423	8.67
C3 <sub>bottom</sub> (%)	2.279	1.71
C4(Tm/h)	16.196	14.51
C3(Tm/h)	7.624	9.71
LPG(Tm/h)	23.92	24.12
Cost func. Value(\$)	-5719.59	-5862.3
Real benefit(\$)	214.77	358

TABLE II. OPTIMAL VALUES OF VARIABLES IN STEADY-STATE

The solution can be visualized on the Figure 7 where the cost function is represented according to Fpv and T when the perturbation  $F = F_0$ , the solution is at the bottom of the surface respecting all constraints.

In this steady-state optimization, the benefits increases by \$143, it is an augmentation of 66%. The constraint on the condensate is an active constraint because the condensate takes its maximum value ( $Fpv_{max}=4.8m^3/s$ ), so the vapor introduced in the column is maximized. The temperature is very close to its upper limit also (the reflux is important).

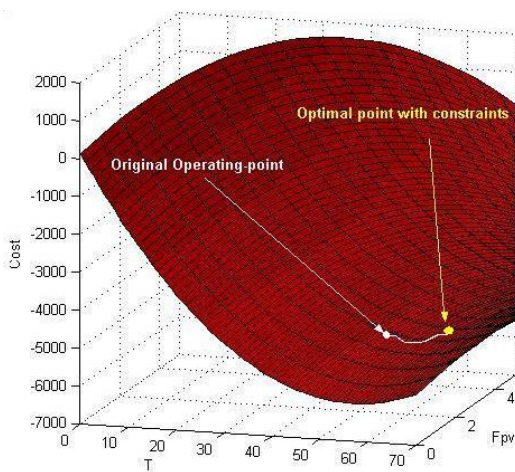


Fig. 7. Cost function representation

*B. Dynamic optimization with HITO*

An iterative dynamic optimization is achieved by HITO using the step responses of the DMC controller (see paragraph 4.1 about HITO). It takes into account the quadratic economic cost function (6) subject to the linear constraints on CVs and on MVs. In the previous optimization in steady-state with GAMS, quadratic constraints were necessary to express constraints on CVs whereas HITO only uses linear constraints because constraints are applied in the optimization (only on u) and in the control (on y, u and Δu). In order to evaluate the performance of this optimization in EcoSimPro we will activate the optimization in the simulation after 7 min when the stationary state of the column is well established. Results of simulation are shown in the figures 8 and 9. The Table 3 contains final values of variables when the steady-state is reached, percentages represent the difference between the optimal values found with GAMS thanks to the steady-state optimization and those found by HITO.

Variables	Optimal values with dynamic optimization
Fpv (m <sup>3</sup> /h)	4.8 : 0%
T(°C)	56.74 : -0.03%
C4 <sub>Top</sub> (%)	8.811 : +1.58%
C3 <sub>bottom</sub> (%)	0.65 : -62%
C4(Tm/h)	14.415 : +1.83%
C3(Tm/h)	9.492 : -1.26%
LPG(Tm/h)	24.103 : -0.09%
Cost func. Value(\$)	-5862 : +0.02%
Real benefit(\$)	429.70 : 33.4%

TABLE III. RESULTS WITH DYNAMIC OPTIMIZATION

In this simulation, the optimization of the HITO function gives more or less the same results than results found with GAMS in steady-state. All variables take values close to estimated values a priori except the value of C3<sub>Bottom</sub>. In both cases, we see that the optimization tries to maximize the quantity of propane produced reducing the quantity of butane because propane is more expensive and the column produced much more butane than propane because the concentration of butane is superior in the feed. We can also note that the two levels (of bottoms in the column and of distillate in the reflux drum) stay in acceptable range during the transitory and remain stable in steady-state.

The error between the steady-state operating point found in GAMS and this dynamic optimization using a linear model is 62% on the C3<sub>Bottom</sub> because the variable C3<sub>bottom</sub> is highly non-linear, so the linear estimation in HITO is not perfect. Hence, we can see in the Figure 8 that this set-point in the simulation can't be reached (0.65%) and the real value of the C3<sub>Bottom</sub> is equal to the value found in GAMS (1.71%) because the bilinear estimation in GAMS is much better. With this optimization, the benefits are multiplied by two (\$429 of benefits with optimization, \$215 before).

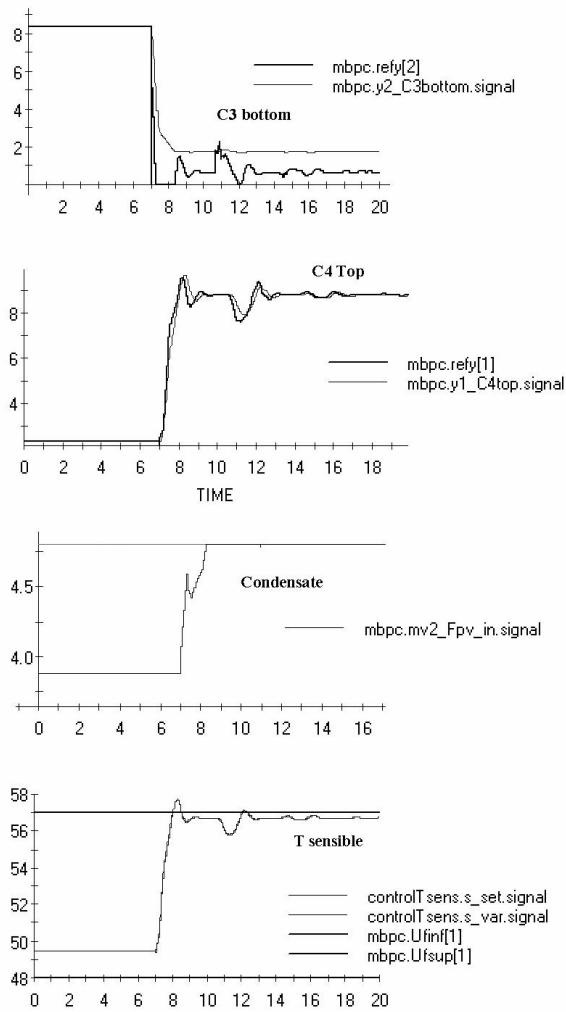


Fig. 8. CVs and MVs during dynamic optimization

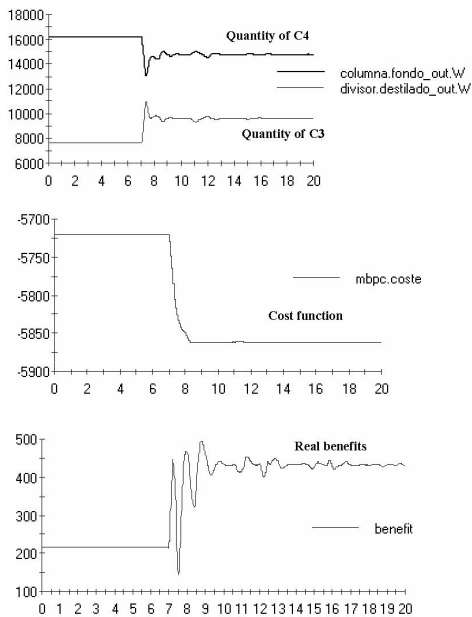


Fig. 9. Economic variables during dynamic optimization

C. Influence of disturbances

A lot of exterior factors can disturb the column. In simulations, all temperatures, pressures and flows of external components are boundary variables which are fixed. Moreover, the composition of the feed can change over time according to the crude which fed the column. The only measurable disturbance takes into account in the DMC (and so, in the optimization) is the flow of the Feed (F) which depends on the crude used.

As the optimization is effectuated in real-time at each sampling-time, the optimal operating point has to move when a measurable disturbance happens to keep an optimal operation of the column. If the composition (which is not measured) moves, a prediction error appears and MVs will move in order to reach the set-point ( $\Delta u \neq 0$ ). In this case, the predictions will be rectified thanks to the equation (2) and as the predictions change during this non-measurable disturbance, the reachable states can be different and in this case, the optimization will find a new optimal set-point in this area whereas this disturbance is not measured. That is the real advantage of this technique when the optimization uses predictions of the DMC.

Table 4 and Figure 10 show results when the composition of the feed change. The concentration of the feed is at the basis 56% of C4 and 44% of C3 and after 15 minutes, the new composition is 65% of C4 and 35% of C3.

Variables	Init opt values	New opt. values
Fpv (m <sup>3</sup> /h)	4.8	4.8
T(°C)	56.74	56.71
C4 <sub>Top</sub> (%)	8.811	9.01
C3 <sub>bottom</sub> (%)	0.65	0.26
C4(Tm/h)	14.415	17.044
C3(Tm/h)	9.492	7.587
LPG(Tm/h)	24.103	24.442
Cost func. Value(\$)	-5862	-5862
Real benefit(\$)	429.70	402

TABLE IV. OPTIMAL STEADY-STATE VALUES WITH DISTURBANCE ON THE COMPOSITION OF THE FEED

When the disturbance occurs, the two set-points are moving: The set-point on C4<sub>Top</sub> increases and the set-point on C3<sub>Bottom</sub> decreases. This natural reaction of the optimization is coherent because there is more butane than propane in the feed. Optimal MVs are the same and so, the economic cost function keeps its value whereas the real benefit decreases a bit because the quantity of propane produced, which is more expensive than the butane, decreases. The error between the set-point and the real value on the C3<sub>Bottom</sub> due to the non-linearity is the same than previously.

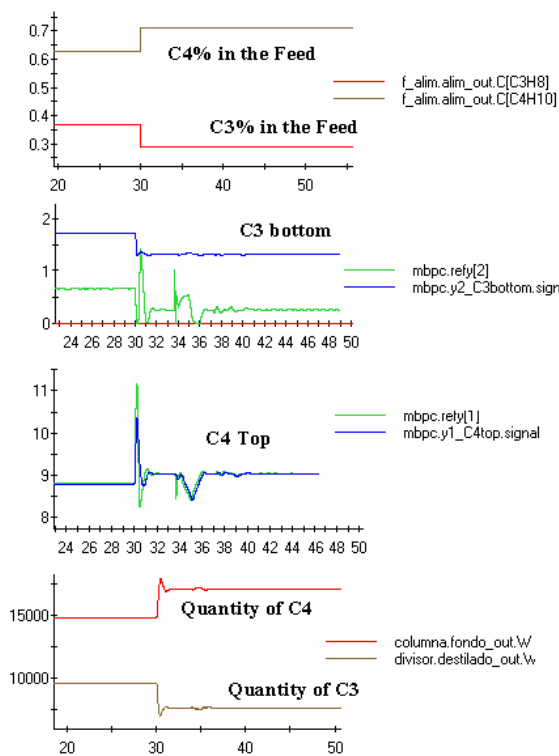


Fig. 10. Disturbance and CVs with disturbance at T=30

ie, steam) fluctuate according to the market. Hence, optimal operating point should move with prices. Moreover butane and propane prices are very close. In previous simulations, butane was cheaper than propane but the inverse can happen on the market. After different simulations, when prices of products are moving in acceptable ranges, the changing of LPcosts and QPcosts are very small, so, the displacement of the optimal operating-point (and so the value of the cost function) is not relevant. Hence, this parameter is not relevant enough to be taken into account for a real process.

## VI. CONCLUSION

A DMC controller with an embedded dynamic optimization is proposed in this paper. The main advantage is that the controller and the optimization are really correlated using the same predictions along the receding horizon. As the optimization is performed at each sampling time, the optimal operating-point is able to move rapidly when disturbances occur or if some constraints move, it is not necessary to wait for a new steady-state to perform the optimization like to the classical Real Time Optimizations (RTO). Moreover the dynamic behavior of the process is taking into account. Nevertheless, when processes are highly non-linear, the linear predictions of the DMC are not so good and the set-points provide by the optimization can be unreachable and there is a static error between the set-point and the real value. But finally, results obtained in simulations with a rigorous model of the depropanizer are positive and benefits are greatly maximized.

## REFERENCES

- [1] P.O. de Castro, E.F. Camacho. *Control e instrumentación de procesos químicos*. Editorial Sintesis, 1997
- [2] C. R. Cutler, B. L. Ramaker. *Dynamic Matrix Control - a computer control algorithm*. Proceedings of the joint automatic control conference (JACC), San Francisco, CA. 1980.
- [3] Liankui Dai, Yang Wang. *A simplified constrained multivariable controller with steady-state optimization*. 4th World Congress on intelligent Control and Automation, 2002
- [4] PE Gill, W Murray, MA Saunders. *SNOPT: An SQP Algorithm for Large-Scale Constrained Optimization*. Numerical Analysis Report 97-2, Department of Mathematics, University of California, San Diego, La Jolla, CA, 1997.
- [5] C. Ramos, J.S Senent, X.Blasco, J.Sanchis. *LP-DMC Control of a chemical plant with integral behaviour*. 15th Triennial World Congress, Barcelona, Spain, 2002
- [6] James B. Rawlings. *Tutorial : Model Predictive Control Technology*. Proceedings of the American Control Conference, San Diego, California, 1999
- [7] Zheng Z. Q. and M. Morari *Stability of model predictive control with mixed constraints*. IEEE Trans. On Automatic Control, 40(10), 1995

## Appendix C: Optimization program and results in GAMS

## PROGRAM:

\$title Economic Optimization of Depropanizer

\$Ontext

*Benjamin Bradu*

*Universidad de Valladolid, Departamento de Ingenieria de Sistemas y Automatica*

\$Offtext

```
Scalars LP_T          "LPcost temperature"      /-216.461/
         LP_Fpv       "LPcost condensate"       /126.282/
         LP_F         "LPcost Feed"            /8.148/
         QP_T         "QPcost Temperature"     /1.908/
         QP_Fpv      "QPcost condensate"      /-19.786/
         QP_F         "QPcost Temperature"     /-0.116/
         G11 "Gain for estimation of C4Top"    /0/
         G12 "Gain for estimation of C4Top"    /0.0068/
         G13 "Gain for estimation of C4Top"    /0.0001/
         G14 "Gain for estimation of C4Top"    /0.8848/
         G15 "Gain for estimation of C4Top"    /-0.0583/
         G16 "Gain for estimation of C4Top"    /-0.0118/
         K1  "cste for estimation of C4Top"    /-41.0612/
         a  "Gain for estimation of C3bot"     /0.2046/
         b  "Gain for estimation of C3bot"     /-12.7105/
         c  "Gain for estimation of C3bot"     /0.5333/
         C30 /8.423/
         T0  /49.5/
         Fpv0 /3.875/ ;
```

### variables

```
F          Objective variable
T          MV : Temperature
Fpv       MV : Condensate
Feed      Disturb : Flow of the Feed
C4_top    CV : Butane in Propane
C3_bot    CV : Propane in Butane
```

### equations

```
Objective Economic Cost Function
estim_C4_top Estimation of C4 top
estim_C3_bot Estimation of C3 bottom
equa_Feed Equality of the Feed Flow;
```

```
Objective.. F=e= LP_T*T + LP_Fpv*Fpv + LP_F*Feed + QP_T*T**2 +
QP_Fpv*Fpv**2 + QP_F*Feed**2;
estim_C4_top.. C4_top =e= G11*T**2 + G12*Fpv**2 + G13*Feed**2 + G14*T
+ G15*Fpv + G16*Feed + K1 ;
estim_C3_bot.. C3_bot =e= C30+a*(T-T0)+b*(Fpv-Fpv0)+c*(T-T0)*(Fpv-
Fpv0);
equa_Feed.. Feed=e=46.9877;
```

```
T.lo = 48;          T.up = 57;
Fpv.lo = 2.7;      Fpv.up = 4.8;
C4_Top.lo = 0;     C4_top.up = 15;
C3_bot.lo = 0;     C3_bot.up = 15;
```

```
model depropanizer /all/;
```

```
solve depropanizer using nlp minimizing f;
```



# RESULTS :

## S O L V E            S U M M A R Y

```

MODEL   depropanizer      OBJECTIVE  F
TYPE    NLP                DIRECTION  MINIMIZE
SOLVER  SNOPT              FROM LINE  59

```

```

**** SOLVER STATUS      1 NORMAL COMPLETION
**** MODEL STATUS      2 LOCALLY OPTIMAL
**** OBJECTIVE VALUE    -5862.2997

```

```

RESOURCE USAGE, LIMIT      0.063      1000.000
ITERATION COUNT, LIMIT    12          10000
EVALUATION ERRORS         0            0

```

SNOPT-Link      Jan 26, 2005 WIN.SN.SN 21.6 040.053.041.VIS SNOPT 6.2-1(1)

GAMS/SNOPT, Large Scale Nonlinear SQP Solver  
S N O P T 6.2-1(1) (Jan 2003)  
P. E. Gill, UC San Diego  
W. Murray and M. A. Saunders, Stanford University

Work space allocated            --      0.20 Mb

EXIT - Optimal Solution found, objective:            -5862.300

```

Major, Minor Iterations      8          12
Funobj, Funcon calls        14          14
Superbasics                  1
Aggregations                 0
Interpreter Usage           0.00        0.0%

```

Work space used by solver            --      0.06 Mb

	LOWER	LEVEL	UPPER	MARGINAL
---- EQU Objective	.	.	.	1.000
---- EQU estim_C4_~	-41.061	-41.061	-41.061	EPS
---- EQU estim_C3_~	47.548	47.548	47.548	EPS
---- EQU equa_Feed	46.988	46.988	46.988	-2.753

	LOWER	LEVEL	UPPER	MARGINAL
---- VAR F	-INF	<b>-5862.300</b>	+INF	.
---- VAR T	48.000	<b>56.725</b>	57.000	-2.26E-10
---- VAR Fpv	2.700	<b>4.800</b>	4.800	-63.664
---- VAR Feed	-INF	<b>46.988</b>	+INF	.
---- VAR C4_top	.	<b>8.672</b>	15.000	.
---- VAR C3_bot	.	<b>1.708</b>	15.000	.

```

**** REPORT SUMMARY :      0      NONOPT
                           0      INFEASIBLE
                           0      UNBOUNDED
                           0      ERRORS

```

## **Título:** Control Predictivo multivariable y optimización de procesos con HITO y EcosimPro

Universidad de Valladolid, Escuela Técnica Superior de Ingenieros Industriales,  
Departamento Ingeniería de Sistemas y Automática

### **Autor:**

- *Benjamin Bradu*

### **Tutores:**

- Director: *Rogelio MAZAEDA*
- Codirector: *César de PRADA MORAGA*

## **RESUMEN**

Este Proyecto Fin de Carrera propone una identificación paramétrica y diferentes tipos de control Predictivo con una optimización de las consignas gracias a HITO. Primero, la identificación y el control Predictivo (GPC y DMC) son realizados en depósitos comunicantes (simulaciones y experimentos en el proceso real). Después, un Dynamic Matrix Control (DMC) se aplica a una columna de destilación usada en las refinerías de petróleo con una optimización dinámica para reducir los costos de operación de este sistema. Esta optimización, incluida en el controlador y usando las mismas predicciones, minimiza una función de coste sujeta a restricciones lineales en las variables manipuladas y controladas. Los resultados se validan gracias a simulaciones en EcosimPro usando un modelo riguroso no lineal de la columna. Se realiza también una comparación con una optimización en estado estacionario. Finalmente, se estudian las influencias de las perturbaciones exteriores y de las evoluciones de los precios en el mercado sobre el punto de operación óptimo.

## **ABSTRACT**

This final year project purposes a parametrical identification and different kinds of predictive control with a set-point optimization thanks to HITO. First, identification and predictive controls (GPC and DMC) are achieved on communicating tanks (simulations and tests on the real process). Then, a Dynamic Matrix Control (DMC) is studied on a distillation column used in the petroleum refineries with a dynamic set-point optimization in order to reduce the operation costs of this system. This optimization, embedded in the DMC controller and using the same model than it, minimizes a quadratic cost function subjects to linear constraints. Results are validated thanks to simulations using a rigorous non-linear model of the column on the software EcosimPro. A comparison with a steady-state optimization is also done. Influences of external disturbances and of market fluctuations on the optimal operating point are studied at the end.

### ***Palabras claves:***

- |                   |                         |                              |
|-------------------|-------------------------|------------------------------|
| 1. Automatic      | 5. Predictive Control   | 9. Steady-state optimization |
| 2. Identification | 6. GPC                  | 10. Distillation column      |
| 3. EcosimPro      | 7. DMC                  | 11. Depropanizer             |
| 4. HITO           | 8. Dynamic Optimization | 12. Economic cost function   |